Investigation of the Synthesis and Thermal Rearrangements of

1,2,3,4,5-Pentaphenyl-2,4,-Cyclopentadiene Alkyl Ethers

by

Patricia Martin

Dissertation submitted to the Faculty of the

Virginia Polytechnic Institute and State University

in partial fulfillment of the requirements for the degree of

Doctor of Philosophy

in

Chemistry

APPROVED:

Michael A. Ogliaruso, Chairman

Harold M. Bell

John G. Mason

Milos Hudlicky

James P. Wightman

November, 1987

Blacksburg, Virginia

Investigation of the Synthesis and Thermal Rearrangements of

1,2,3,4,5-Pentaphenyl-2,4,-Cyclopentadiene Alkyl Ethers

by

Patricia Martin

Michael A. Ogliaruso, Chairman

Chemistry

(ABSTRACT)

A comparative synthetic study of a series of six 1,2,3,4,5-pentaphenyl-2,4-cyclopentadiene alkyl ethers was investigated. It was determined that the most efficient route to these ethers was not the most generally accepted route to ethers - the Williamson Reaction - but rather a solvolysis reaction between 1-bromo-1,2,3,4,5-pentaphenyl-2,4-cyclopentadiene and the appropriate alcohol.

Thermal rearrangement of the ethers had been expected to rearrange by a [1,5]-sigmatropic shift of the phenyl group in the 1-position to yield the corresponding enol ether. However, this appeared to occur only as a trace in some cases. Rather, the major product of the thermal rearrangements of these ethers was actually the elimination product, the hydrocarbon, 1,2,3,4,5-pentaphenyl-2,4-cyclopentadiene. The elimination is most likely the result of a retro-ene reaction.

Acknowledgements

I very gratefully thank Dr. Ogliaruso for his guidance, encouragement, support and friendship during my time at Virginia Tech. He will *always* remain on my "most respected" list.

I would also like to thank the other members of my committee, Dr.'s Bell, Hudlicky and Mason. Their respective contributions to this dissertation were greatly appreciated. Special thanks to Dr. Wightman for filling in at the last minute. I also owe my thanks to Dr. Tanko for his understanding and generous patience in sharing the lab as well as his generous offer for using his computer to help prepare this dissertation. I wish him much luck in his future at Virginia Tech.

I am very thankful for the friendships I made while at Virginia Tech. From the "early years" I am grateful for having known Frank Koehan, Patti Andolino-Brandt and Pradip Das.

Also my many thanks to the members of my research group Dwaine Davis, Alan Davis and Bob Eagan. Alan was definitely the most unique person I've ever shared a lab with and Bob probably the most patient when posed a thousand questions.

For the "final phase" of my time at Tech I would like to acknowledge Dr. Kingston's research group for my adoption. I especially found great support from friends

and .. I very gratefully thank Mike for his chemical input, fantastic ability at fixing aging HPLC equipment and especially for sharing a craving of homemade ice cream, which probably got us both through those final months. It is difficult to find words to thank Tom. Most importantly

I was always grateful for his companionship and doubt I had a better pal. However, Tom stands out for his willingness to *really* listen to my chemistry and *really* make excellent suggestions. For many reasons Tom will never cease to amaze me, he just never stops thinking. I believe he is truly one of the most intelligent and versatile chemists I have ever met. I would also like to thank my roommate for her generous help and patience with helping me use the computer and the preparation of the graphs for this dissertation.

Many thanks to Cindy Koning for typing this dissertation. Her excellent skills made the preparation of this dissertation as painless as possible.

My very special thanks to Chris for the friendship I have found with him. The patience and support he so generously gave will never be forgotten, only gratefully remembered and returned.

And lastly, I very gratefully and proudly acknowledge my parents for both the strong emotional support and financial support they have given throughout my education.

Table of Contents

List of Figures

Figure Page

List of Tables

Introduction

Youssef and Ogliaruso[1] showed the thermally induced isomerization of 1,2,3,4,5-pentaphenyl-2,4-cyclopentadien-1-ol to 2,2,3,4,5-pentaphenyl-3-cyclopenten-1-one to be a symmetry allowed [1,5]-sigmatropic phenyl rearrangement. Ogliaruso's group[2-3] has investigated the nature of the transition state for this rearrangement to determine its sensitivity to electronic effects. Several series of p-substituted phenyl derivatives of 1,2,3,4,5-pentaphenyl-2,4-cyclopentadien-1-ol were synthesized with the substituted phenyl positioned at either the migration origin, migration terminus or along the π backbone of the cyclopentadienol ring. They concluded from their results that the positioning of the substituents did not illustrate any detactable linear free energy relationship. Therefore, they proposed a neutral transition state devoid of charge separation for this phenyl migration.

However, more recently, Eagan[4] synthesized a series of 1-substituted-2,3,4,5-tetraphenyl-2,4-cyclopentadien-1-ols and studied the rates of rearrangement. His results showed that electron donating groups increased the rate of migration and electron withdrawing substituents slowed the rate of migration. These results supported the originally proposed charge separated transition state. Eagan's results were explained by the fact that a more

direct effect was being exerted on the ($\delta+$) charged area of the transition state than could possibly be made by a para substituent on a phenyl ring.

The fundamental point of this dissertation was to study the thermal rearrangement of a series of 1,2,3,4,5-pentaphenyl-2,4-cyclopentadiene alkyl ethers. The ethers were most efficiently prepared by a solvolysis reaction between 1-bromo-1,2,3,4,5-pentaphenyl-2,4-cyclopentadiene and the appropriate alcohol. A [1,5]-sigmatropic phenyl shift had been the anticipated thermal rearrangement, however this particular system apparently was better suited for rearranging via a retro-ene elimination giving the corresponding hydrocarbon. The rates of rearrangement were determined and the activation energies (Ea) and entropies of activation ($\Delta S^{\neq}$) were calculated. The results of this investigation form the thrust of this dissertation.

Historical

In 1943, Allen and Van Allen[5] reported the synthesis of 2,3,3,4,5-pentaphenyl-1,4-cyclopentadiene-1-ol (1) by means of two different methods. The first method was by a direct 1,4-Grignard addition of phenyl magnesium bromide to 2,3,4,5-tetraphenyl-2,4-cyclopentadien-1-one (tetracyclone, 2) in refluxing isoamyl ether (BP 173°).

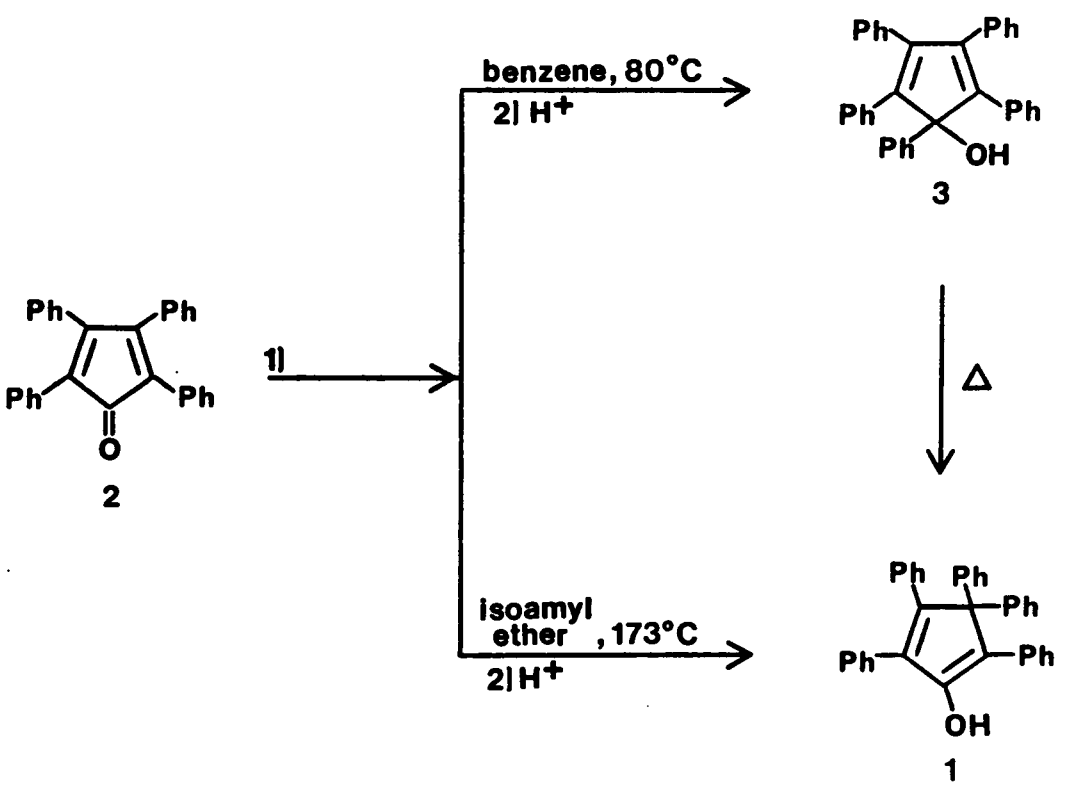

The second method was by a 1,2-Grignard addition of phenyl magnesium bromide to **2** in refluxing benzene (BP 80°) to give 1,2,3,4,5-pentaphenyl-2,4-cyclopentadien-1-ol **3** which could be thermally isomerized at 173° to the reported product **1**.

In 1961, Dufraisse, Rio and Ranjon[6] reinvestigated the thermal isomerization of **3** in the absence of solvent and reported that, in addition to two minor products formed, the actual structure of the major product was not **1**, but rather 2,2,3,4,5-pentaphenyl-3-cyclopenten-1-one **4**. For the mechanism of formation of **4** from **3** they proposed a thermally induced pinacol type rearrangement.

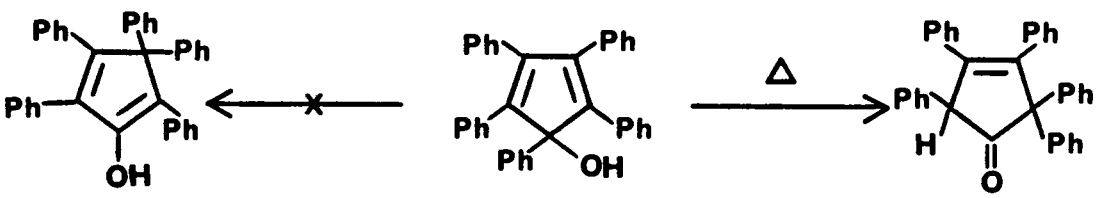

1 **3** **4**

In 1965, Woodward and Hoffmann[7] put forth the fundamental basis for the theoretical treatment of all concerted reactions. Their basic principle stated that reactions will readily occur when there is congruence between the orbital symmetry characteristics of reactants and products. And in addition, that reactions in which that congruence is not obtained will proceed only with great difficulty. In other words, orbital symmetry is conserved in concerted reactions. They also defined a sigmatropic reaction of the order [i,j] as the migration of a σ bond, flanked by one or more π electron systems, to a new position whose termini are i-1 and j-1 atoms removed from the original bonded loci, in an uncatalyzed intramolecular process.

Also in 1965, McLean and Haynes[8] studied [1,5]-hydrogen migrations in methyl substituted cyclopentadienes. They synthesized 5-methyl cyclopentadiene **5**, 1-methyl cyclopentadiene **6** and 1,5-dimethyl cyclopentadiene **7**, and measured the rates of hydrogen migration. The rearrangement

of **5** to **8** was found to proceed the fastest due to stabilization of the partial positive charge associated with C5 in the transition state. Most likely the methyl group stabilizes the $\delta+$ charge through its inductive effect and by facilitating rehybridization of the (C5) sp^3 carbon to the more electronegative sp^2. The conversion of **6** to **9** proceeded with the slowest rate which is explained by the fact that the methyl substituent lies along the π-backbone, an area which would bear a partial negative charge in the transition state. In this way, the inductive effect of the electron-donating methyl substituent destabilizes the transition state by increasing the electron density in this partial negative area. And finally the conversion of **7** to **10** proceeded at an intermediate rate. In this case the methyl groups are located in both a $\delta+$ (C5) area and a $\delta-$ (C1) area which essentially negates any electronic effect.

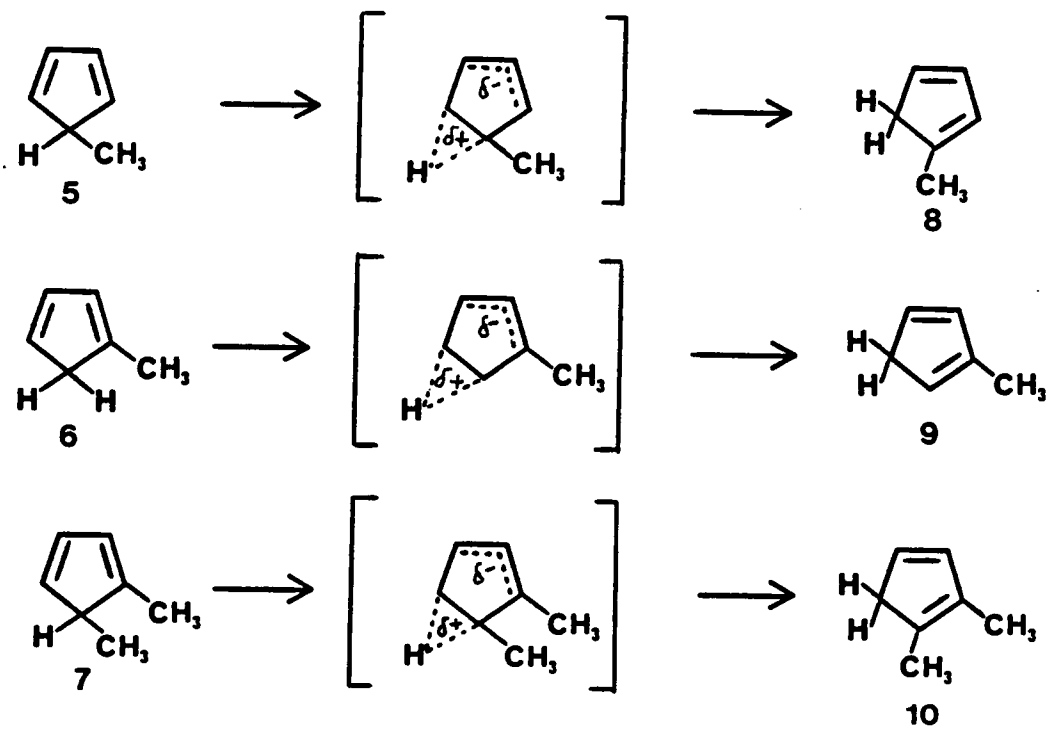

In 1969, Miller, Greisinger and Boyer[9,10] first studied the migratory aptitudes of methyl, phenyl, and hydrogen during thermal sigmatropic rearrangements within the indene system. They

reported that a [1,5]-sigmatropic phenyl shift in indene substituted systems was associated with a ΔE_a and $\Delta S^{\neq}$ of 27.2 kcal/mole and -27.2 eu respectively.

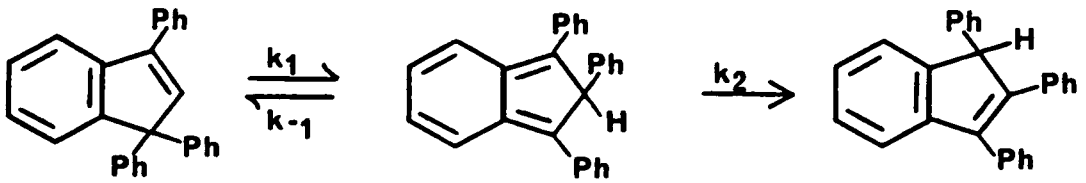

In 1972, Youssef and Ogliaruso[1] reinvestigated the direct 1,4-Grignard addition of phenyl magnesium bromide to tetracyclone 2 and the thermally induced isomerization of 3 to 4. Due to the work of Woodward and Hoffmann[7], this rearrangement under investigation could now be classified as a thermally-allowed [1,5]-sigmatropic phenyl rearrangement. The enol 13 initially formed could then rapidly tautomerize to the more stable keto form 4.

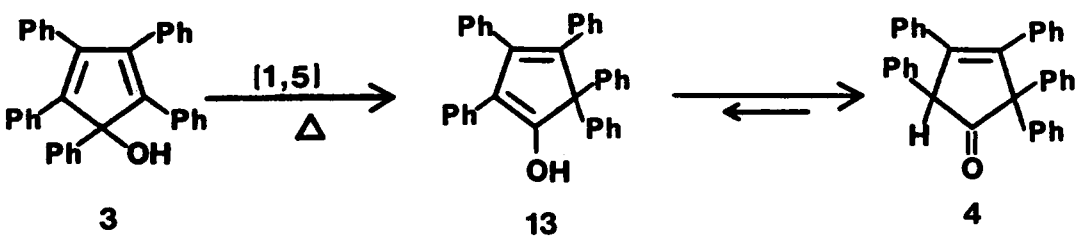

3 13 4

In order to establish that the rearrangement of 3 to 4 proceeded by an initial [1,5]-sigmatropic rearrangement followed by a keto-enol tautomerization, Youssef and Ogliaruso[1] performed the series of experiments illustrated in Scheme 1.

The possibility of a direct 1,6-addition was eliminated by showing that 11, the product of a 1,2-addition to be an intermediate in the reaction. This was done by performing the addition of

Scheme I

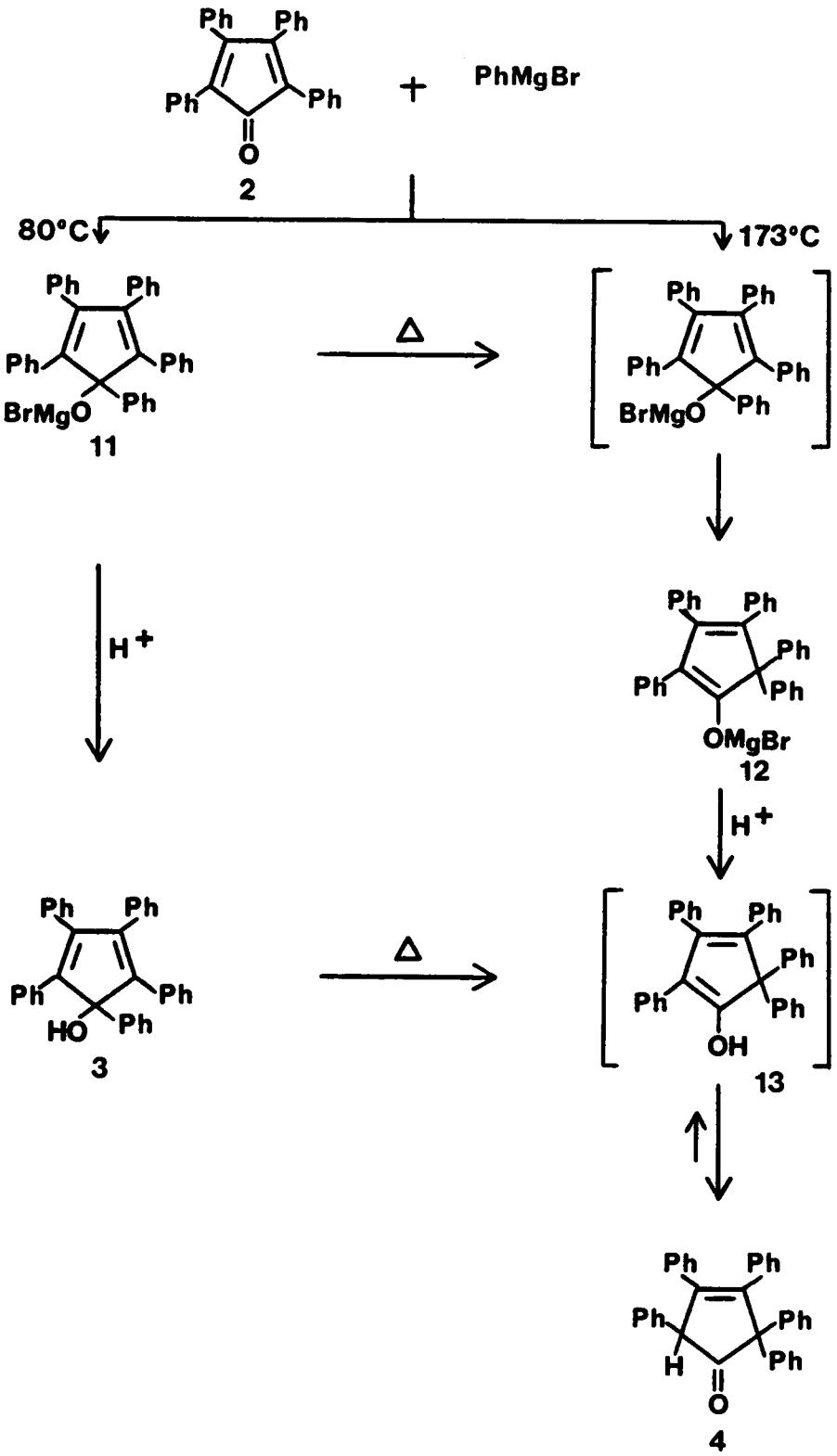

phenyl magnesium bromide to tetracyclone **2** in refluxing benzene (BP 80°C). The 1,2 addition produce **11** was formed since quenching an aliquot of the reaction mixture afforded the dienol **3**. The dienol **3** could then be isomerized in refluxing isoamyl ether (BP 173°C) to the enol form **13** which rapidly tautomerizes to the keto form **4**. Alternatively, the Grignard salt **11** could be rearranged to **12** which upon hydrolysis also affords **4** This was the first reported case of a thermally induced sigmatropic rearrangement of a magnesium salt of a Grignard reaction. The above series of reactions concludes that the reaction under investigation proceeded via 1,2-addition of phenylmagnesium bromide to **2** to yield the Grignard salt **11**, which could be hydrolyzed to give the alcohol **3**. The alcohol **3** under high temperature rearranges by a phenyl shift to give the enol **13** which immediately tautomerizes to the ketone **4**.

In order to establish the concertedness of the phenyl shift, two other possible pathways had to be eliminated. The first possibility, an ionic pathway, was eliminated by heating **3** in both isoamyl ether (E = 2.8) and dimethyl sulfoxide (E = 46.6) at the same temperature for the identical amount of time (i.e. 3 hours @ 173°C). Even though these solvents have greatly varied dielectric constants the percentage of rearranged product (determined by chromatography) was identical. The second possibility, a free radical pathway, was eliminated by refluxing **3** in isoamyl ether with a steady stream of oxygen continuously bubbling through the solution. The yield of **4** was identical to that obtained when the reaction was run in the absence of oxygen, indicating that the reaction must not be free-radical in nature since the presence of a radical inhibitor did not effect the yield of **4**. With these possibilities eliminated, the reaction could be classified as a thermally-induced [1,5]-sigmatropic phenyl rearrangement. The phenyl group proceeds by way of a suprafacial shift in accordance with the Woodward-Hoffmann rules.

In 1973, Breslow, Hoffman, and Perchonock[11] looked at the relative reactivities of a series of 5-halocyclopentadienes in relation to a [1,5]-hydrogen migration. They confirmed a definite substituent effect associated with these [1,5]-hydrogen migration when the rates of rearrangement of the C_5-halogen substituted cyclopentadienes were compared to the rate of the parent compound.

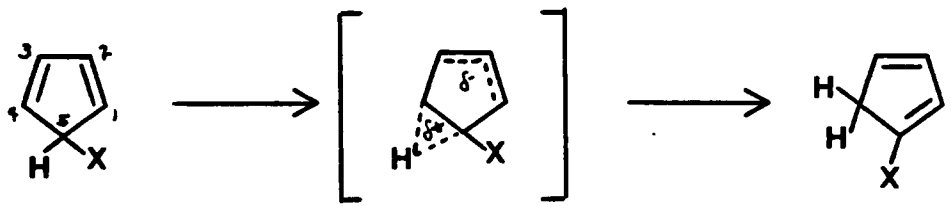

X	Relative Rate
H	1.0
Cl	0.67
Br	0.64
I	0.17

In all cases, halogen substitution slowed the rearrangement relative to the parent compound. These results were consistent with the proposed transition state, since the electron-withdrawing halogen at C-5 effectively destabilizes the $\delta+$ charge at that position in the transition state. Therefore, the destabilizing electron-withdrawal through induction must be predominating over the ability to stabilize through π-donation via resonance.

In 1973, Youssef and Ogliaruso[11] investigated the kinetics of the conversion of 3 to 4. First order kinetics were observed for this rearrangement which is consistent with a sigmatropic rearrangement. The activation energy (E_a) for this process was calculated to be 36.1 ± 3.6 kcal/mol and the entropy of activation ($\Delta S^{\neq}$) to be -7.5 eu.

Youssef and Ogliaruso proposed a transition state for the phenyl migration that was similar to that proposed by McLean and Haynes[8] and Breslow[11] for [1,5]-hydrogen migrations in substituted cyclopentadienols involving partial positive charge formation at the migration origin and

terminus and partial negative charge formation at the opposite end of the molecule.

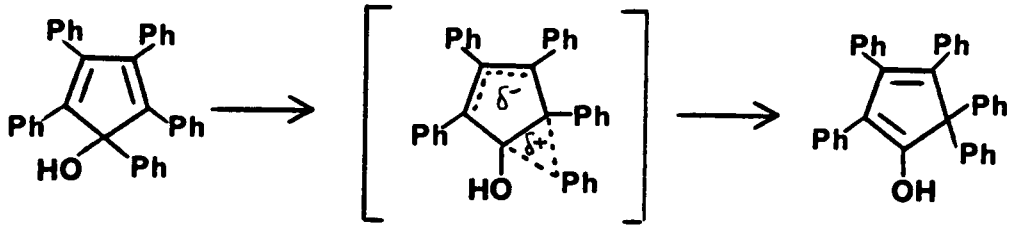

In 1974, McCullough and McClory[13] investigated the migratory aptitudes of substituted aryl groups during the sigmatropic rearrangements of 1,1-diarylindenes to determine the transition state structure for the migration.

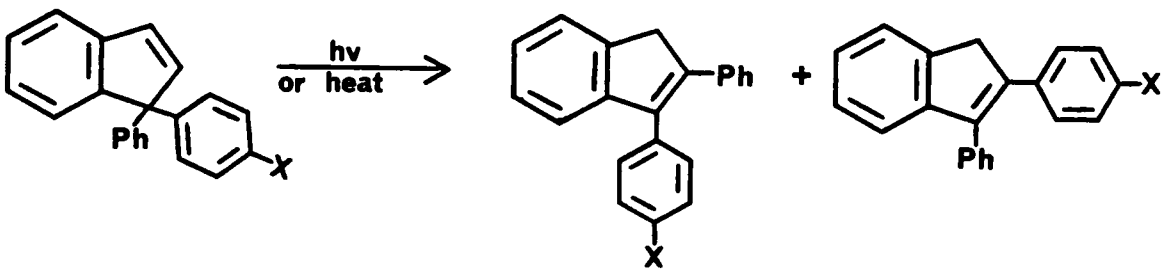

In reviewing the work of the others discussed as well as their own, Ogliaruso felt the 1,2,3,4,5-pentaphenyl-2,4-cyclopentadiene-1-ol **3** system was an excellent system for probing the electronic nature of the sigmatropic rearrangement. A series of substituted phenyl cyclopentadienols could be synthesized and studied to examine the electronic effects operating on the cyclopentadienol ring.

Youssef also initiated this study in 1973, with the synthesis and isomerization of a series of 1-(p-substituted phenyl)-2,3,4,5-tetraphenyl-2,4,-cyclopentadien-1-ols **14**. A comparison of the relative rates of rearrangement would be used to determine the existence (or non-existence) of a linear free energy relationship. The substituents initially examined included p-bromo, p-chloro, p-methoxy and p-tert-butyl. The results of this study were inconclusive. Although the rates

differed, no free energy relationship was observed. However there was concern that the gas chromatographic analysis employed in the study may have affected the results. Theoretically it was possible that further rearrangement of the alcohol **14** to the ketone **15** could occur on the heated column of the GC during the 30 minutes required for elution of the compounds. This possibility would yield measured rates greater than the true rates and activation energies less than the actual values.

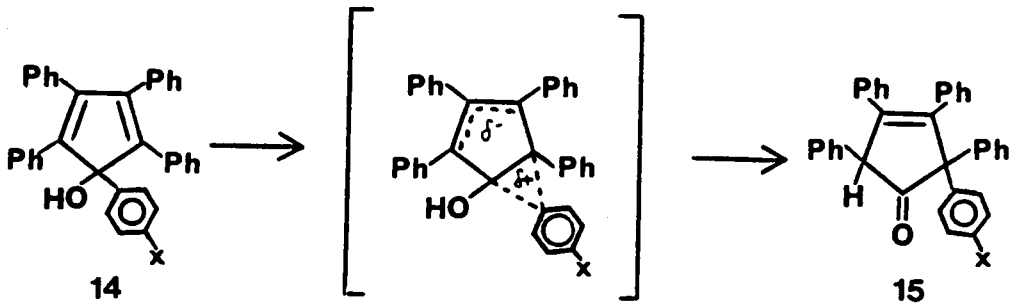

14 15

X = Br, Cl, Me, MeO, H, t-butyl, Ph, CF_3

In 1975, Berg, Ogliaruso and McNair[14] developed a liquid chromatographic procedure which could analyze the alcohol **3**/ketone **4** reaction mixtures.

Equipped with the LC procedure, Oldaker[2] in 1979 was able to extend the series of 1-(p-substituted phenyl) alcohols **14** for kinetic study of the rearrangement initiated by Youssef. These 1-(p-substituted phenyl) cyclopentadienols are exerting their electronic effects on the area of the proposed transition state which bears a $\delta+$ charge. Therefore, electron-donating substituents would be expected to increase the rates of rearrangement by stabilizing the transition state whereas electron-withdrawing substituents should slow the rates of migration. Oldaker's results indicated that the rates of rearrangement were nearly identical and no free energy correlations were observed.

Also in 1979, Perfetti[2] was investigating the kinetics of 3,4-bis (p-substituted phenyl)-1,2,5-triphenyl-2,4-cyclopentadien-1-ols **16** rearranging to the corresponding ketones **17** for any possible electronic effects. With these compounds the substituted phenyls are located along the

π-backbone of the cyclopentadienyl ring in the proposed transition state, an area which bears a δ- charge. In this study, electron-donating substituents would be expected to decrease the rates of rearrangement by destabilizing the transition state, while electron-withdrawing substituents should increase the rates of rearrangement. Perfetti's results found the rates to be essentially the same and no correlation of rate to substituent could be established for this series.

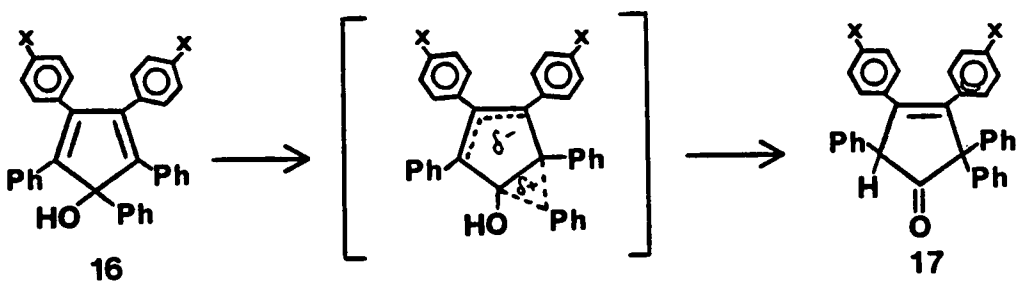

X = Br, Cl, *t*-Bu, Me

In 1982, Brubaker[3] synthesized and thermally isomerized a series of 2- and/or 5-(p- or m-substituted phenyl)-1,3,4-triphenyl-2,4-cyclopentadien-1-ols **18**. In this system more than one migration pathway is possible, therefore substituents should interact with the transition state in a way which would influence the direction of migration.

For the case where Y is electron-donating and X = H, pathway 1 yielding **19** would be preferred since the Y-substituent is stabilizing the $\delta+$ region in the proposed transition state relative to the unsubstituted phenyl. However if the phenyl migrates toward the side where X = 1 (pathway 2), the electron-donating effect of the Y-substituent is forced to interact with a δ- charge region, resulting in destabilization of the transition state. For the case where Y is electron-withdrawing and X = H, pathway 2 yielding **20**, would be favored since the substituent stabilizes the region associated with a δ- charge in the transition state. Migration toward the Y-substituent (pathway 1) would produce a transition state in which the electron-withdrawing substituents would intensify and thereby destabilize the developing $\delta+$ charge.

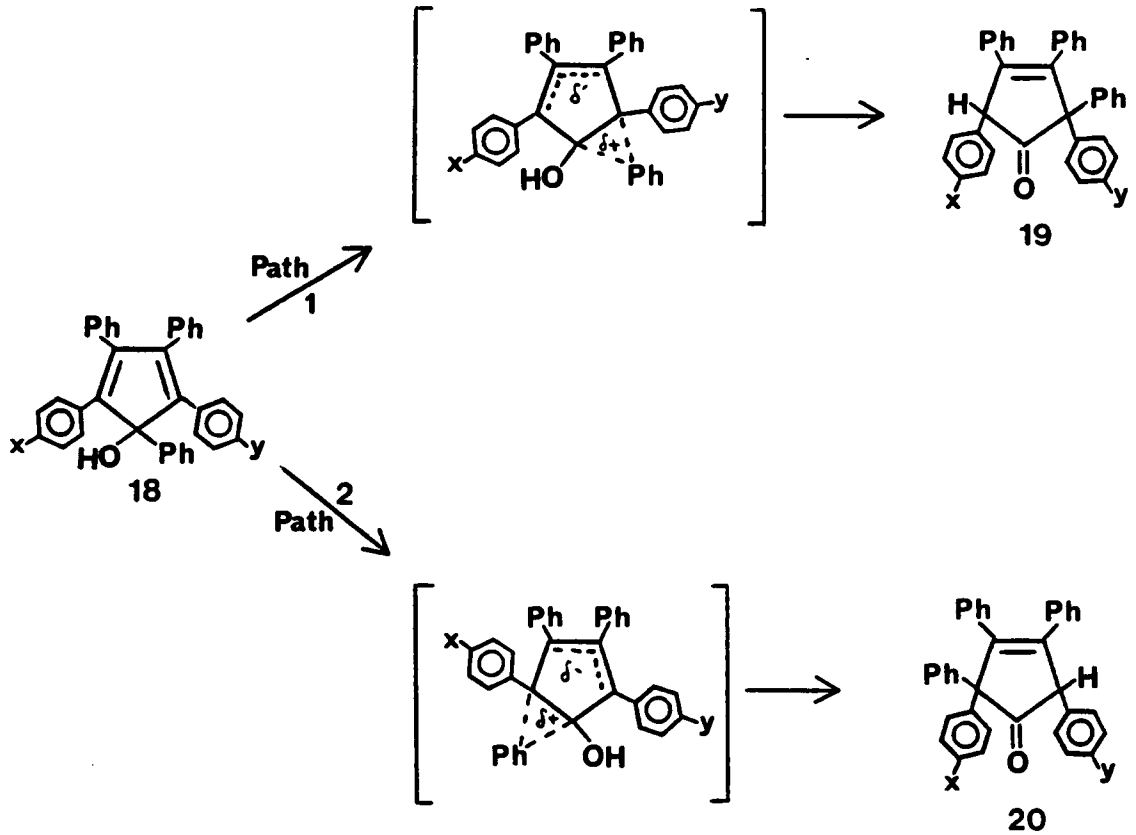

The effects of this system would be even more pronounced in the case where X is electron-withdrawing and Y is electron-donating, since pathway 1 allows the Y-substituent to stabilize the $\delta+$ area of the transition state while the X-substituent could simultaneously stabilize the $\delta-$ area. If the phenyl group attempted to migrate by path 2 it would require a transition state where both $\delta+$ and $\delta-$ charges are destabilized by the electronic effects of the substituents.

Brubaker's results showed very slight differences in the product ratios. Therefore this series of rearrangements were stated as being random in nature and not attributable to either resonance or inductive effects due to the substituents.

Oldaker's, Perfetti's and Brubaker's results allow for the conclusion that the originally proposed transition state does not apply in the pentaphenylcyclopentadienol system. A transition state devoid of charge separation was consistent with their findings. They concluded that this

particular system rearranges by a truly neutral mechanism like that shown below in Scheme II.

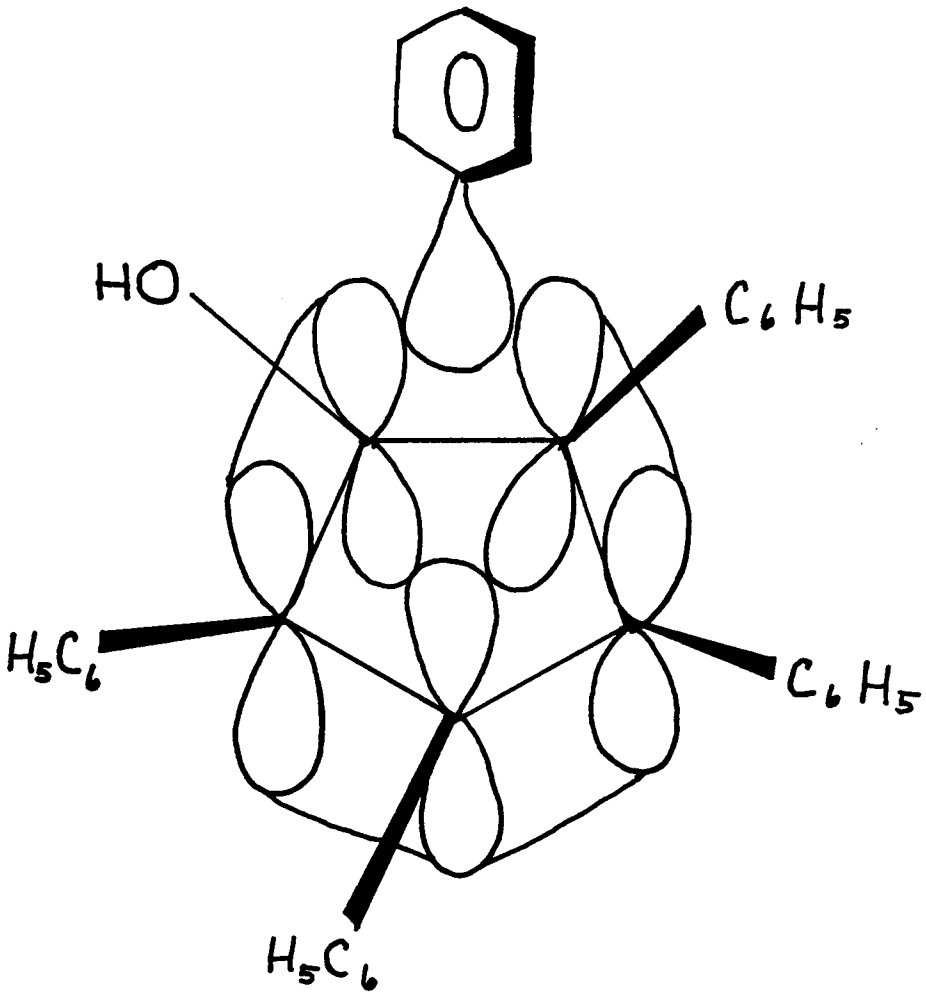

In 1985, Davis[15] investigated the thermal rearrangement of 2,5-dialkyl-1,3,4-triphenyl-2,4-cyclopentadien-1-ols **21** to the corresponding ketones **22**. This work was undertaken to study the effect of steric interactions at the migration terminus on the energy of activation for the phenyl migration. Davis' results indicated that the activation energy remained

essentially the same regardless of the nature of the alkyl substituent.

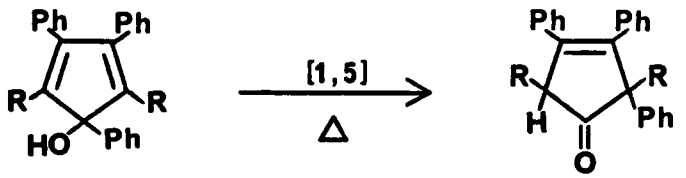

21 22

In 1986, Eagan[4] synthesized a series of 1-substituted-2,3,4,5-tetraphenyl-2,4-cyclopentadien-1-ols 23 and studied the rate of their rearrangement to the corresponding ketone 24.

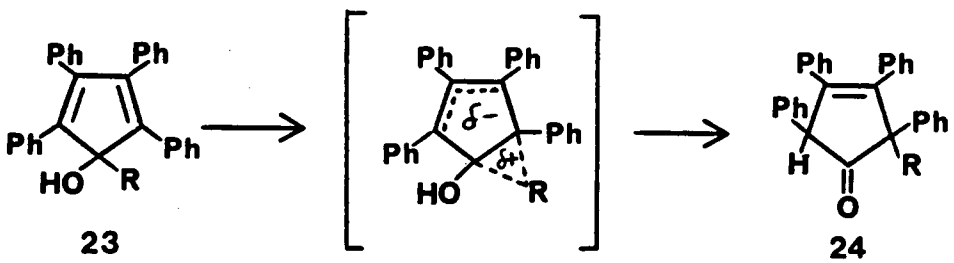

23 24

R = Ph, Ph—C≡C—, CH_2=CH—, *t*-Bu,

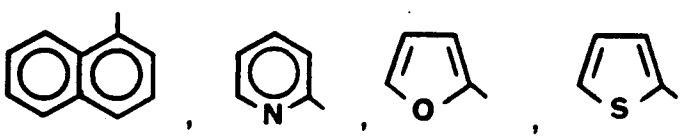

The basis for this study came from the argument that the substituents used by Oldaker, Perfetti and Brubaker did not interact to a significant degree with the $\delta+$ and $\delta-$ charged areas of the proposed transition state due to the distance between the substituents and the cyclopentadienol ring system. It would be more desirable to have the substituents as close as possible to the sites of interaction, since inductive effects fall off with the square of the distance. Eagan's results determined that both electronic and steric effects of the migrating group played a role in the [1,5]-sigmatropic rearrangement of the 1-substituted tetraphenylcyclopentadienols. In this series the substituted phenyl group is exerting its electronic effects in the $\delta+$ region of the proposed transition state. And accordingly, electron donating groups increased the rate of migration whereas electron

withdrawing substituents decreased the rate of rearrangement. Also, in contrast to Davis' work, when comparing groups of similar electronic nature, smaller substituents rearranged faster while bulky groups slowed the migration. This work supported the originally proposed charged separated transition state.

In view of Eagan's results, it would be interesting to study other systems which have a more direct effect on influencing the rate of rearrangement in the transition state on the cyclopentadienyl ring. Thus for this study it was decided to synthesize a series of 1,2,3,4,5-pentaphenyl-2,4-cyclopentadiene alkyl ethers **25** and investigate the rate of rearrangement. This series is again probing the electronic nature of the transition state in the $\delta+$ region. The ether linkages would be expected to exert a stabilizing effect due to their electron donating ability and therefore the rates of rearrangement would be expected to increase. Also since an ether **26** rather than an alcohol is being rearranged the product will be an enol ether **26** instead of a ketone. This fact would also lend more support for the proposed intermediate enol form. In this case, the enol would be essentially "trapped" as an enol ether **26**. Since this system is slightly different than the cyclopentadienol system previously studied it was necessary to go back to the literature to obtain information on any previous relevant work in this area.

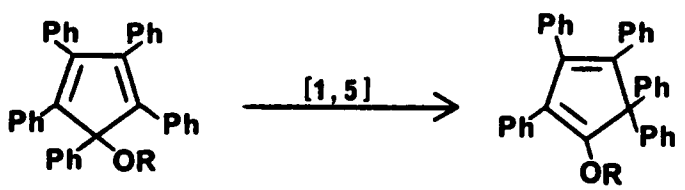

25 **26**

In 1954, Dufraisse, Etienne and Aubry[16] investigated the photooxidation of polyarylcyclopentadienes. In order to prove a point on a suspected mechanism of the photooxidation of polyarylcyclopentadienols they chose to try the photooxidation of 1,2,3,4,5-pentaphenyl-2,4-cyclopentadiene-1-methyl ether **25a**. Surprisingly, after irradiation of **25a**

in air, the product was the photooxide of 1,2,3,4,5-pentaphenylcyclopentadiene **28**. Upon irradiation in the absence of oxygen, the methyl ether **25a** rapidly and quantitatively afforded the hydrocarbon **27** and formaldehyde. Therefore the photooxide of the methyl ether **25a** could not be obtained even in the presence of oxygen since the elimination proceeds rapidly enough to precede photooxidation. They also stated further investigation was underway for this phenomenon.

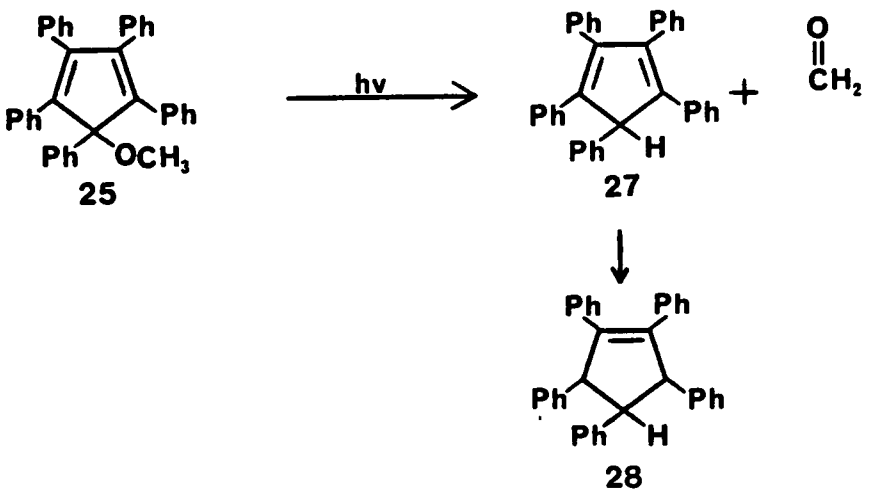

The mechanism proposed[17] for this photolysis reaction is essentially one of a concerted circular electron transfer. The mechanism begins with the photochemical formation of a diradical **29** at the 2 and 5 positions of the ether **25**, followed by one of the radicals capturing one of the hydrogens from the methoxy group, and concludes with the scission of the new diradical **30** into the cyclopentadiene **27** and the aldehyde.

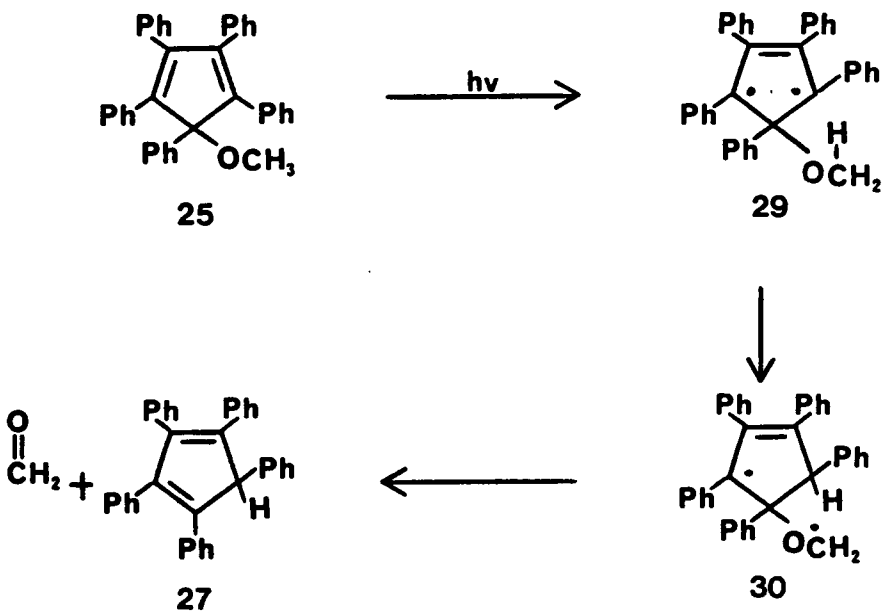

25 29 30 27

Between the years of 1959 and 1962 Dufraisse and his coworkers[18, 19, 20] continued studying the phenomena of this photolysis reaction of the methyl ether **25a** to the hydrocarbon compound **27**. In order to study a less symmetrically substituted ether than **25a** they synthesized a series of p-tolyl (T)-tetraphenyl cyclopentadiene methyl ethers **33a-c**. The ethers were prepared by the action of phenyl lithium on the appropriately substituted tetracyclone **2a-c** to give the corresponding alcohols **31a-c**. The alcohols **31a-c** when treated with thionyl chloride diluted with ether in the presence of pyridine gave the corresponding chlorides **32a-c**. The action of sodium methoxide on the appropriate chloride gives the corresponding methyl ether **33a-c**. The methyl ethers **33a-c** were also obtained by treating the alcohols **31a-c** with methyl iodide in the presence of solid potassium and heating.

Their results of the photolysis of the p-tolyl-substituted-tetraphenylcyclopentadiene methyl ethers **33a-c** were not exactly what had been expected. Although the p-tolyl (T) substituted hydrocarbons **34a-c** were the products of the photolysis, it appears that all 3 isomers of the p-tolyl substituted hydrocarbon **34a-c** were produced for *each* p-tolyl substituted

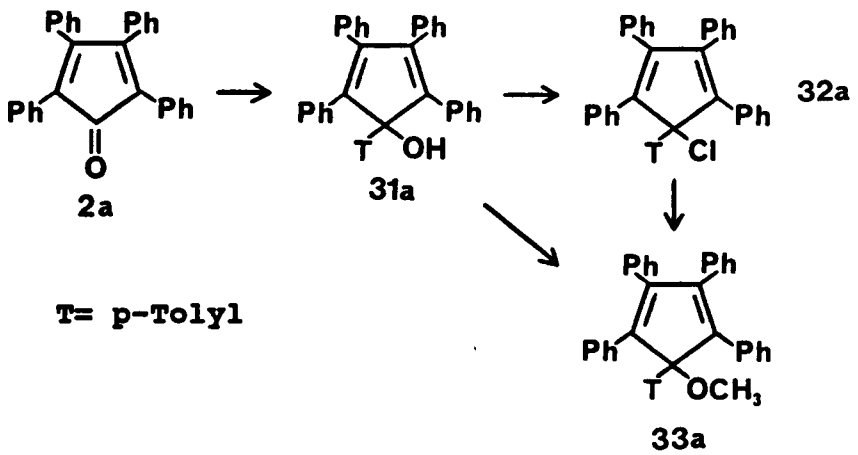
Ph
Ph
Ph
Ph
O
2a
T OH
31a
T Cl
32a
T= p-Tolyl
T OCH3
33a

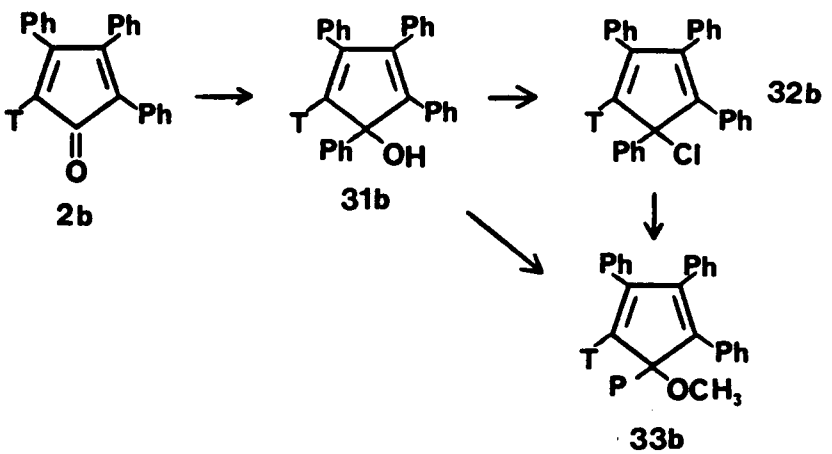
T
Ph
Ph
Ph
O
2b
Ph OH
31b
Ph Cl
32b
P OCH3
33b

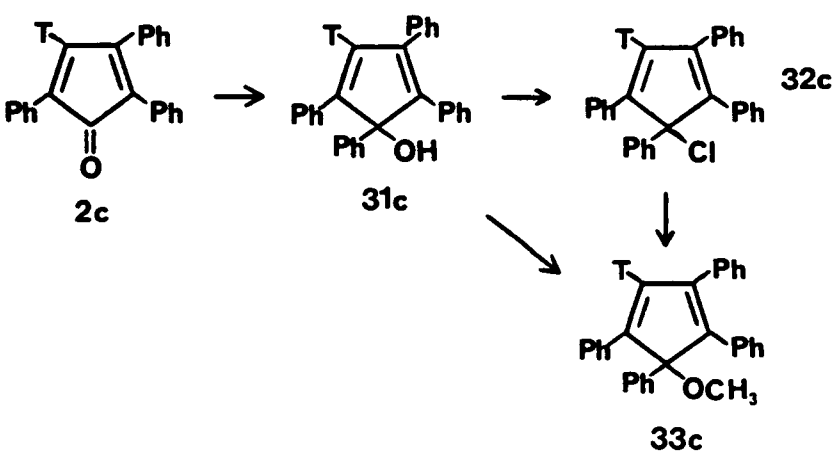
T
Ph
Ph
Ph
O
2c
Ph OH
31c
Ph Cl
32c
OCH3
33c

tetraphenylcyclopentadiene methyl ether 33a-c.

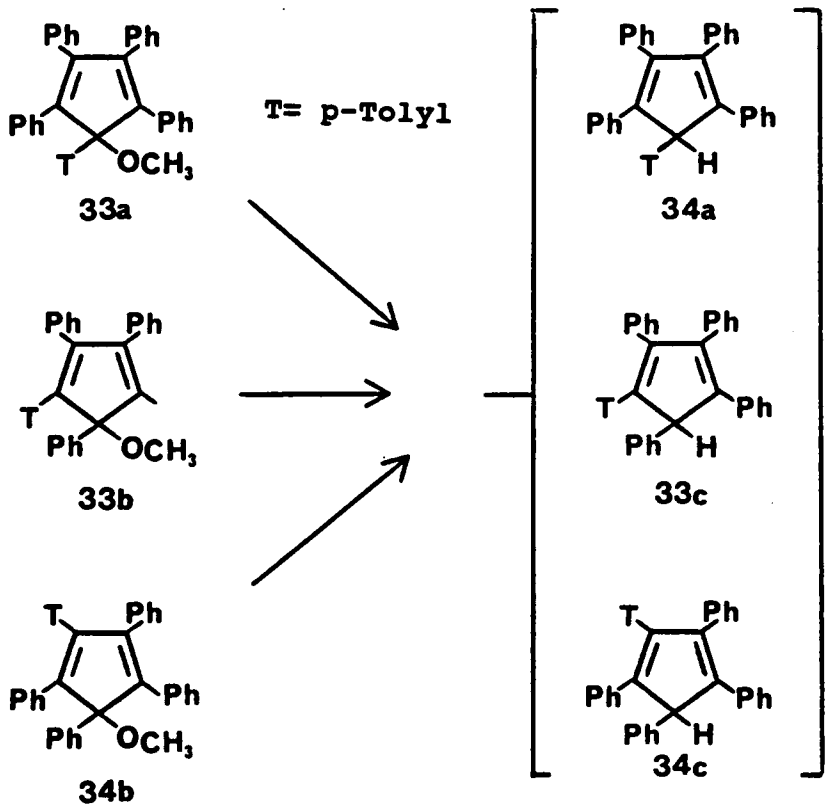

Therefore the mechanism originally proposed by Dufraisse, *et al.* is not acceptable, since mixtures were obtained and they reported that they would continue investigating the photolysis and its mechanism.

In 1963, Dufraisse, Rio, and Liberles[21] investigated the photochemistry of the pentaphenylcyclopentadienol system 3 and a few of the pentaphenyl cyclopentadiene alkyl ethers 25. They report that the compound 3 is photooxidizable and that the photooxide 35 is converted

to the tetraphenylfuran **36** and benzoic acid by heating **35** in acetic acid.

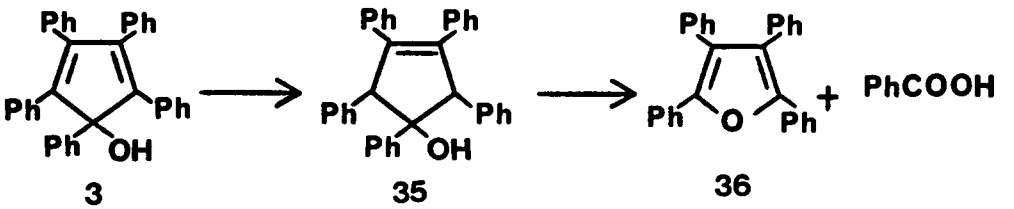

However the methyl **25a** and ethyl **25b** ethers were not susceptible to photooxidation but rather to photolysis giving the hydrocarbon, 1,2,3,4,5-pentaphenylcyclopentadiene **27** and the corresponding aldehyde trapped as the dinitrophenyl hydrazone derivatives.

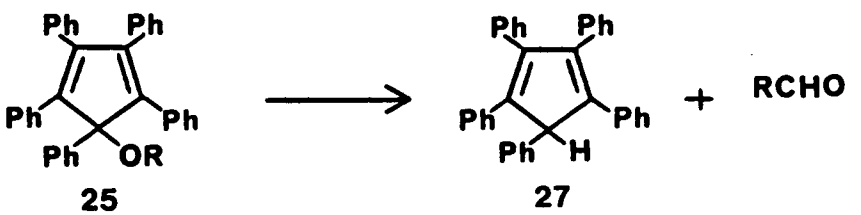

In order to test the generality of this photolysis reaction several other ether derivatives were chosen to study. However, several problems associated with the attempted syntheses of these compounds redirected their attention towards a more detailed study of the preparation of three of the ethers. They report that in using the Williamson reaction the benzyl ether **25** is easily obtained (90% yield) by heating the alcohol **3** and benzyl bromide at 100°, in the presence of potassium hydroxide for 1 hour. They also claim a similar procedure was used to obtain both the methyl **25a** and ethyl **25b** ethers. They also report a faster reaction time in synthesizing the benzyl ether, explained by the reactivity of the halogen employed. However, they report that the corresponding ethers cannot be obtained with the procedure stated above if either benzyl chloride or n-propyl iodide are employed. In these two cases the isomers of the ethers, the α-alkylated (benzyl and

n-propyl) ketones 39 are obtained.

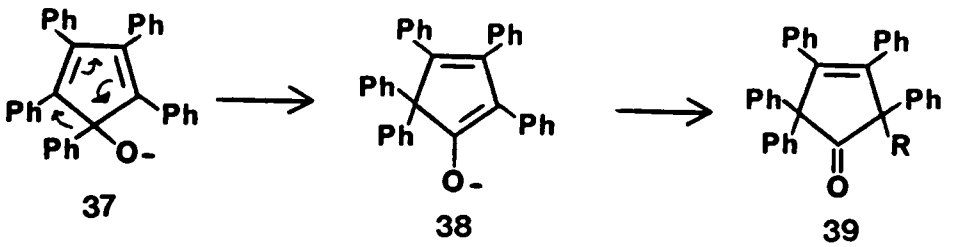

This rearrangement is similar to that of the parent alcohol 3 upon heating at high temperatures (178°). Because n-propyliodide and benzylchloride are slower to react with the enolate 37, the enolate 37 can isomerize to the enolate 38 by migration of phenyl. Enolate 38 is then essentially quenched by the alkyl halide giving the corresponding α-alkylated ketones 39.

In order to synthesize the n-propyl ether a different technique was needed. This method allows the reaction to be run at room temperature thereby decreasing the possibility of any rearrangement taking place. They treated the alcohol 3 with sodium hydride in THF to yield the sodium salt of the alcohol 3 then reacted with n-propyl iodide (85% yield).

No further work by the authors on this particular system was located in the literature. Therefore in examining the information that was available on ethers of the pentaphenylcyclopentadienol system **25a** we decided to first do a comparative synthetic study on the ethers **25a**. The second phase of the project looks at the kinetics of the attempted thermal rearrangement of the ethers **25a**.

Experimental

General Procedures

Melting points were determined on a Thomas-Hoover melting point apparatus and are uncorrected. The infrared spectra were recorded on a Perkin-Elmer 710B spectrophotometer using solution cells with NaCl salt windows. The ^{1}H NMR spectra were recorded at 270 MHz on a Bruker Wp-270SY. The ^{13}C NMR were recorded at 67.4 MHz also on the Bruker WP-270SY. The NMR chemical shifts are reported in parts per million (ppm) for both ^{1}H NMR and ^{13}C NMR relative to tetramethylsilane and chloroform respectively, as the internal standards. Mass spectra were determined on a VG 7070 E-HF mass spectrometer at 70 eV. Elemental analyses were performed by Multi Chem Laboratories, Inc., Lowell, MA. All solvents were purified by standard methods prior to use.

Synthesis of Starting Materials

2,3,4,5-Tetraphenyl-2,4-Cyclopentadien-1-one[22](tetracyclone; **2**). In a 1-liter round bottom flask equipped with a reflux condenser was placed 31.5 g (0.15 mol) of benzil and 31.5 g (0.15 mol) of

dibenzyl ketone and 225 mL of 95% ethanol. The temperature of the solution was raised almost to the boiling point (BP 78°C). A solution of 4.5 g of potassium hydroxide in 22.5 mL of 95% ethanol was slowly added dropwise through the condenser. When the frothing had subsided, the mixture was refluxed for an additional 30 minutes and then cooled to 0°C. The dark crystalline product is visible at the bottom of the solution. The crystalline product was filtered with suction then washed with 3-20 mL portions of cold 95% ethanol. The product was spread on a watchglass and dried in the oven overnight before taking the melting point. The reaction yielded 55.3 g (0.144 mol, 96%) of purple black crystals: mp 217-218°C (lit[22] mp 218-220°C); IR (CCl_4) 1760 cm^{-1} (C=O); mass spectrum, m/z 384 (M^+).

1,2,3,4,5-Pentaphenyl-2,4-cyclopentadiene-1-ol (3). Into a 500 mL three necked round bottom flask equipped with a reflux condenser, nitrogen inlet and addition funnel was placed 0.44 g (0.063 g atoms) lithium in 10 mL of anhydrous ethyl ether. A solution of 4.71 g (0.03 mol) of bromobenzene in 20 mL anhydrous ether was placed in the addition funnel. Approximately 2 drops of pure bromobenzene was added to the reaction flask to initiate the reaction. A slow dropwise addition of the bromobenzene/ethyl ether solution was used in order to maintain a good reflux ratio. After the addition was completed the reaction was allowed to go to completion then heated the solution to the reflux for one half hour. A separate solution of 7.7 g of 2,3,4,5-tetraphenyl-3-cyclopenten-1-one **2** dissolved in 200 mL dry benzene was placed in the addition funnel. The reaction flask was placed in an ice water bath and proceeded with a slow dropwise addition of the tetracyclone/benzene solution. After the addition was completed, the reaction mixture was allowed to stir for an additional hour. The reaction mixture was quenched with 24 g ammonium chloride/200 mL water, then separated. The aqueous layer was extracted twice with 25 mL portions of benzene. The combined organic layers were washed twice with 25 mL portions of water, dried over anhydrous magnesium sulfate, filtered and concentrated. A dark yellow oil resulted which was crystallized by dissolving it in 30 mL benzene then slowly adding 90 mL petroleum ether. The reaction yielded 7.85 g (0.017 mol; 85% yield) of bright yellow crystals of 1,2,3,4,5-pentaphenyl-2,4-cyclopentadien-1-ol: mp 176-177°C (lit[1] mp 176-177°C); IR (CCl_4)

3645 cm^{-1} (O-H); ^1H NMR ($CDCl_3$) δ 6.8-7.7 (m, 25H), 2.45 (s, 1H); ^{13}C NMR δ 90.0 (C-OH); mass spectrum, m/z 462 (M^+).

1-Bromo-1,2,3,4,5-pentaphenyl-2,4-cyclopentadiene (40). Into a 100 mL single-necked round bottom flask equipped with a magnetic stirring bar and a reflux condenser was placed 2.0 g (4.3 mmol) of 1,2,3,4,5-pentaphenyl-2,4-cyclopentadien-1-ol 3, 5 mL dry benzene, 25 mL glacial acetic acid and let stir 20 minutes. To the above soultion 5 mL hydrobromic acid (30 wt % solution in acetic acid; Aldrich Chemical Co.) was added and the solution allowed to stir 1 hour at room temperature. The stirring was continued for an additional hour with gentle heating. Let cool to room temperature then placed in an ice water bath for 15 minutes. During the cooling process, orange crystals formed in the flask. Filtering with suction yielded 2.18 g (4.2 mmol, 96.4%) of orange powder. The crystals were recrystallized by dissolving in 10 mL benzene then slowly adding 25 mL petroleum ether. The recrystallization yielded 2.07 g (0.0039 mol, 91%) of orange crystals of 1-bromo-1,2,3,4,5-pentaphenyl-2,4-cyclopentadiene: mp 191-193°C (lit[21] mp 189-191°C); mass spectrum m/z 524.9 (M^+).

2,2,3,4,5-Pentaphenyl-3-cyclopentene-1-one (4). Into a 100 mL round bottom flask equipped with a reflux condenser, nitrogen inlet and magnetic stir bar was placed 1.5 g (3.25 mmol) of 1,2,3,4,5-pentaphenyl-2,4-cyclopentadien-1-ol 3 and 35 mL decane. The solution was refluxed for 8 hours then cooled to room temperature. The decane was removed on a rotary evaporator. The crude compound was recrystallized from 8 mL benzene and 40 mL petroleum ether yielding 1.16 g (2.5 mmol; 77%) of white crystals: mp 192-193°C (lit[1] mp 194-195°C); IR (CCl_4) 1770 cm^{-1} (C=O); ^1H NMR ($CDCl_3$) δ 6.7-7.5 (m, 25H), 4.94 (s, 1H); ^{13}C NMR δ 212.4 (C=O); mass spectrum m/z 462 (M^+).

1,2,3,4,5-Pentaphenyl-2,4-cyclopentadiene (27). Into a 250 mL three-necked round bottom flask equipped with a reflux condenser, nitrogen inlet, stopper, septum and magnetic stirrer were placed 2.0 g (3.81 mmol) of 1-bromo-1,2,3,4,5-pentaphenyl-2,4-cyclopentadiene **40** and 130 mL dry

tetrahydrofuran. The reaction flask was placed in an ice bath and 0.14 g (3.2 mmol) of lithium aluminum hydride (LAH) was added slowly by small microspatulafuls. The addition of LAH was carried out over 1 hours time. After the addition was completed the solution was allowed to stir for an additional 30 minutes. The reaction mixture was then quenched by adding 1 drop of water and letting stir 20 minutes, adding 2 drops 10% NaOH and stirring for 20 mintues and finally adding 3 drops water and letting stir 30 minutes. The solution was then filtered, dried over anhydrous magnesium sulfate, filtered again and concentrated. The compound was then refluxed in 100 mL benzene incorporating a Dean Stark apparatus to remove water left behind during the quenching process. The reaction yielded 1.5 g (3.36 mmol; 88%) of white crystals: mp 252-254°C (Lit[21] mp 254-255°C); ^{1}H NMR ($CDCl_3$) δ 5.1 (s, 1H); ^{13}C NMR ($CDCl_3$) δ 62.3 (C-H); mass spectrum m/z 446 (M^+).

Synthesis of the Pentaphenylcyclopentadiene Alkyl Ethers

1,2,3,4,5-Pentaphenyl-2,4-cyclopentadiene-1-methyl Ether (25a).

Via 40 and methanol. Into a 100 mL round bottom flask, equipped with a reflux condenser and magnetic stir bar was placed 1.0 g (1.9 mmol) of the bromo compound **40** and 25 mL of dry methanol. (The bromo compound was not very soluble in the methanol). The mixture was refluxed for 5 hours during which time the color of the solution and the undissolved bromo compound changed from orange to bright yellow. The reaction mixture was allowed to cool to room temperature then further cooled by means of an ice bath. The yellow crystals which separated were filtered with suction and allowed to further air dry. The crystals were recrystallized from 5 mL benzene and 25 mL petroleum ether. The recrystallization yielded 0.84 g (1.77 mmol; 93%) of fluorescent yellow crystals; mp 196-198°C (lit[21] mp 197-198°C); IR (CCl_4) 1080 cm^{-1} (-O-CH_3); ^{1}H NMR ($CDCl_3$) δ 6.8-7.7 (m, 25H), 3.5 (s, 3H); ^{13}C NMR δ 95.34 (C-O), 51.35

(-O-CH_3); mass spectrum, m/z 476 (M^+). Anal. Calcd. for $C_{36}H_{28}O$: C, 90.76; H, 5.88. Found: C, 90.51; H, 6.02.

25a via 40 and sodium methoxide. Into a 100 mL three-necked round bottom flask equipped with a reflux condenser, nitrogen inlet, addition funnel and magnetic stir bar was placed 0.51 g (9.5 mmol) of sodium methoxide and 35 mL of dry methanol. The solution was stirred at room temperature until the sodium methoxide dissolved. Meanwhile a separate solution of 1.0 g (1.9 mmol) of 1-bromo-1,2,3,4,5-pentaphenyl-2,4-cyclopentadiene **40** in 25 mL dry benzene was placed in the addition funnel. This solution was slowly added dropwise at room temperature. At the end of the addition the solution was orange in color. The mixture was then refluxed for 3 hours during which the solution turned cherry red. As the solution cooled to room temperature, it became yellow. The reaction mixture was poured into a separatory funnel containing 100 mL of cold water and extracted 3 times with 50 mL portions of benzene. The combined benzene layers were then washed with 100 mL water, dried over anhydrous magnesium sulfate, filtered and concentrated. The resulting yellow oil was crystallized from 50 mL of a 1:5 (by volume) mixture of benzene-petroleum ether. The reaction yielded 0.67 g (1.4 mmol; 74%) of yellow crystals: mp 196-198°C (lit[21] mp 197-198°C); ^{1}H NMR ($CDCl_3$) δ 6.8-7.7 (m, 25H), 3.5 (s, 3H).

25a via 40, Sodium Methoxide and Dimethyl Sulfoxide. Into a 250 mL three necked round bottom flask equipped with a reflux condenser, nitrogen inlet, addition funnel and magnetic stir bar was placed 0.51 g (9.5 mmol) of sodium methoxide and 30 mL dry methanol and 30 mL of dimethyl sulfoxide. The flask was placed in an ice bath and the mixture was allowed to stir until the sodium methoxide dissolved. In the meantime, a solution of 1.0 g (1.9 mmol) of 1-bromo-1,2,3,4,5-pentaphenyl-2,4-cyclopentadiene **40** dissolved in 25 mL of dry benzene was placed in the addition funnel and added dropwise to the sodium methoxide solution. After the addition was completed the ice bath was removed and the solution allowed to warm to room temperature. Next, a heating mantle was placed around the flask and the mixture was refluxed for 3 hours, then the solution cooled to room temperature. The solution was poured into a separatory

funnel containing 200 mL cold water, then extracted 3 times with 50 mL portions of benzene. The combined benzene layers were washed 3 times with 100 mL portions of water. The resulting orange-yellow oil was crystallized from 50 mL of a 1:5 (by volume) mixture of benzene-95% ethanol. The reaction yielded 0.44 g (0.92 mmol; 48%) of yellow crystals: mp 196-198°C (lit[21] mp 197-198°C); ^{1}H NMR ($CDCl_3$) δ 6.8-7.7 (m, 25H), 3.5 (s, 3H).

25a via 3, Potassium t-Butoxide and Methyl Iodide. Into an oven dried 250 mL 3-necked round bottom flask with nitrogen inlet was placed 1.0 g (2.2 mmol) of 1,2,3,4,5-pentaphenyl-2,4-cyclopentadien-1-ol **3** with 40 mL of dry benzene and 40 mL dimethyl sulfoxide and stirred until dissolved. In a separate 50 mL single-necked round bottom flask was placed 0.37 g (3.3 mmol) of potassium t-butoxide with 10 mL dimethyl sulfoxide and 20 mL of t-butyl alcohol and allowed to stir until dissolved. The potassium t-butoxide solution was added to the cyclopentadienol solution, then allowed to stir for 15 minutes. The solution turned a dark cherry color indicating the enolate had been formed. The enolate was quenched with 1 mL (large excess) of methyl iodide and allowed to stir for 1.25 hrs. The reaction mixture was transferred to a separatory funnel containing a dilute acid solution (5 mL conc. HCl in 150 mL H_2O) and the layers were separated. The aqueous layer was extracted with 40 mL of benzene and the combined benzene layers were washed three times with 100 mL portions of water. The solution was dried over anhydrous magnesium sulfate, filtered and concentrated. The resulting yellow oil was crystallized from 50 mL of a 1:5 (by volume) mixture of benzene-petroleum ether. The reaction yielded 0.5 g (1.1 mmol; 48%) of the yellow methyl ether crystals: mp 196-198°C (lit[21] mp 197-198°C); ^{1}H NMR ($CDCl_3$) δ 6.8-7.7 (m, 25H), 3.5 (s, 3H).

1,2,3,4,5-Pentaphenyl-2,4-cyclopentadiene-1-methyl (d_3) Ether (25f)

via 40 and methyl-d_3 alcohol. Into a 50 mL round bottom flask, equipped with a reflux condenser, nitrogen inlet and magnetic stir bar was placed 1.0 g (1.9 mmol) of the bromo compound **40** and 20 g of methyl-d_3 alcohol (Aldrich Chemical Co.). (The bromo compound was not very soluble

in the methanol). The mixture was refluxed for 5 hours during which time the color of the solution and the undissolved bromo compound changed from an orange color to bright yellow. The reaction mixture was allowed to cool to room temperature then further cooled by means of an ice bath. The crystals were recrystallized from 4 mL benzene and 20 mL petroleum ether. The recrystallization yielded 0.80 g (1.66 mmol; 87%) of fluorescent yellow crystals; mp 194-195°C; IR (CCl_4) 1071 cm^{-1} (-O-CD_3); mass spectrum, m/z 479 (M^+).

1,2,3,4,5-Pentaphenyl-2,4-cyclopentadiene-1-ethyl Ether (25b)

via 40 and Ethanol. Into a 100 mL single-necked round bottom flask equipped with a reflux condenser and magnetic stir bar was placed 1.0 g (1.9 mmol) of the bromo compound **40** and 20 mL of dry absolute ethanol. (The bromo compound was only slightly soluble in the ethanol but as the solution heated it dissolved in the ethanol and the solution gradually turned a light yellow color.) The solution was refluxed for 6.5 hours. The solution was allowed to cool to room temperature during which yellow crystals separated. The mixture was further cooled with an ice water bath. The yellow crystals were filtered with suction and dried. The crystals were recrystallized from 100 mL of 95% ethanol. The reaction yielded 0.81 g (1.64 mmol; 86%) of pale yellow crystals: mp 127-128°C; IR (CCl_4) 1078 cm^{-1} (-O-CH_2CH_3); ^1H NMR ($CDCl_3$) δ 6.9-7.7 (m, 25H), 3.6-3.8 (q, 2H), 1.1-1.3 (t, 3H); ^{13}C NMR δ 94.72 (C-O-), 58.78 (-O-CH_2), 15.33 (-CH_3); mass spectrum, m/z 490 (M^+). Anal. Calcd. for $C_{37}H_{30}O$: C, 90.61; H, 6.12. Found: C, 90.54; H, 6.23.

25b via 40 and Sodium Ethoxide. Into a 100 mL three-necked round bottom flask equipped with a reflux condenser, nitrogen inlet, addition funnel and magnetic stir bar was placed 0.65 g (9.5 mmol) of sodium ethoxide and 35 mL of absolute ethanol. The solution was allowed to stir at room temperature until the sodium ethoxide dissolved. Meanwhile a solution of 1.0 g (1.9 mmol) of 1-bromo-1,2,3,4,5-pentaphenyl-2,4-cyclopentadiene **40** dissolved in 25 mL dry benzene was placed in the addition funnel. The solution was slowly added dropwise to the sodium ethoxide solution

at room temperature. As the bromo compound was added the solution became orange in color. The solution was then allowed to reflux for 4 hours during which the color changed from orange to black-brown to greenish blue black to a pale yellowish brown. As the solution cooled to room temperature it turned green. The reaction mixture was poured into a separatory funnel containing 100 mL of water. (During the time period the solution was in contact with water it turned a light yellow color.) The solution was extracted 3 times with 50 mL portions of benzene. The combined benzene layers were then washed with 100 mL water, dried over anhydrous magnesium sulfate, filtered and concentrated. The resulting yellow oil was dissolved in 50 mL of a 1:5 (by volume) mixture of benzene-95% ethanol. The reaction yielded 0.52 g (1.07 mmol; 56%) of yellow crystals: mp 127-128°C; ^{1}H NMR ($CDCl_3$) δ 6.9-7.7 (m, 25H), 3.6-3.8 (q, 2H), 1.1-1.3 (t, 3H).

25b via 40, Sodium Ethoxide and Dimethyl Sulfoxide. Into a 250 mL three-necked round bottom flask equipped with a reflux condenser, nitrogen inlet, addition funnel and magnetic stir bar was placed 0.65 g (9.5 mmol) of sodium ethoxide, 30 mL absolute ethanol and 30 mL dimethyl sulfoxide. The flask was placed in an ice bath and allowed to stir until dissolved. In the meantime, a solution of 1.0 g (1.9 mmol) of 1-bromo-1,2,3,4,5-pentaphenyl-2,4-cyclopentadiene **40** dissolved in 25 mL of dry benzene was placed in the addition funnel and added dropwise to the sodium ethoxide solution. After the addition was completed the ice bath was removed and the solution allowed to warm to room temperature. To insure complete reaction a heating mantle was placed around the flask and the solution allowed to reflux for 4 hours, then cooled to room temperature. The solution was poured into a separatory funnel containing 200 mL cold water and then extracted 3 times with 50 mL portions of benzene. The combined benzene layers were washed 3 times with 100 mL portions of water. The resulting yellow-orange oil was crystallized from 50 mL of a 1:5 (by volume) mixture of benzene-95% ethanol. The reaction yielded 0.31 g (0.63 mmol; 33%) of yellow crystals; mp 126-127°C; ^{1}H NMR ($CDCl_3$) δ 6.9-7.7 (m, 25H), 3.6-3.8 (q, 2H), 1.1-1.3 (t, 3H).

25b via 3, Potassium t-Butoxide and Ethyl Iodide. Into a 250 mL 3 necked round bottom flask with nitrogen inlet was placed 1.0 g (2.2 mmol) of 1,2,3,4,5-pentaphenyl-2,4-cyclopentadiene **3** with 40 mL of dry benzene and 40 mL dimethyl sulfoxide and the mixture was stirred until dissolved. In a separate 50 mL single-necked round bottom flask was placed 0.37 g (3.3 mmol) of potassium t-butoxide with 10 mL dimethyl sulfoxide and 20 mL of t-butyl alcohol and the mixture allowed to stir until dissolved. The potassium t-butoxide solution was added to the cyclopentadienol solution and stirred for 15 minutes. The solution turned a dark cherry color indicating the enolate had been formed. The enolate was quenched with 1 mL (large excess) of ethyl iodide and allowed to stir for 1.25 hours. The reaction mixture was transferred to a separatory funnel containing a dilute acid solution (5 mL conc. HCl in 150 mL H_2O) then the layers were separated. The aqueous layer was extracted with 40 mL of benzene and the combined benzene layers washed 3 times with 100 mL portions of water. The solution was dried over anhydrous magnesium sulfate, filtered and concentrated. The resulting yellow oil was crystallized from 25 mL 95% ethanol. The reaction yielded 0.43 g (0.87 mmol; 40%) of the pale yellow ethyl ether crystals: mp 126-127°C, ^{1}H NMR ($CDCl_3$) δ 6.9-7.7 (m, 25H), 3.6-3.8 (q, 2H), 1.1-1.3 (t, 3H).

1,2,3,4,5-Pentaphenyl-2,4-cyclopentadiene-1-n-propyl Ether (25c)

via 40 and n-Propanol. Into a 100 mL round bottom flask equipped with a reflux condenser and magnetic stir bar was placed 1.0 g (1.9 mmol) of the bromo compound **40** and 25 mL of dry (HPLC Grade) 1-propanol. The reaction mixture was refluxed for 8 hours. As the solution heated up the bromo compound became soluble in the n-propanol and then gradually changed from an orange color to pale yellow. Upon cooling to room temperature yellow crystals may or may not form. However, further cooling the reaction mixture in an ice water bath and initiating crystal growth by scratching the inside of the flask with a glass rod always brought the crystals out of solution. The crystals which separated were filterd with suction and allowed to air dry. The n-propyl ether crystals were recrystallized from 75 mL of 95% ethanol. The reaction yielded 0.82 g (1.59 mmol; 84%) fluorescent pale yellow crystals: mp 142-144°C; IR (CCl_4) 1085 cm^{-1} (-O-nPr); ^{1}H NMR

($CDCl_3$) δ 6.8-7.7 (m, 25H), 3.5-3.7 (t, 2H), 1.4-1.7 (m, 2H), 0.7-0.9 (t, 3H); ^{13}C NMR δ 94.49 (-C-O-), 64.79 (-O-CH_2-), 23.23 (-CH_2-), 10.80 (-CH_3); mass spectrum, m/z 504 (M^+). Anal. Cald. for $C_{38}H_{32}O$: C, 90.48; H, 6.35. Found: C, 90.58; H, 6.49.

25c via 3, Potassium t-Butoxide and n-Propyl Iodide. Into a 250 mL 3-necked round bottom flask with nitrogen inlet was placed 1.0 g (2.2 mmol) of 1,2,3,4,5-pentaphenyl-2,4-cyclopentadien-1-ol 3 with 40 mL of dry benzene and 40 mL dimethyl sulfoxide and stirred until dissolved. In a separate 50 mL single-necked round bottom flask was placed 0.37 g (3.3 mmol) of potassium t-butoxide with 10 mL dimethyl sulfoxide and 20 mL of t-butyl alcohol and the mixture allowed to stir until dissolved. The potassium t-butoxide solution was added to the cyclopentadienol solution and stirred for 15 minutes. The solution turned a dark cherry color indicating the enolate had been formed. The enolate was quenched with 1 mL (large excess) n-propyl iodide and allowed to stir for 45 minutes. The reaction mixture was transferred to a separatory funnel containing a dilute acid solution (5 mL conc HCl in 150 mL H_2O) and the layers were separated. The aqueous layer was extracted with 40 mL of benzene and the combined benzene layers were washed three times with 100 mL portions of water. The solution was dried over anhydrous magnesium sulfate, filtered and concentrated. A yellow oil resulted which was recrystallized from 25 mL of 95% ethanol yielding 0.56 g (1.32 mmol; 56%) of pale yellow crystals: mp 142-144°C; ^1H NMR ($CDCl_3$) δ 6.8-7.7 (m, 25H), 3.5-3.7 (t, 2H), 1.4-1.7 (m, 2H), 0.7-0.9 (t, 3H).

1,2,3,4,5-Pentaphenyl-2,4-cyclopentadiene-1-isopropyl Ether (25d)

via Sealed Tube, 40 and 2-propanol. Into a 7 inch tube was placed 1.0 g (1.9 mmol) of the bromo compound **40** and 15 mL of HPLC grade 2-propanol. The tube was cooled in a Dewar of dry ice and acetone and then sealed. The tube was placed in an oven at 140°C for 24 hours. After the tube was cooled and opened the yellow crystals which separated were filtered with suction. The crystals were recrystallized from 100 mL of 95% ethanol yielding 0.75 g (1.49 mmol; 78%) of pale yellow isopropyl ether crystals: mp 144-145°C, IR (CCl_4) 1085 cm^{-1}; ^1H NMR ($CDCl_3$) δ 6.8-7.7 (m,

25H), 4.0-4.18 (m, 1H), 1.05-1.15 (d, 6H); ^{13}C NMR δ 94.23 (C-O-), 68.40 (-O-CH), 24.36 ($-CH_3$); mass spectrum, m/z 504 (M^+).

25d via 40 and 2-propanol (reflux). Into a 100 mL round bottom flask equipped with a reflux condenser and magnetic stir bar was placed 1.0 g (1.9 mmol) of the bromo compound **40** and 25 mL of dry HPLC grade isopropanol. (The bromo compound was only slightly soluble in the isopropanol until heated.) The solution was allowed to reflux for 1 week. During this time period the solution *very* gradually turned from an orange color to a yellowish color, with the most change being seen between the 4th and 5th days. After 1 week's time the reaction was allowed to cool to room temperature then further cooled by means of an ice water bath. The crystals which separated were filtered with suction and allowed to air dry. The crystals were recrystallized from 95% ethanol which yielded 0.73 g (1.46 mmol; 77%) of isopropyl ether crystals: mp 144-145°C; ^1H NMR ($CDCl_3$) δ 6.8-7.5 (m, 25H), 4.0-4.18 (m, 1H), 1.05-1.15 (d, 6H).

1,2,3,4,5-Pentaphenyl-2,4-cyclopentadiene-1-benzyl Ether (25e).

via 40 and Benzyl Alcohol. Into a 100 mL round bottom flask equipped with a reflux condenser and magnetic stir bar was placed 2.0 g (3.8 mmol) of the bromo compound **40** and 20 mL benzyl alcohol. The mixture was refluxed for 1.5 hours. (During the refluxing period, the bromo compound dissolved in the benzyl alcohol.) As the reaction proceeds, the solution turns from orange to a bright yellow color, but with no visible precipitate. It was necessary to remove the benzyl alcohol by means of a Kugelrohr apparatus. The yellow oil is then crystallized by refluxing in an excess of 95% ethanol. The oil will become crystalline, however the crystals are not totally soluble in the 95% ethanol. The reaction yielded 0.92 g (1.67 mmol; 88%) of pale yellow benzyl ether crystals: mp 180-181°C (lit[21] mp 180-182°C); IR (CCl_4) 1080 cm^{-1} ($-O-CH_2Ph$); ^1H NMR ($CDCl_3$) δ 6.9-7.8 (m, 36H), 4.75 (s, 2H); ^{13}C NMR δ 94.95 (C-O-), 65.73 ($-O-CH_2Ph$); mass spectrum, m/z 552 (M^+).

25e via 3, Potassium t-Butoxide and Benzyl Bromide. Into a 250 mL 3-necked round bottom flask with nitrogen inlet was placed 1.0 g (2.2 mmol) of 1,2,3,4,5-pentaphenyl -2,4-cyclopentadien-1-ol 3 with 40 mL of dry benzene and 40 mL dimethyl sulfoxide and stirred until dissolved. In a separate 50 mL single-necked round bottom flask placed 0.37 g (3.3 mmol) of potassium t-butoxide with 10 mL dimethyl sulfoxide and 20 mL of t-butyl alcohol and allowed to stir until dissolved, then the potassium t-butoxide solution was added to the cyclopentadienol solution and stirred for 15 mintues. The solution turned a dark cherry color indicating the enolate had been formed. The enolate was quenched with 1 mL (large excess) of benzyl bromide and allowed to stir for 45 minutes. The reaction mixture was transferred to a separatory funnel containing a dilute acid solution (5 mL conc. HCl in 150 mL H_2O) and the layers separated. The aqueous layer was extracted with 40 mL benzene and the combined benzene layers washed three times with 100 mL portions of water. The solution was dried over anhydrous magnesium sulfate, filtered and concentrated. The resulting yellow oil was crystallized from 25 mL 95% ethanol which yielded 0.44 g (1.05 mmol; 42%) of the benzyl ether crystals: mp 180-181°C (lit[21] mp 180-182°C); ^{1}H NMR ($CDCl_3$) δ 6.9-7.8 (m, 36H), 4.75 (s, 2H).

2,3,4,5,5-Pentaphenyl-1,3-cyclopentadiene-1-Ethyl Ether (26B). Into a 50 mL round bottom flask equipped with a nitrogen inlet, stopper, septum, and magnetic stir bar was placed 1.0 g (2.17 mmol) of 2,2,3,4,5-pentaphenyl-3-cyclopenten-1-one 4 and 25 mL HPLC grade methylene chloride. The solution was allowed to stir until the compound was completely dissolved, approximately 10 minutes. Next, 0.48 g (4.33 mmol) of potassium t-butoxide was added and allowed to stir 30 minutes. The solution turned an orange red color indicating the enolate was formed. Next, 5.4 mL (5.4 mmol) of a 1.0 M solution of triethyl oxonium tetrafluoroborate (Aldrich Chemical Co.) was added and allowed to stir for 30 minutes. The reaction mixture was then poured into a separatory funnel containing 100 mL water and extracted with 50 mL benzene. The aqueous layer was extracted with 50 mL benzene and the combined organic layers were washed 3 times with 100 mL portions of water. The organic layers were then dried over anhydrous magnesium sulfate, filtered and concentrated. The resulting yellow oil was crystallized by dissolving in 95% ethanol

(~25 mL), cooling to room temperature, then adding water dropwise to precipitate the pale yellow ethyl enol ether crystals. The reaction yielded 0.75 g (1.54 mmol; 71%) of the ethyl enol ether: mp 125-126°C; IR (CCl_4) 1075 cm^{-1} (-O-CH_2CH_3); ^1H NMR ($CDCl_3$) δ 6.8-7.7 (m, 25H), 3.2-3.3 (q, 2H), 0.55-0.65 (t, 3H); ^{13}C NMR δ 167.17 (=C-O-), 69.11 (-O-CH_2), 14.80 (-CH_3); mass spectrum, m/z 490 (M^+).

2-Benzyl-2,3,4,5,5-pentaphenyl-2-cyclopenten-1-one (39e). Into a single-necked 50 mL round bottom flask equipped with a nitrogen inlet and magnetic stir bar was placed 0.5 g (1.08 mmol) of 2,2,3,4,5-pentaphenyl-3-cyclopentene-1-one **4** and 25 mL THF and the solution stirred until dissolved, approximately 10 minutes. Next, 0.24 g (2.2 mmol) of potassium t-butoxide was added and the solution allowed to stir for 30 minutes. With the cherry-colored enolate being formed, then ~0.26 mL (2.2 mmol) of benzyl bromide was added and stirred for 1 hour. The solution was poured into a separatory funnel containing 100 mL water and extracted with 50 mL benzene. The aqueous layer was extracted once with 50 mL benzene. The combined benzene layers were washed 3 times with 100 mL portions of water, dried over anhydrous magnesium sulfate, filtered and concentrated. The resulting yellow oil was crystallized from 5 mL benzene and 25 mL petroleum ether which yielded 0.25 g (0.51 mmol; 47%) of white crystals: mp 164-166°C; IR (CCl_4) 1760-1775 cm^{-1} (C=O); ^1H NMR ($CDCl_3$) δ 6.8-7.7 (m, 36H), (dd, 2H); ^{13}C NMR δ 212 (C=O), 67.5 (-CH_2Ph); mass spectrum, m/z 552 (M^+).

Kinetic Investigation

To study the kinetics of the thermal rearrangement of the ethers, the following procedures were performed:

All glassware and parts of apparatus that could come into contact with the reaction mixture were washed (0.5 M HCl), rinsed with distilled water and dried in an oven overnight (105°C). The glassware was assembled and cooled to room temperature under a nitrogen atmosphere. Due to

the high temperatures being used, the glass joints were wrapped with teflon tape instead of using stopcock grease.

Into a 50 mL, three-necked round bottom flask equipped with a reflux condenser, nitrogen inlet, septum inlet adapter, thermometer adapter and thermometer, and magnetic stir bar was placed 35 mL of diphenyl ether. The flask was placed in an electrical heating mantle which was attached to a THERM-O-WATCH L7/600 temperature controller and the solvent raised to the desired temperature for the rearrangement. In addition, to minimize heat loss, the flask was further insulated by wrapping with electrical heating tape and several layers of aluminum foil. The electrical heating tape was also connected to a POWERSTAT variable autotransformer. The THERM-O-WATCH and POWERSTAT were adjusted to maintain a stable temperature range of ± 0.5°C. Once the desired temperature had stabilized, 0.43 mmol of the ether was added to the solvent and the timer was started.

During the rearrangement, 0.4-0.5 mL samples were removed by means of a syringe, placed in vials and frozen, to prevent further decomposition, until the samples could be analyzed. Each sample was analyzed by High Performance Liquid Chromatography (HPLC) using a Waters Association M6000 Chromatographic Pump in combination with a Waters series 440 Absorbance Detector operating at 254 nm. For the ethers **25a-c** and **25f** a hexane/THF mixture (Appendix L) with a flow rate of 1 mL/min. was used, and the separation was performed on a Micro Pak NH_2-10 column (30 cm x 4 mm). However, the benzyl ether **25e** had slightly different solubility properties along with the fact that its thermolysis produced the hydrocarbon compound **27** *and* the more polar benzyl ketone **39e**. Therefore, reverse phase HPLC was required in order to analyze the thermolysis of the benzyl ether. This separation used a methanol/THF/water mobile phase (Appendix L) with a flow rate of 2 mL/min and was performed on a radial-pak C-18 column. The spectra were recorded on a Linear Instruments Corp. Model 250/MM chart recorder recording at 0.5 cm/min. and the resulting peak heights were used to measure the concentration.

The concentration of each ether was obtained by comparison with a calibration curve constructed from peak heights of known concentration. The points on the calibration curve were the result of triple injections. The concentration of product (hydrocarbon compound **27**) was also

compared with a calibration curve, again constructed from peak heights of known concentration and also compared with its rate of decomposition. The points for the kinetic runs were the result of averaging duplicate injections. The results of the kinetic investigation are summarized graphically in Figures 1-47 and in tabular form in Appendix E.

Results and Discussion

Synthesis of Pentaphenylcyclopentadiene Alkyl Ethers

For this investigation, six 1,2,3,4,5-pentaphenyl-2,4-cyclopentadiene alkyl ethers **25a-f** were prepared by traditional methods appearing in the literature and by solvolysis in order to determine the best method for synthesizing these ethers. The results are illustrated in Tables I-III. The Williamson reaction[23] is usually considered the best general method for the preparation of symmetrical or unsymmetrical ethers. The Williamson synthesis of ethers consists of an S_{n2} reaction of a sodium alkoxide with an alkyl halide. However, in this particular system, the possibility of a rearrangement can occur once the anion has been generated in the cyclopentadienol system.

The first attempt at synthesizing the desired ethers using the Williamson reaction (Table I) uses the cyclopentadiene system as the "alkyl halide" **40** and the "R" substituent as the "alkoxide". The overall reaction proceeds fairly smoothly, however the low yields are most likely due to losses associated with extractions and washes used to eliminate excess alkoxide and also some loss is attributed to the recrystallization process. The same reaction was also run in the presence of dimethyl sulfoxide (DMSO) (Table I), a polar aprotic solvent which generally strongly favors S_{n2} reactions. In these cases, however, the isolated yields were even lower than in the absence of DMSO. This again is probably due to losses associated with excess water washes of the reaction

mixture to eliminate excess alkoxide as well as the DMSO. Also, the possibility of side reactions occurring between the DMSO and the alkyl halides is present.

The second method used for comparison, illustrated in Table II, was again a variation of the Williamson ether synthesis, however this time the alkoxide was the cyclopentadienol 3 system and the "R" substituent came from the alkyl halide. In these cases, the yields are considerably lower due to generation of the "alkoxide" from the 1,2,3,4,5-pentaphenyl-2,4-cyclopentadienol system 3. It has previously been shown that 3 in the presence of base can lead to rearrangement in the system. Also the nature of the enolate formed lends itself to the possibility of both C- and O- alkylated products. Here again, there are also losses associated with water washes and recrystallization.

The third and most efficient route to these ethers is illustrated in Table III. By using the bromo compound **40** in a solvolysis reaction with the appropriately substituted alcohol, the corresponding ether, which precipitates out of solution after cooling, is produced in relatively high yield even after recrystallization. The reaction can be classified as either an S_{N2} or $S_{N2'}$ type mechanism. Although technically different from the Williamson reaction, some consider this type of reaction a variation of the Williamson reaction. The lower yield of the isopropyl ether synthesized from **40** and isopropyl alcohol (a secondary alcohol) is due to the fact that some of the elimination product (the hydrocarbon **27**) was formed during the course of the reaction. This solvolysis type Williamson ether synthesis was also attempted using t-butyl alcohol and phenol. However, the only isolated product (as might be expected) was the elimination product (hydrocarbon **27**).

The initial thoughts anticipating the outcome of this project were based somewhat on work done by Robert Eagan.[4] His work had supported the charge separated transition state originally proposed by Youseff and Ogliaruso.[1] And, it was from these results that it was felt that by showing further stabilization of the transition state in close proximity to the area of positive charge with an electron donating group, such as an ether group, that the 1,5-sigmatropic phenyl migration would occur at an accelerated rate. If this occurred, the resulting product would be an enol ether. Since

there would be

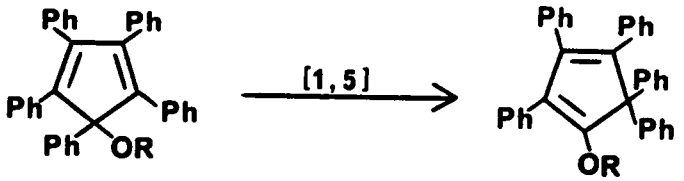

25 26

essentially minor differences in structure, the difficulty would be in determining whether the reaction had proceeded or not. Therefore, independent syntheses were needed for the enol ethers. All the syntheses centered around generation of the enolate **38** from the unconjugated ketone **4** and quenching with an electrophile under conditions which would favor O-alkylation.

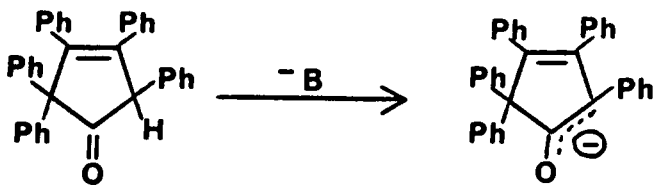

4 38

With this particular ambident nucleophile C-alkylation appears to predominate. By considering just the structure of the enolate, it is easy to explain this fact. First of all, carbon, being less electronegative than oxygen, will be more polarizable, and therefore it follows that it should also be more nucleophilic.[24] Also, in terms of stabilization of the enolate, although oxygen (being electronegative) can stabilize a negative charge, the carbon of the enolate has an electron withdrawing phenyl group which helps to pull the negative charge in the direction of the carbon atom. It is also known that in cases where an alkyl halide is the alkylating agent, C-alkylation usually predominates. Since the nature of the enolate alone will produce C-alkylation other factors were required to force O-alkylation.

If one considers the hard and soft acid base principle (HSAB), it offers an explanation of the results. The HASB principle basically states that hard acids bind strongly to hard bases and soft acids bind strongly to soft bases and that the terms acid and electrophile, base and nucleophile, respectively, can be used interchangeably.[25]

The alkylating agents which were used were methyl iodide, benzylbromide and triethyloxonium tetrafluorborate. If these alkylating agents are ranked as electrophiles in terms of being hard acids, they would have the following order: MeI < $PhCH_2Br$ < $Et_3O^+\bar{B}F_4$. Both methyl iodide and benzyl bromide gave predominately C-alkylation. Both were also used in the reaction in the presence of dipolar aprotic solvents such as dimethyl sulfoxide and N, N^1-dimethyl-N,N^1-propylene urea (DMPU).[26] However, again C-alkylation was the predominent product, which may very well have been anticipated with the use of MeI, but surprisingly the benzyl cation was still not a strong enough acid (electrophile) even in the presence of DMPU to give significant O-alkylation. Only in the case where triethyloxonium tetrafluoroborate, a very hard acid (strong electrophile) was used did O-alkylation predominate, and in most runs exclusively.

Therefore, from the synthesis of the ethyl enol ether and also considering the other cases where small amounts of O-alkylation occurred, it was discovered that the starting allylic ethers **25a-f** could be distinguished from the anticipated rearranged products, the enol ethers **26**, by ^1H NMR. Due to the arrangement of the phenyl groups (especially on C-5) in the enol ether the protons of the ether group experience a shielding effect and therefore their signals appear upfield from those of the starting allylic ethers.

Table I.

Synthesis of Pentaphenylcyclopentadiene Alkyl Ethers
via Williamson Ether Synthesis-A

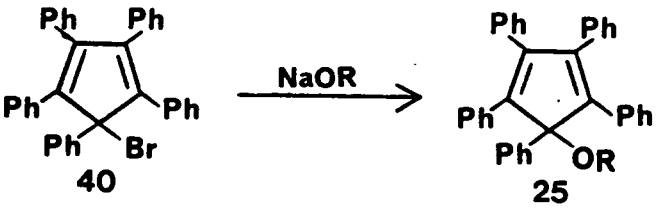

R	Ether	% Yield	MP (°C)
$-CH_3$	25a	74	196-198
$-CH_2CH_3$	25b	56	127-128
↓ + DMSO			
$-CH_3$	25a	48	196-198
$-CH_2CH_3$	25b	33	127-128

Table II.

Synthesis of Pentaphenylcyclopentadiene Alkyl Ethers
via Williamson Ether Synthesis-B

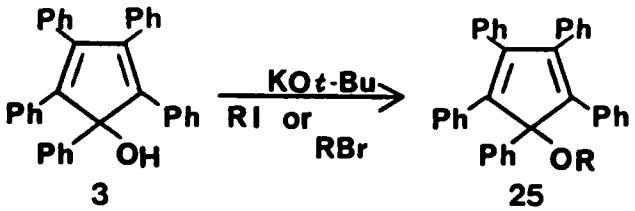

3 25

R	Ether	% Yield	MP (°C)
$-CH_3$	25a	48	196-198
$-CH_2CH_3$	25b	40	127-128
$-CH_2CH_2CH_3$	25c	30	142-144
$-CH_2Ph$	25e	43	180-181

Table III.

Synthesis of Pentaphenylcyclopentadiene Alkyl Ethers via Solvolysis

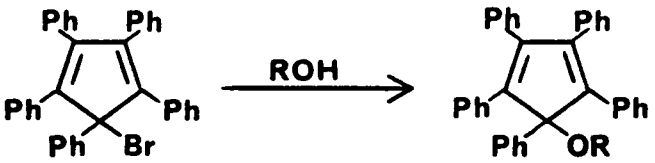

40 25

R	Ether	% Yield	MP (°C)
$-CH_3$	25a	93	196-198
$-CH_2CH_3$	25b	86	127-128
$-CH_2CH_2CH_3$	25c	84	142-144
$-CH(CH_3)_2$	25d	78	144-145
$-CH_2Ph$	25e	88	180-181
CD_3	25f	90	196-198

Kinetic Investigation

The results of the thermolysis of the 1,2,3,4,5-pentaphenyl-2,4-cyclopentadiene alkyl ethers are graphically displayed in Figures 1-32 and the data summarized in Tables IV-XXXIII (Appendix E). The results obtained, but not anticipated with the 1,2,3,4,5-pentaphenyl-2,4-cyclopentadiene alkyl ethers (**25a-f**) were the relative ease with which these allylic ethers could undergo a retro ene elimination. It was determined that the major product of the thermolysis of allylic ethers (**25a-f**) is the hydrocarbon compound (**27**).

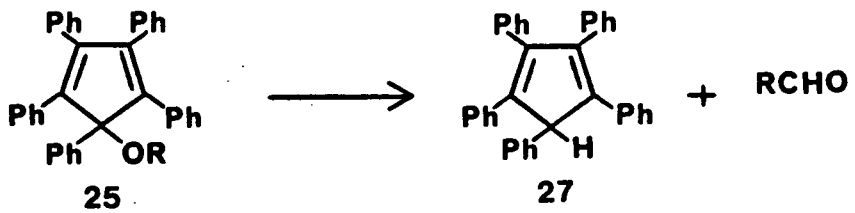

Much work has been reported on this type of elimination in the case of esters[27], but little study has been done with ethers until approximately the last 20 years.[28-30] Most reported cases[28-30] of retro ene eliminations occurred in small allylic ethers and have been observed to occur in the gas phase at extremely high temperatures (400-500°C). The anticipated product of the thermolysis of these allylic ethers (**25e-f**) was the enol ether (**26**) being produced by a [1,5]-sigmatropic phenyl shift. That result would have lent more support to the proposed[1] intermediate enol structure since enol ethers would not immediately tautomerize to a ketone as in the case with the alcohols. It was also expected, based on Robert Eagan's[4] work, that the [1,5]-sigmatropic phenyl shift would occur at a faster rate due to stabilization of the transition state by the electron-donating ether group. However, the surprising results of this thermolysis can be explained by taking a closer look at the structural features of this molecule and comparing them with the known information on retro ene reactions, specifically in allylic ethers, to learn how structure facilitated the retro ene elimination to occur in the 1,2,3,4,5-pentaphenyl-2,4-cyclopentadiene alkyl ether system (**25a-f**).

The general process shown below[31] illustrates the well known ene reaction of which the

reverse process is the retro ene reaction or elimination. The retro ene process

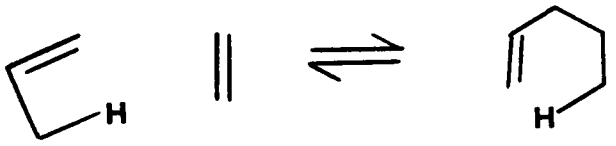

is considered to bear a close resemblence to the [1,5]-sigmatropic shift of hydrogen. The main difference being that in the retro ene reaction, a σ bond breaks instead of a π bond. The temperature required varies widely depending upon the substitution pattern. However, on thermodynamic grounds[32], the retro ene reaction is favored by increasing temperature. The process is also favored by electron-withdrawing substituents on the hydrogen acceptor (enophile), by geometrical constraints that hold the components in favorable relative positions, and by strain in the double bonds. Since the retro ene reaction is considered a concerted cyclic elimination, the following criteria[33] must also be met:

- stereospecific in cis sense
- unimolecular
- shows deuterium isotope effect
- and generally a negative entropy of activation is observed.

An example of a heteroatom analog of the retro ene reaction is illustrated below[32].

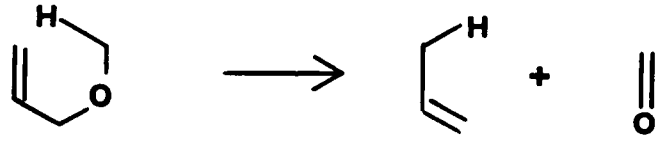

This process would clearly be kinetically controlled and first order kinetics would be expected. This retro ene cleavage of allylic ethers constitutes the microscopic reverse of the "wrongly oriented"

addition of a carbonyl compound to an ene component and has been studied by several investigators. The mechanism is also considered closely related to the Ei mechanism, although not entirely analogous. One particular system investigated by G. Ohloff[34] and illustrated below, goes through an ene cleavage which is presumably facilitated by the rigidity of the allylic system, which allows the transition state to be reached more readily.

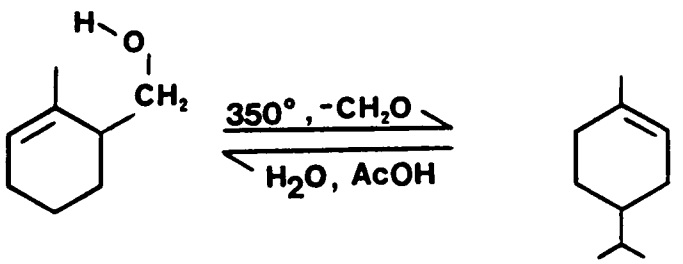

By looking at the 3-dimensional structure of the 1,2,3,4,5-pentaphenyl-2, 4-cyclopentadiene alkyl ether shown below and considering its substitution pattern and its geometrical restraints, we can see why the retro ene elimination occurred in this system in preference to the [1,5]-sigmatropic phenyl shift which was expected.

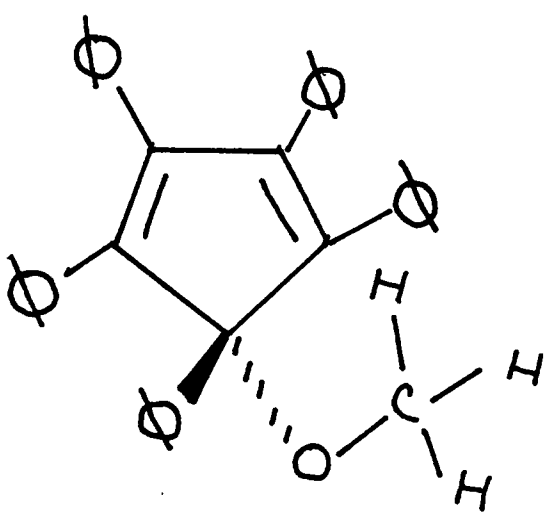

The pentaphenyl cyclopentadiene alkyl ether system is obviously a fairly rigid system due to the five membered ring, the double bonds and also the steric factor of all the phenyl substituents. The diagram also shows that the α-hydrogen of the methyl group is in very close proximity to the C-5 carbon of the cyclopentadiene ring (numbering through the π system). This C-5 carbon to which the hydrogen will be transferred also has an electron-withdrawing phenyl substituent which

will further favor the retro ene reaction. The reaction is also unimolecular and has displayed first order kinetics (Figures 1-32). In 2 cases, very slight traces of the anticipated enol ether from a [1,5]-sigmatropic phenyl shift occurred. However, the products were produced in less than 5 percent yield and were observed to occur only in a few cases. Detection of the enol ether products was difficult, because their retention time in the HPLC corresponded closely to the retention time of the peak resulting from the decomposition of the hydrocarbon compound (**27**). In order to help establish the mechanism for this elimination reaction, the deuterated methyl ether (**25f**) was synthesized and then thermolyzed in the same manner as the other ethers. A primary kinetic isotope effect was observed (illustrated below) indicating that the breaking of a carbon-(α)-hydrogen bond of the alkyl moiety of these "alkyl allylic" ethers is involved in the transition state. A primary isotope effect can be detected by kinetic measurement only if the bond to the isotopically labeled atom is broken during or before the rate determining step[35]. In the case of the allylic ethers, we have concluded that the C-D or C-H bond must be broken during the rate determining step since we are dealing with a concerted cyclic process.

Temperature°C	k_H/k_D
240	2.60
225	2.23
210	3.09

The last criteria needed in order to establish our mechanism as a concerted cyclic elimination was that the processes generally showed a negative entropy of activation. This result is illustrated below for each substituent and the calculations are listed in Appendix J.

Ether	ΔS
methyl (**25a**)	-3.7
ethyl (**25b**)	-3.48
n-propyl (**25c**)	-17.8
benzyl (**25e**)	-7.8

Due to the fact that very slight amounts of enol ether were detected in some cases (possibly produced by a parallel pathway) led us to use the appearance of hydrocarbon (**27**) as a means of determining the rate of this retro ene reaction. However, the hydrocarbon compound (**27**) apparently decomposed at the temperatures used and during the times being studied. These facts made determination of the *exact* rate constants very difficult. It was necessary to consider the reaction as a consecutive first order reaction[36].

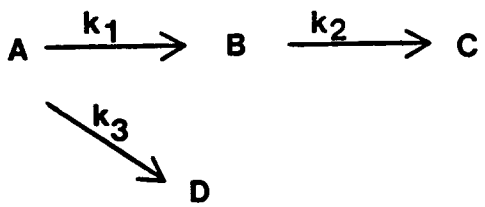

where A = starting allylic ether (**25a-f**)

B = hydrocarbon compound (**27**)

C = decomposition products

D = enol ether

This also made it necessary to perform an independent study of k_2, the decomposition rate of the hydrocarbon compound (**27**). By comparing the rate of disappearance of the allylic ether (k_1 + k_3) with the rates of formation (k_1) and disappearance (k_2) of hydrocarbon compound (**27**), as in Figures 21-32, we illustrated that mass balance had essentially been achieved within reasonable error limits and that k_3 could be considered approximately equal to zero. In order to help illustrate our conclusions, Figures 33-41 show comparisons of the experimentally obtained data points with a theoretical plot generated from the calculated rate constants based on the assumption stated above ($k_3 = 0$). These graphs imply that we have identified the major rearrangement (or reaction) occurring in the themolysis of the allylic ethers **25a-c** . Realizing that this approach introduces some error into the kinetic data, we are only able to consider broad generalizations for this retro ene elimination based on:

$$k_{obs} = k_1 \text{ at its maximum value}$$

$$k_{obs} = \text{disappearance of starting allylic ether (25a-f)}$$

The activation energies are in very close proximity to one another which is in good agreement with a cyclic, concerted transition state (Appendix I).

The benzyl ether **25e**, however, disappears at a much faster rate than the other ethers due to another very strongly competing pathway. Thermolysis of the benzyl ether (**25e**) yields not only the hydrocarbon compound (**27**) but also the benzyl ketone (**39e**) (Appendix I).

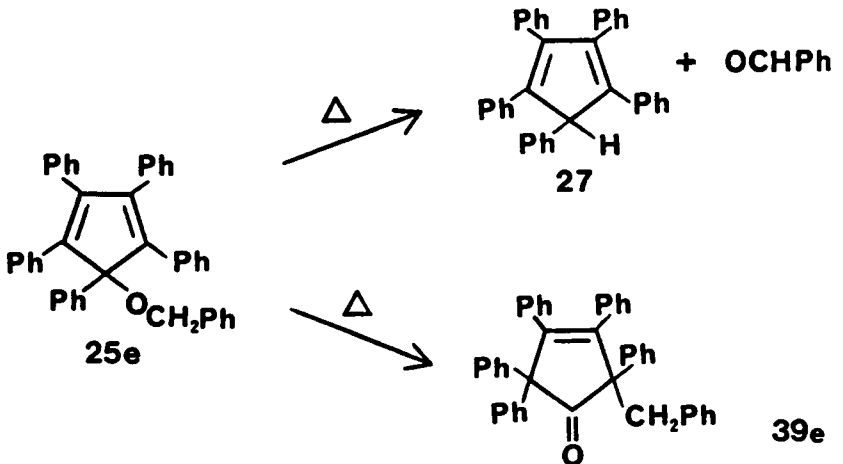

To help illustrate these conclusions, Figures 42-47 show comparisons of the experimentally obtained data with theoretically generated plots. These graphs again help prove the accuracy of our conclusions within reasonable experimental error. This competing pathway probably occurs by formation of the fairly stable benzyl cation ($\pm$ *CH_2Ph*) which then reattacks the molecule which has rearranged to the more stable enolate (as discussed in the synthetic portion of the Results and Discussion section of this thesis) giving the benzyl ketone (**39e**). (A table summarizing the calculated [B] max and t_{max} for each of the rearrangements is located in Appendix H).

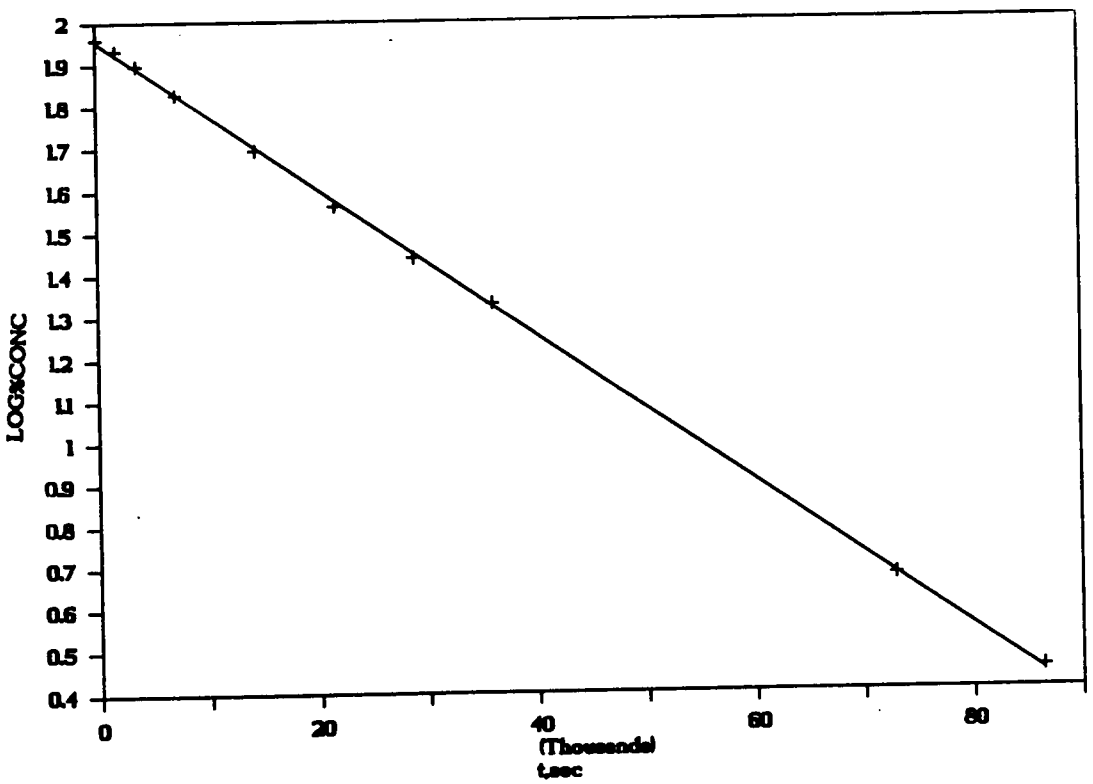

k

plotting log (% conc) versus time	slope = -1.75×10^{-5}
k = -2.303 (slope)	y intercept = 1.96
$k = 4.04 \times 10^{-5} sec^{-1}$	corr = 0.999

Figure 1. First-order plot of the thermolysis of 1,2,3,4,5-pentaphenyl-2, 4-cyclopentadiene-1-methyl ether (25a) @ 240.0 ± 0.5°C.

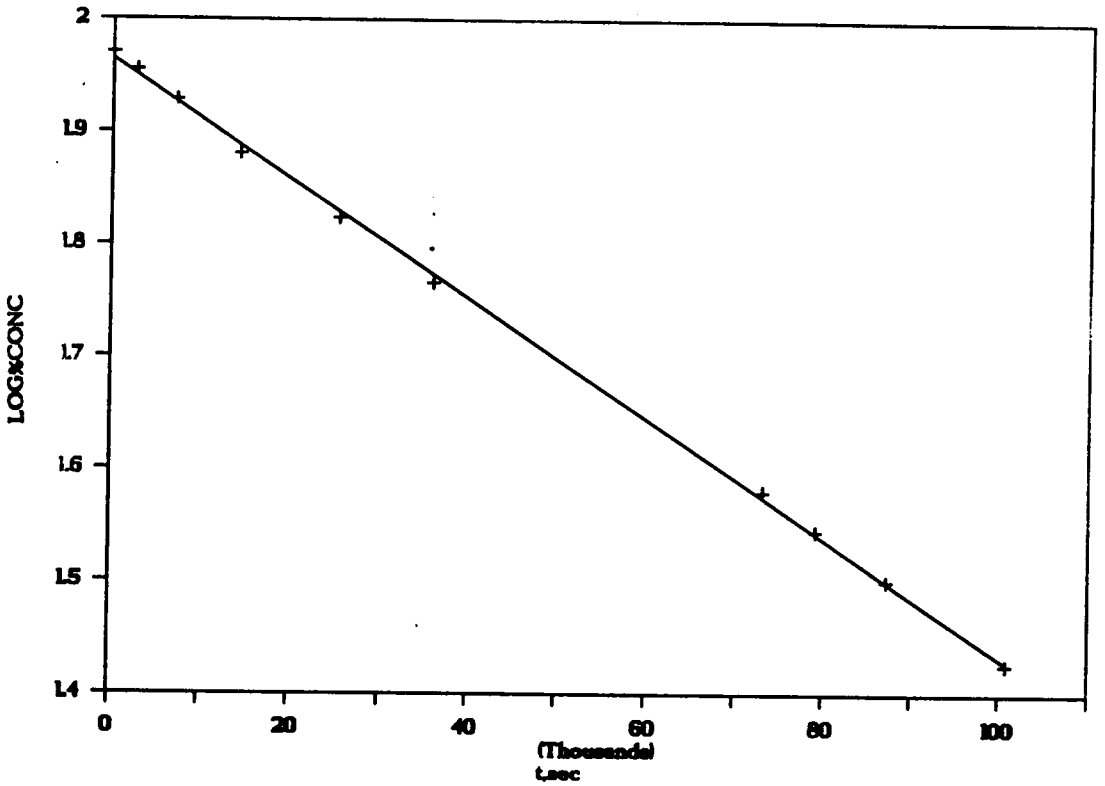

k

plotting log (% conc) versus time	slope = -5.33×10^{-6}
k = -2.303 (slope)	y intercept = 1.96
k = $1.23 \times 10^{-5} sec^{-1}$	corr = 0.999

Figure 2. First-order plot of the thermolysis of 1,2,3,4,5-pentaphenyl-2, 4-cyclopentadiene-1-methyl ether (25a) @ 225.0 ± 0.5°C.

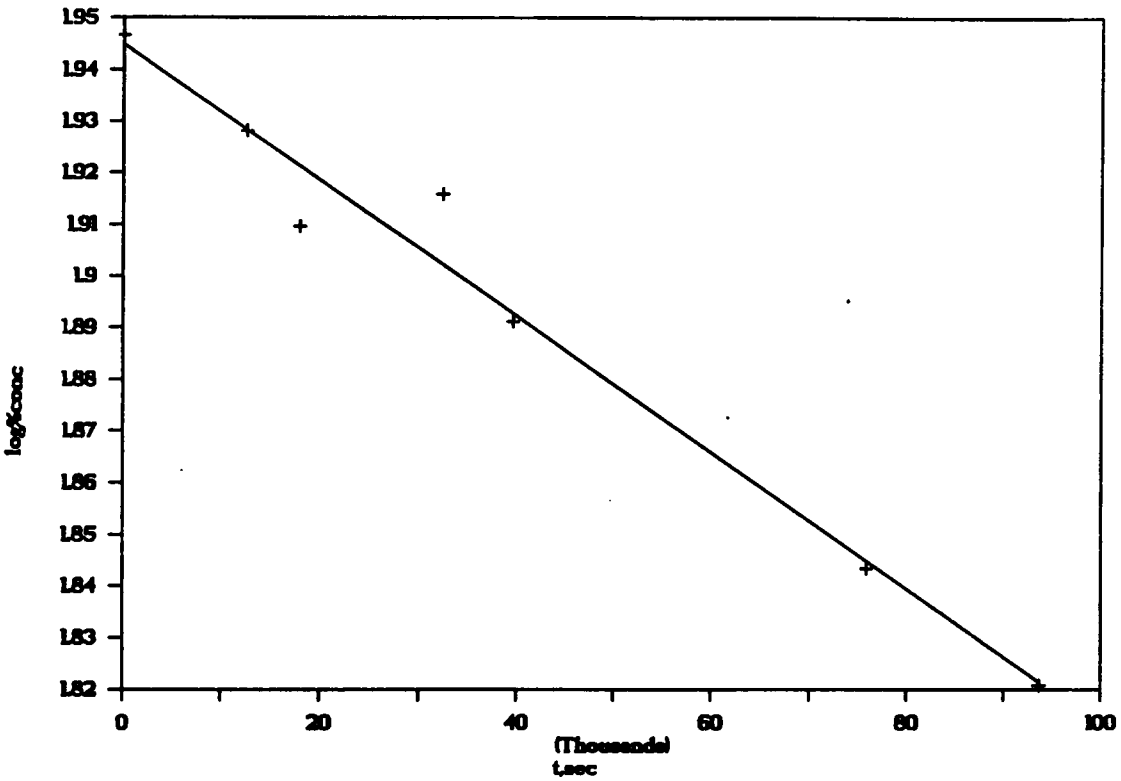

k

plotting log (% conc) versus time	slope = -1.27×10^{-6}
k = -2.303 (slope)	y intercept = 1.94
k = $3.04 \times 10^{-6} sec^{-1}$	corr = 0.974

Figure 3. First-order plot of the thermolysis of 1,2,3,4,5-pentaphenyl-2, 4-cyclopentadiene-1-methyl ether (25a) @ 210.0 ± 0.5°C.

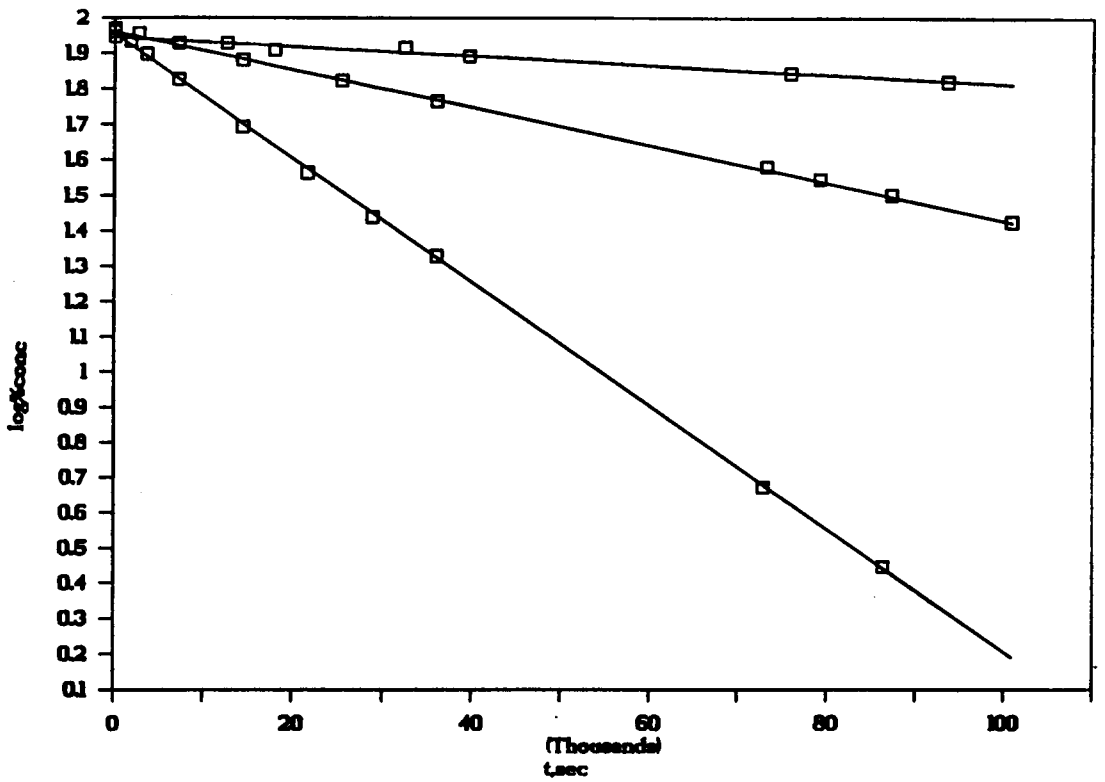

Figure 4. First-order plot of the thermolysis of 1,2,3,4,5-pentaphenyl-2, 4-cyclopentadiene-1-methyl ether (25a) @ 240.0-210.0°C.

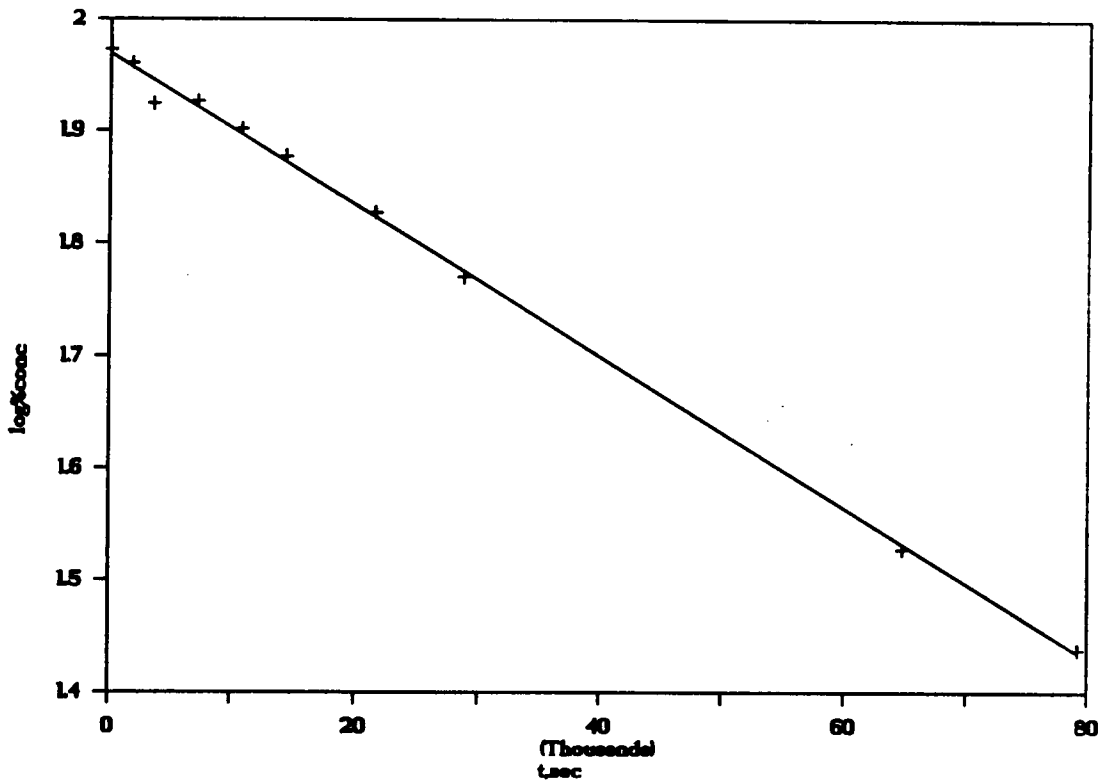

k

plotting log (% conc) versus time	slope = -6.75×10^{-6}
k = -2.303 (slope)	y intercept = 1.97
k = $1.55 \times 10^{-5} sec^{-1}$	corr = 0.998

Figure 5. First-order plot of the thermolysis of 1,2,3,4,5-pentaphenyl-2, 4-cyclopentadiene-1-methyl (d_3) ether (25f) @ 240.0 ± 0.5°C.

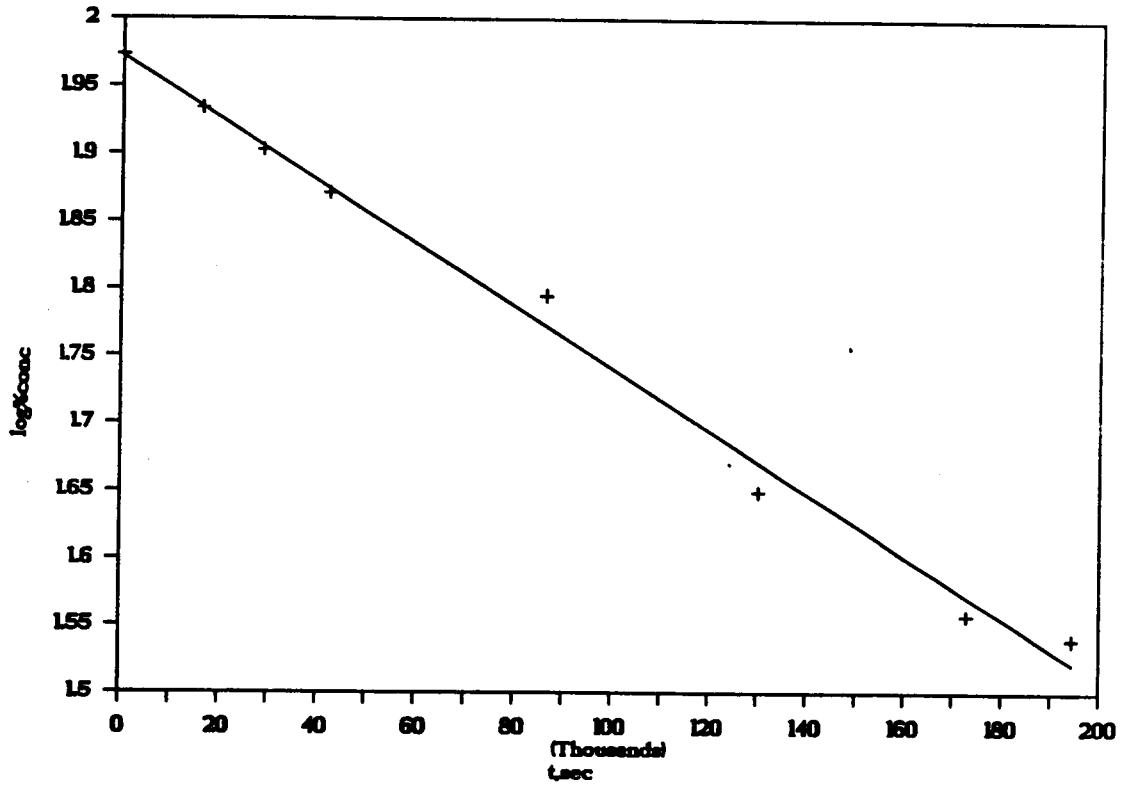

k

plotting log (% conc) versus time	slope = -2.27×10^{-6}
k = -2.303 (slope)	y intercept = 1.97
k = $5.34 \times 10^{-5} sec^{-1}$	corr = 0.993

Figure 6. First-order plot of the thermolysis of 1,2,3,4,5-pentaphenyl-2, 4-cyclopentadiene-1-methyl (d_3) ether (25f) @ 225.0 ± 0.5°C.

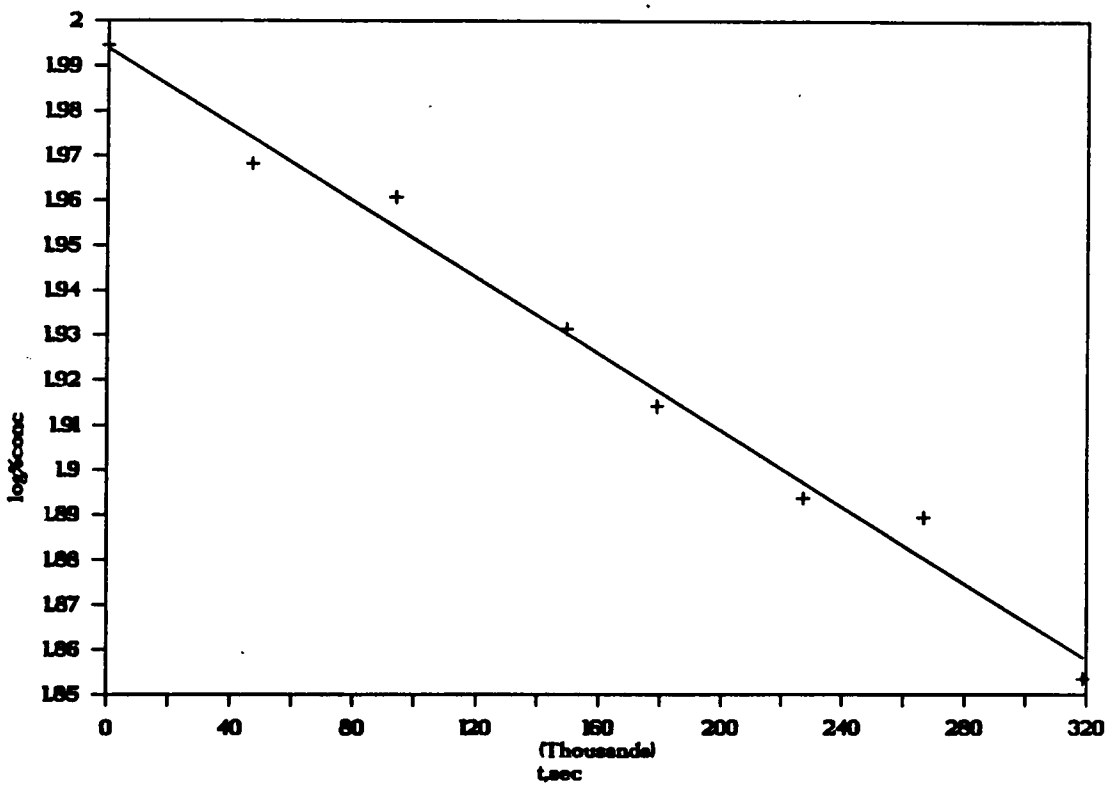

k

plotting log (% conc) versus time	slope = -4.26×10^{-7}
k = -2.303 (slope)	y intercept = 1.99
k = $9.81 \times 10^{-7} sec^{-1}$	corr = 0.986

Figure 7. First-order plot of the thermolysis of 1,2,3,4,5-pentaphenyl-2, 4-cyclopentadiene-1-methyl (d_3) ether (25f) @ 210.0 ± 0.5°C.

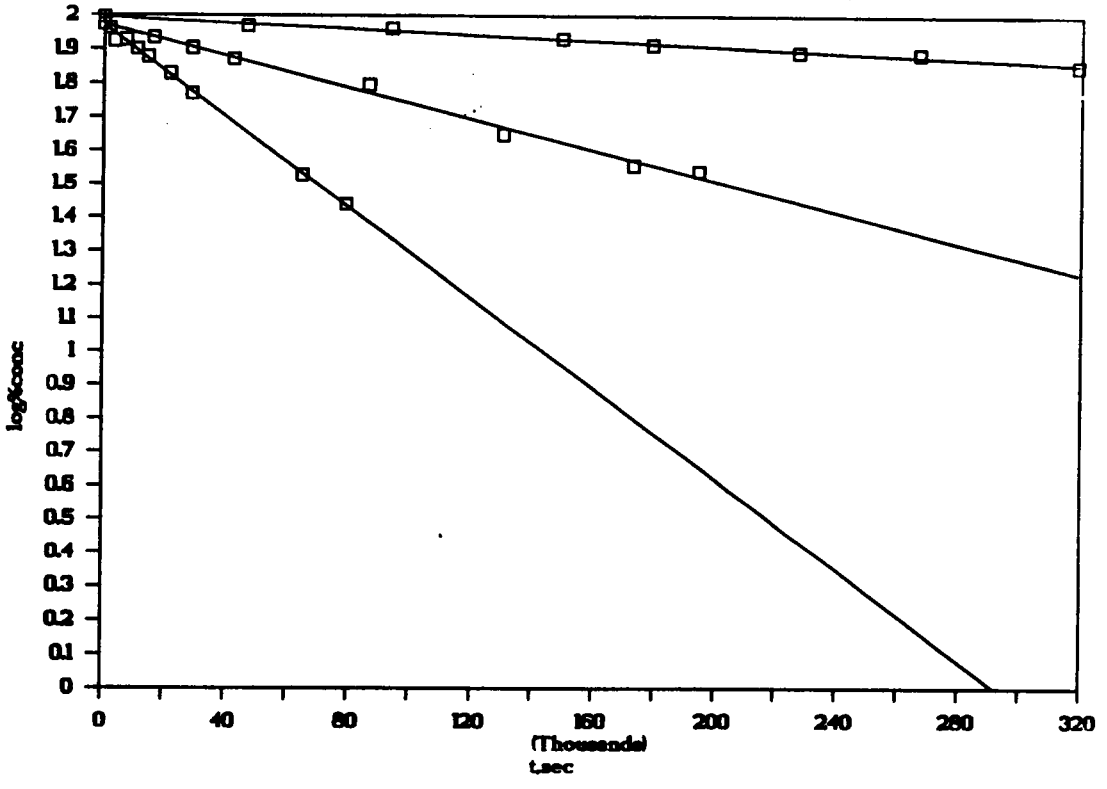

Figure 8. First-order plot of the thermolysis of 1,2,3,4,5-pentaphenyl-2, 4-cyclopentadiene-1-methyl (d_3) ether (25f) @ 240.0-210.0°C.

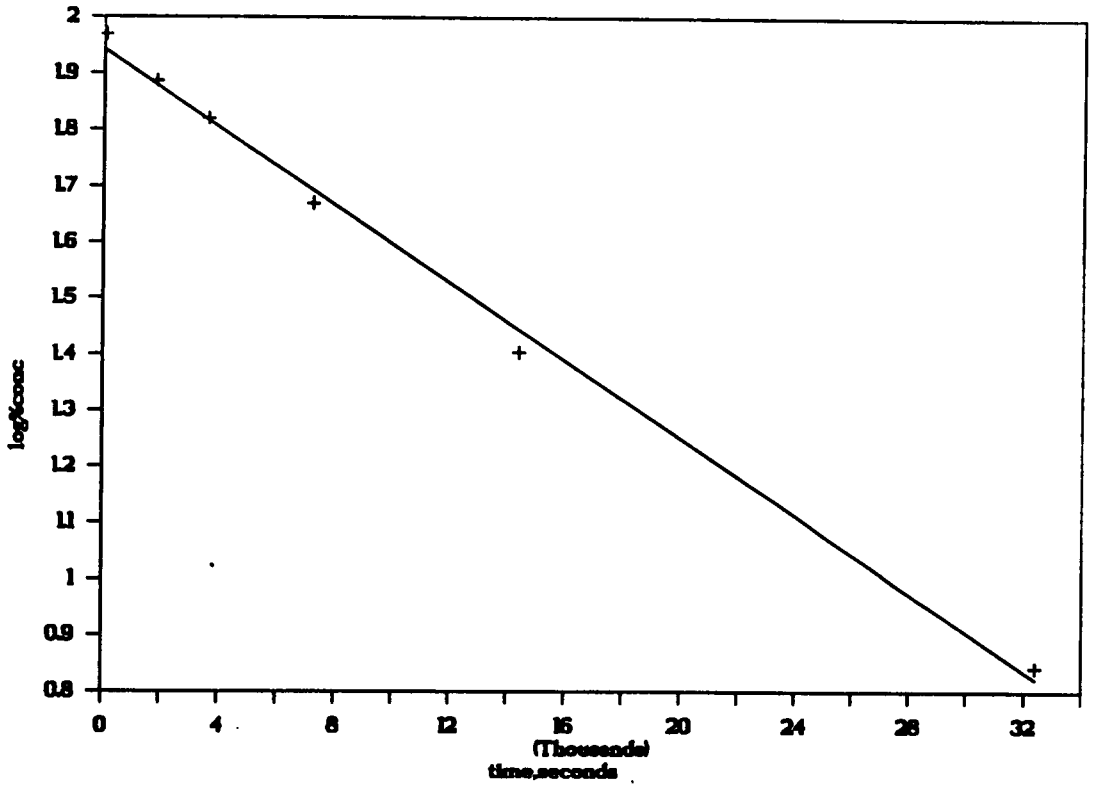

k

plotting log (% conc) versus time	slope = -3.46×10^{-5}
k = -2.303 (slope)	y intercept = 1.94
k = $7.96 \times 10^{-5} sec^{-1}$	corr = 0.996

Figure 9. First-order plot of the thermolysis of 1,2,3,4,5-pentaphenyl-2, 4-cyclopentadiene-1-ethyl ether (25b) @ 240.0 ± 0.5°C.

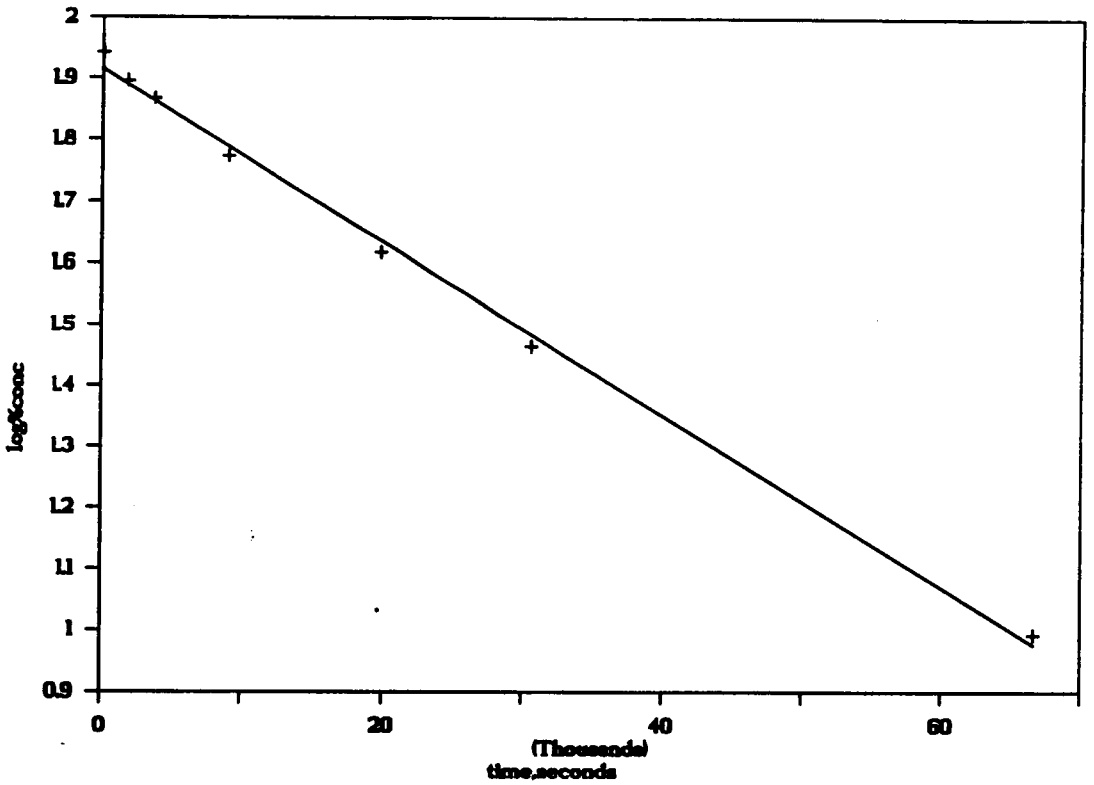

k

plotting log (% conc) versus time	slope = -1.41×10^{-5}
k = -2.303 (slope)	y intercept = 1.92
k = $3.25 \times 10^{-5} sec^{-1}$	corr = 0.996

Figure 10. First-order plot of the thermolysis of 1,2,3,4,5-pentaphenyl-2, 4-cyclopentadiene-1-ethyl ether (25b) @ 230.0 ± 0.5°C.

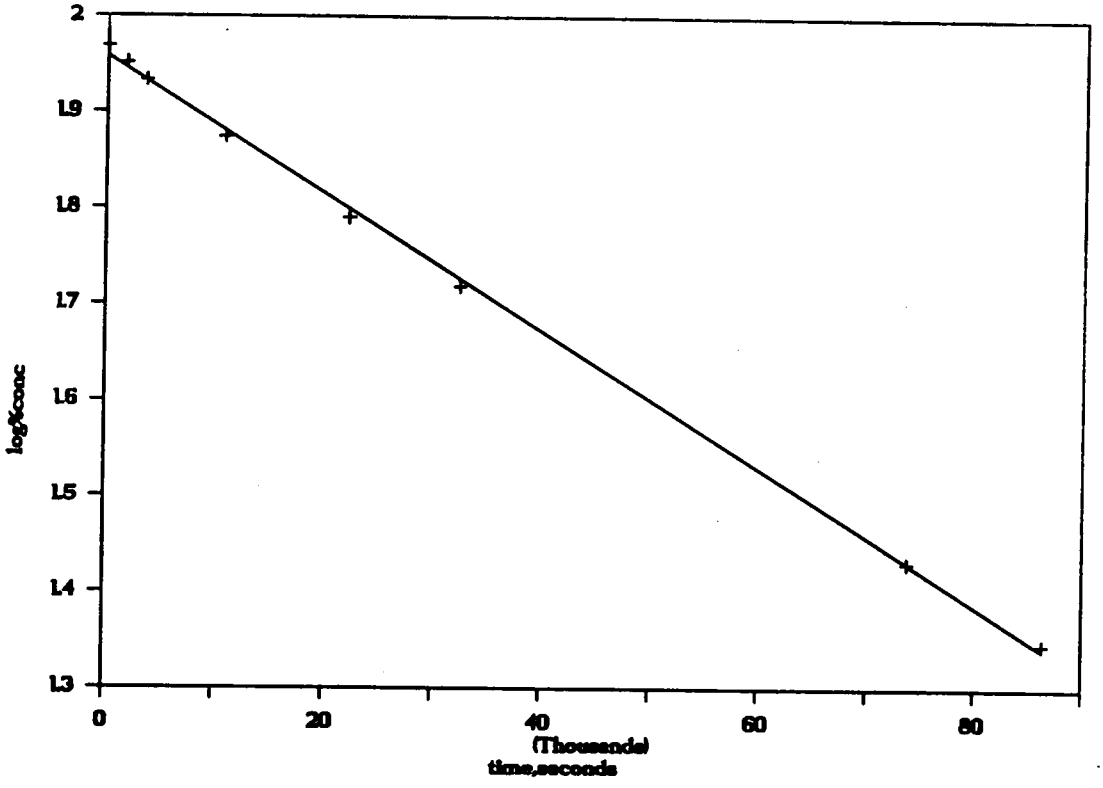

k

plotting log (% conc) versus time	slope = -7.14×10^{-6}
k = -2.303 (slope)	y intercept = 1.96
k = $1.65 \times 10^{-5} sec^{-1}$	corr = 0.999

Figure 11. First-order plot of the thermolysis of 1,2,3,4,5-pentaphenyl-2, 4-cyclopentadiene-1-ethyl ether (25b) @ 220.0 ± 0.5°C.

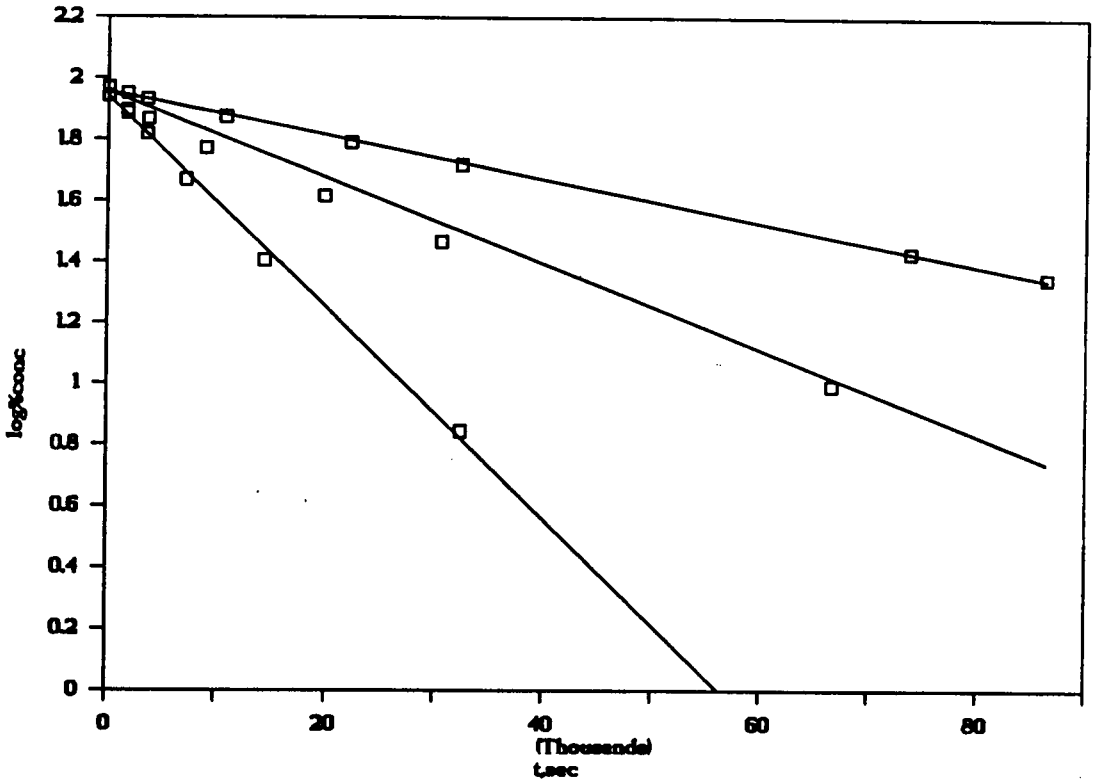

Figure 12. First-order plot of the thermolysis of 1,2,3,4,5-pentaphenyl-2, 4-cyclopentadiene-1-ethyl ether (25b) @ 240.0-220.0°C.

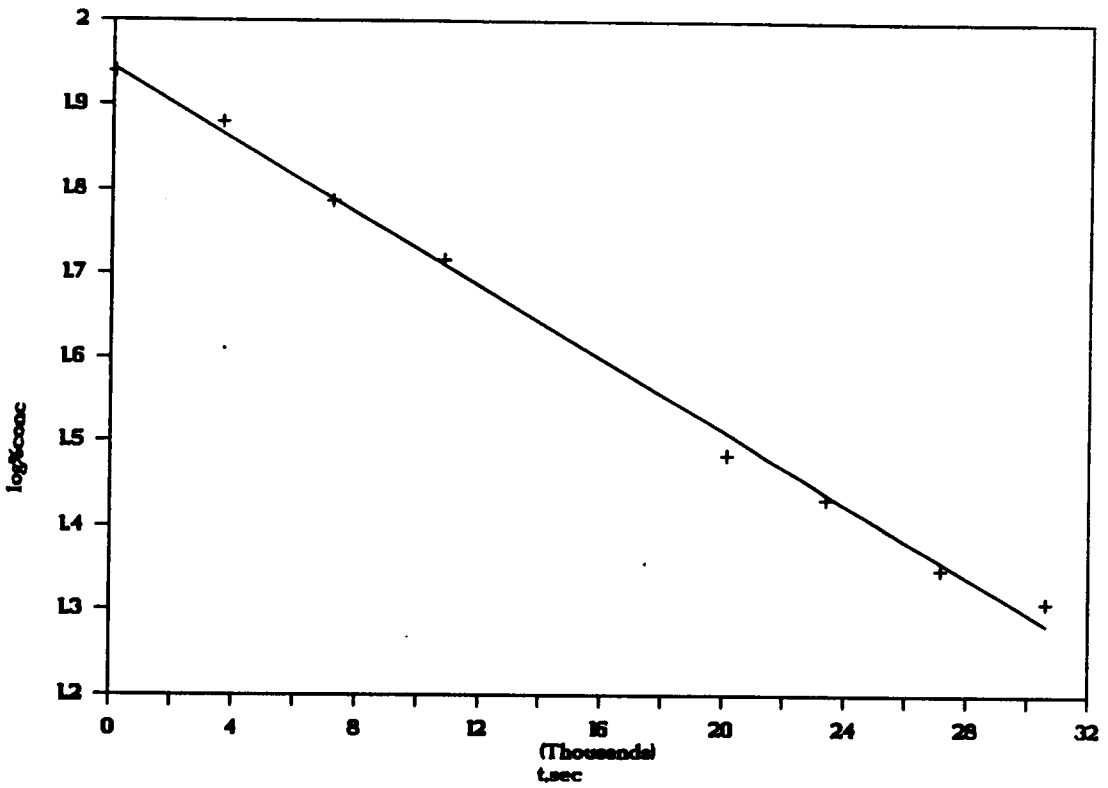

k

plotting log (% conc) versus time	slope = -2.16×10^{-5}
k = -2.303 (slope)	y intercept = 1.94
k = $4.97 \times 10^{-5} sec^{-1}$	corr = 0.996

Figure 13. First-order plot of the thermolysis of 1,2,3,4,5-pentaphenyl-2, 4-cyclopentadiene-1-n propyl ether (25c) @ 240.0 ± 0.5°C.

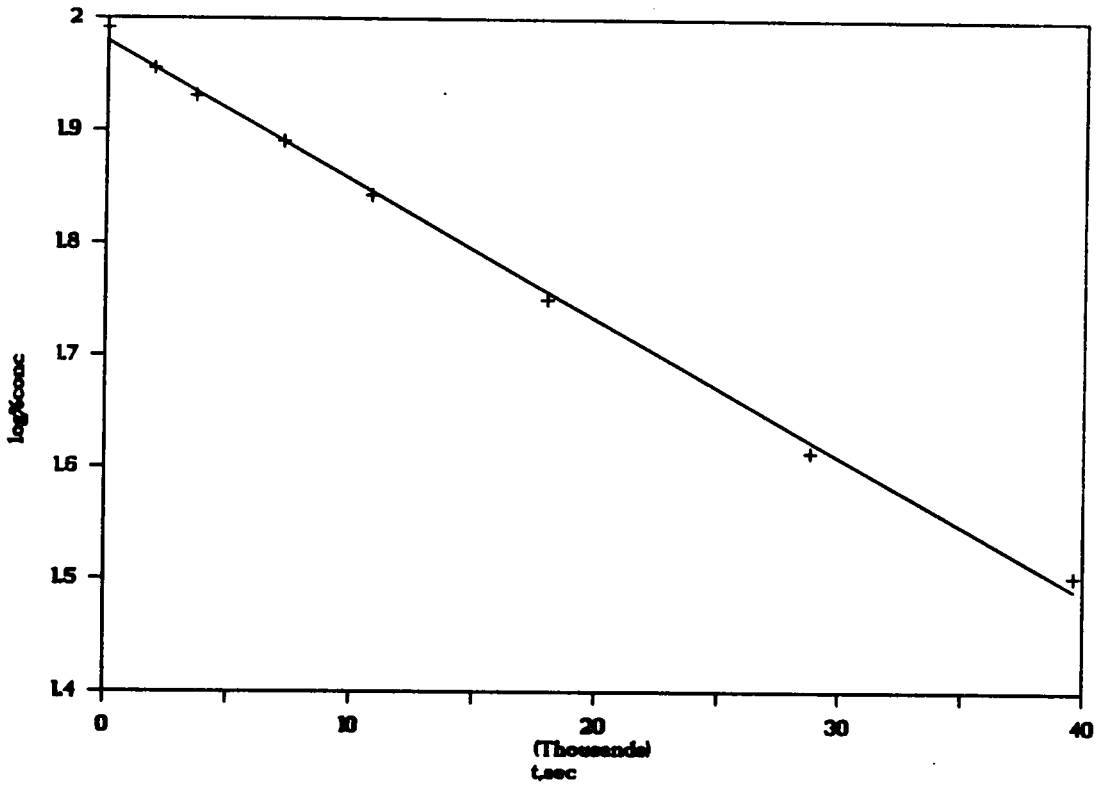

k

plotting log (% conc) versus time	slope = -1.23×10^{-5}
k = -2.303 (slope)	y intercept = 1.98
$k = 2.84 \times 10^{-6} sec^{-1}$	corr = 0.997

Figure 14. First-order plot of the thermolysis of 1,2,3,4,5-pentaphenyl-2, 4-cyclopentadiene-1-n-propyl ether (25c) @ 230.0 ± 0.5°C.

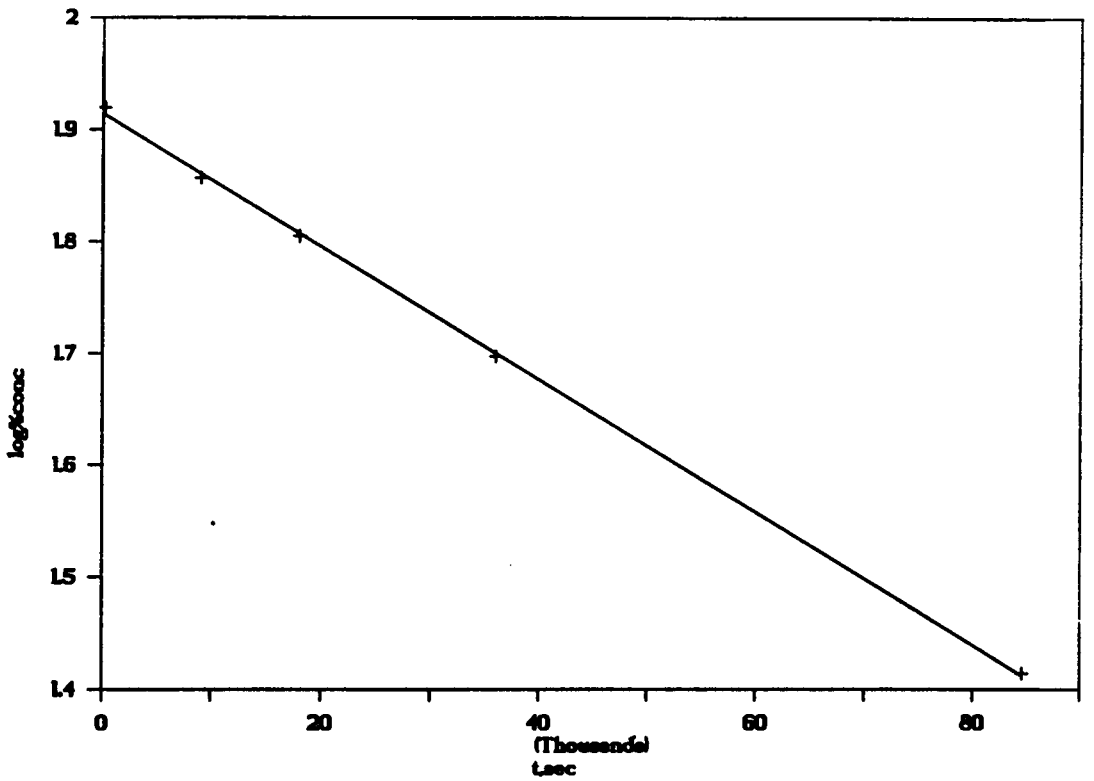

k

plotting log (% conc) versus time	slope = -6.01×10^{-6}
k = -2.303 (slope)	y intercept = 1.90
k = $1.39 \times 10^{-5} sec^{-1}$	corr = 0.998

Figure 15. First-order plot of the thermolysis of 1,2,3,4,5-pentaphenyl-2, 4-cyclopentadiene-1-n-propyl ether (25c) @ 220.0 ± 0.5°C.

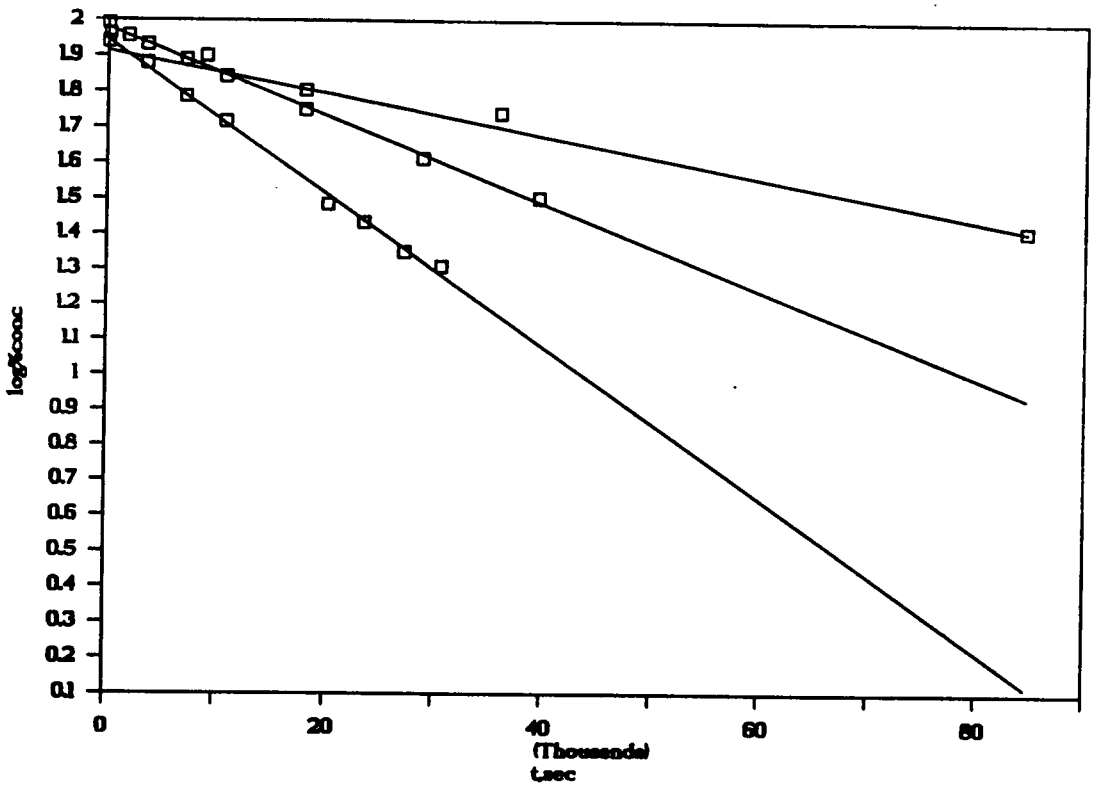

Figure 16. First-order plot of the thermolysis of 1,2,3,4,5-pentaphenyl-2, 4-cyclopentadiene-1-n-propyl ether (25c) @ 240.0-220.0°C.

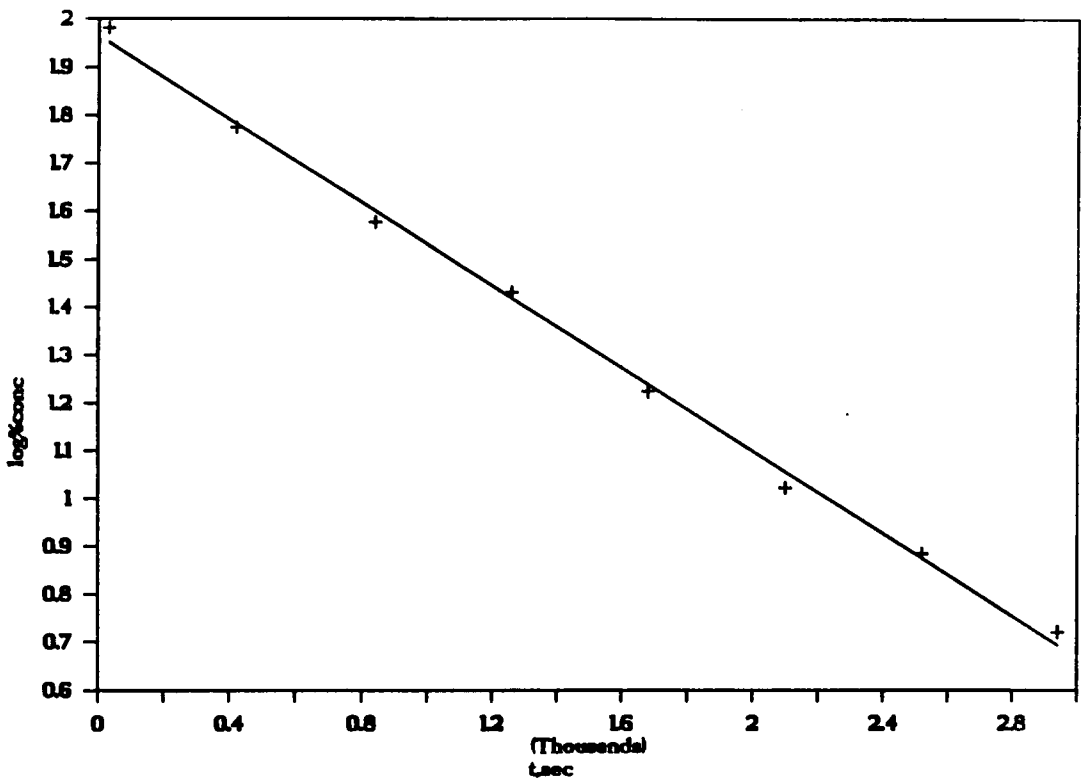

k

plotting log (% conc) versus time	slope = -4.27×10^{-4}
k = -2.303 (slope)	y intercept = 1.96
k = $9.95 \times 10^{-4} sec^{-1}$	corr = 0.997

Figure 17. First-order plot of the thermolysis of 1,2,3,4,5-pentaphenyl-2, 4-cyclopentadiene-1-benzyl ether (25e) @ 240.0 ± 0.5°C.

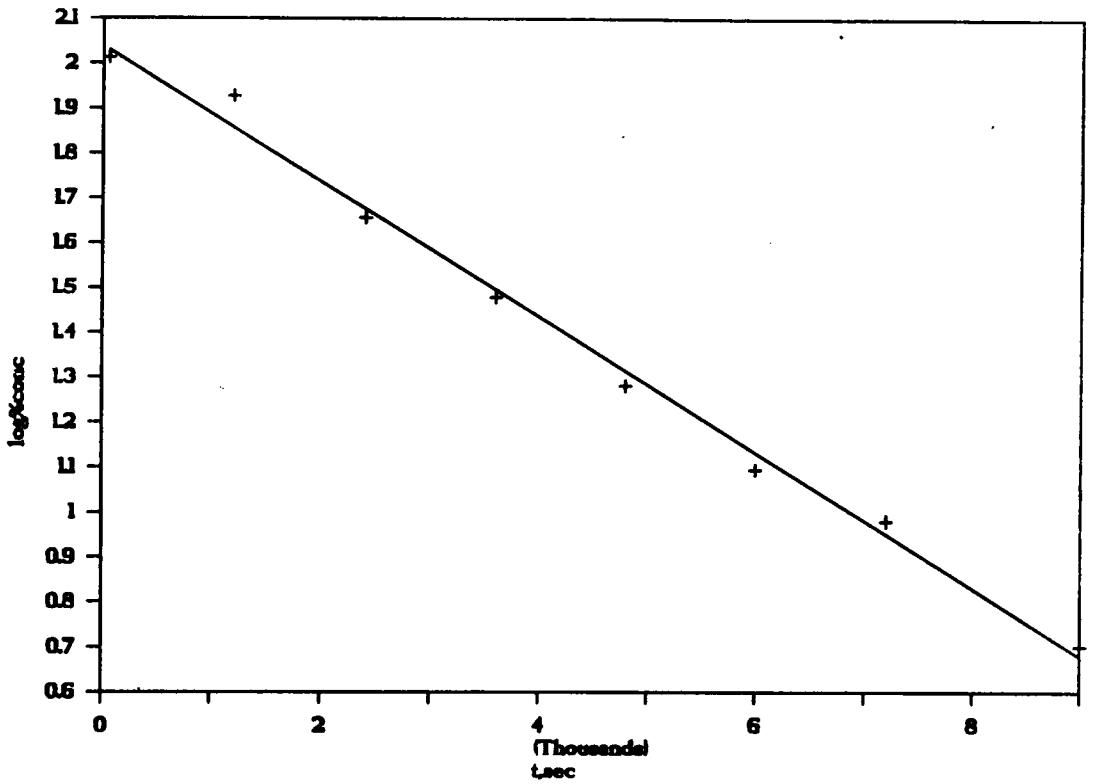

k

plotting log (% conc) versus time	slope = -1.51×10^{-4}
k = -2.303 (slope)	y intercept = 2.03
$k = 3.48 \times 10^{-4} sec^{-1}$	corr = 0.993

Figure 18. First-order plot of the thermolysis of 1,2,3,4,5-pentaphenyl-2, 4-cyclopentadiene-1-benzyl ether (25e) @ 225.0 ± 0.5°C.

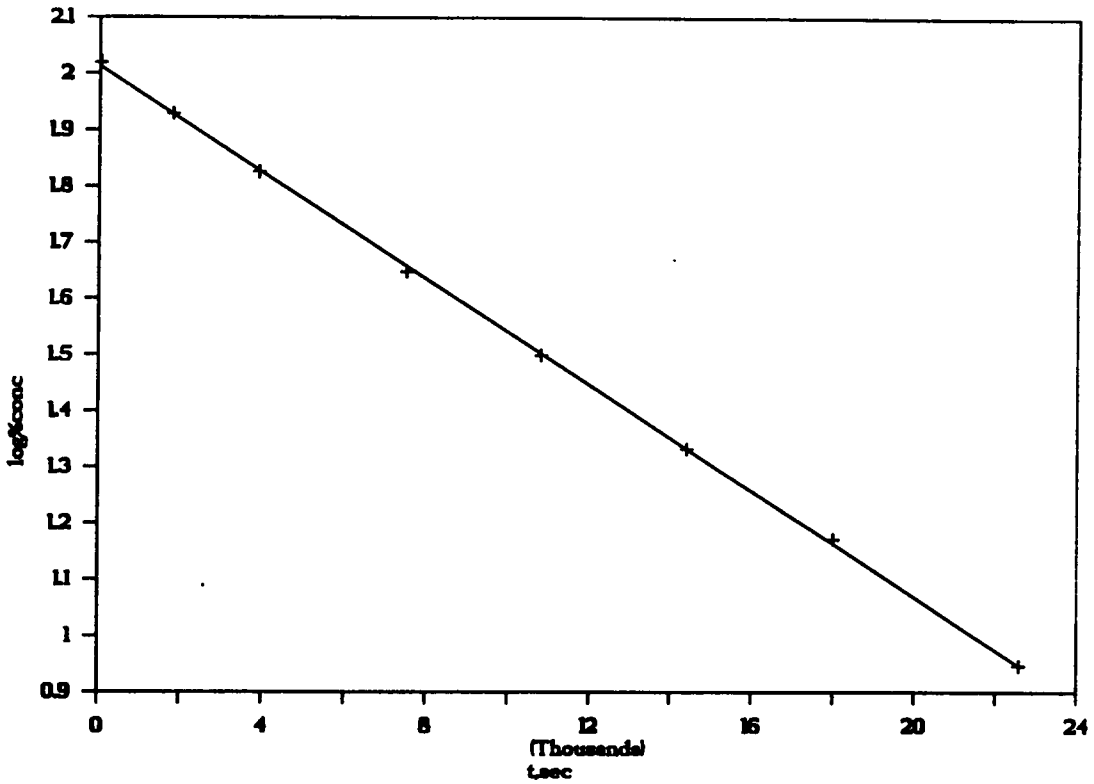

k

plotting log (% conc) versus time	slope = $-4.72 \times 10^{-5} sec^{-1}$
k = -2.303 (slope)	y intercept = 2.01
$k = 1.09 \times 10^{-4} sec^{-1}$	corr = 0.999

Figure 19. First-order plot of the thermolysis of 1,2,3,4,5-pentaphenyl-2, 4-cyclopentadiene-1-benzyl ether (25e) @ 210.0 ± 0.5°C.

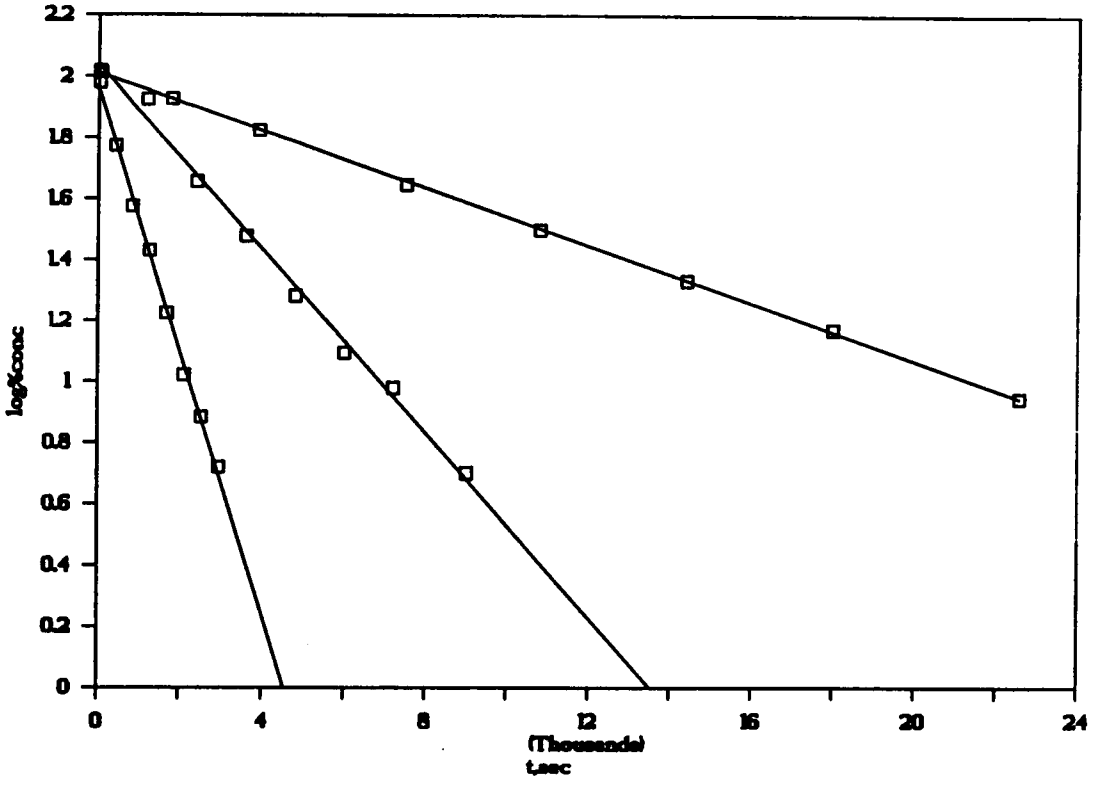

Figure 20. First-order plot of the thermolysis of 1,2,3,4,5-pentaphenyl-2, 4-cyclopentadiene-1-benzyl ether (25e) @ 240.0-210.0°C.

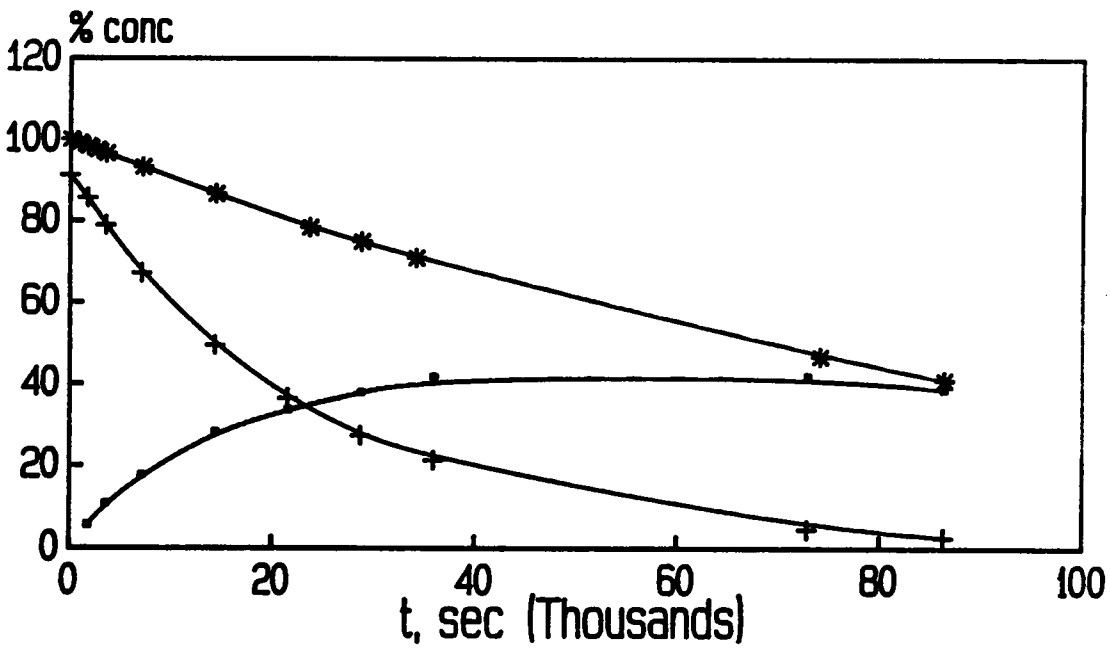

+ Represents methyl ether (25a) thermolysis.

■ Represents hydrocarbon (27) formation.

* Represents independent study of hydrocarbon (27) decomposition.

Figure 21. Comparison plot of % concentration versus time for thermolysis of methyl ether (25a), formation of hydrocarbon (27), and independent study of hydrocarbon (27) decomposition all measured @ 240.0 ± 0.5°C.

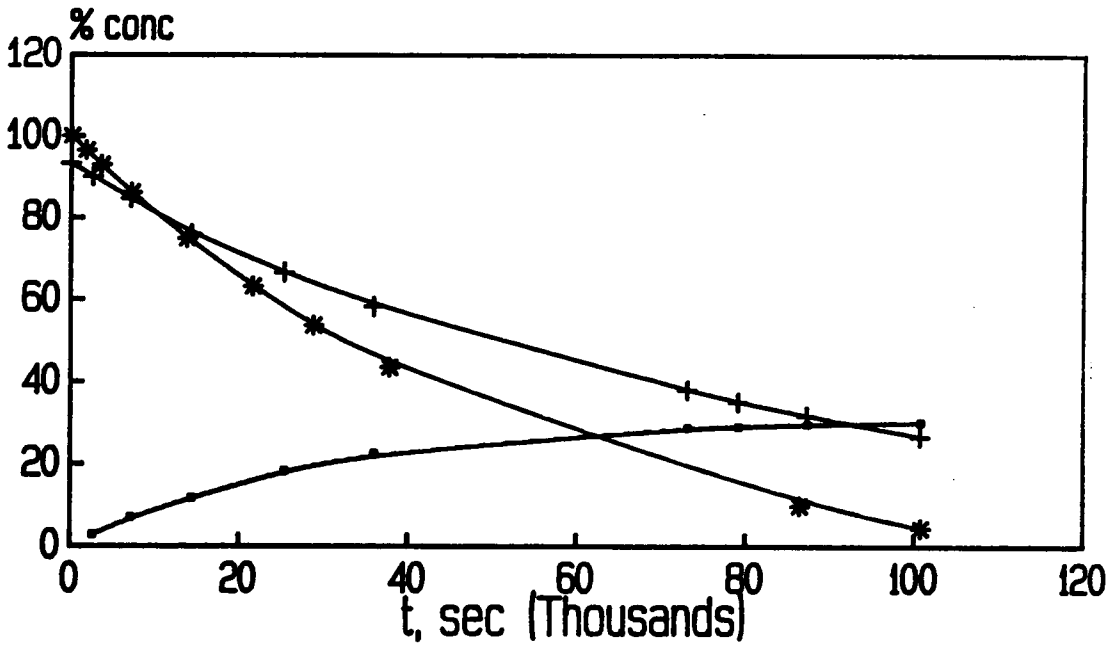

\+ Represents methyl ether (25a) thermolysis.

■ Represents hydrocarbon (27) formation.

* Represents independent study of hydrocarbon (27) decomposition.

Figure 22. Comparison plot of % concentration versus time for thermolysis of methyl ether (25a), formation of hydrocarbon (27), and independent study of hydrocarbon (27) decomposition all measured @ 225.0 ± 0.5°C.

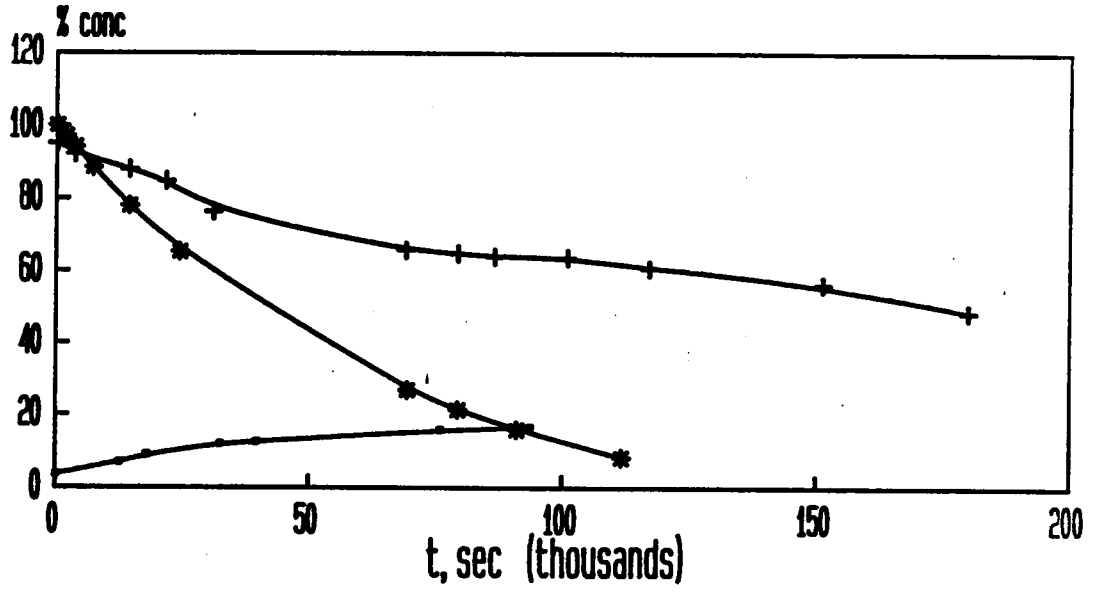

\+ Represents methyl ether (25a) thermolysis.

■ Represents hydrocarbon (27) formation.

* Represents independent study of hydrocarbon (27) decomposition.

Figure 23. Comparison plot of % concentration versus time for thermolysis of methyl ether (25a), formation of hydrocarbon (27), and independent study of hydrocarbon (27) decomposition all measured @ 210.0 ± 0.5°C.

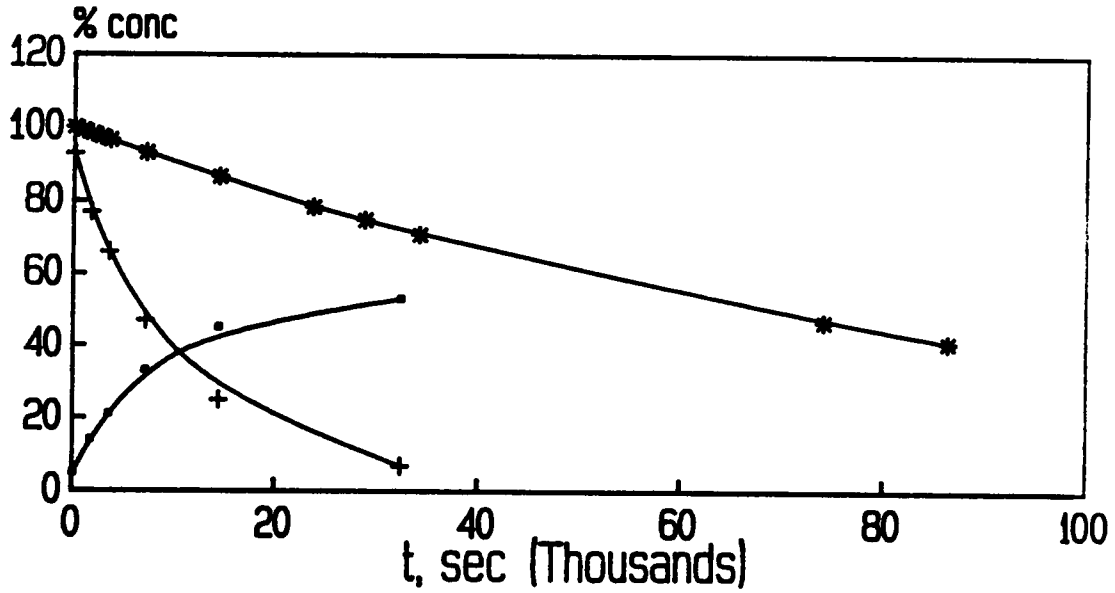

\+ Represents ethyl ether (25b) thermolysis.

▪ Represents hydrocarbon (27) formation.

* Represents independent study of hydrocarbon (27) decomposition.

Figure 24. Comparison plot of % concentration versus time for thermolysis of ethyl ether (25b), formation of hydrocarbon (27), and independent study of hydrocarbon (27) decomposition all measured @ 240.0 ± 0.5°C.

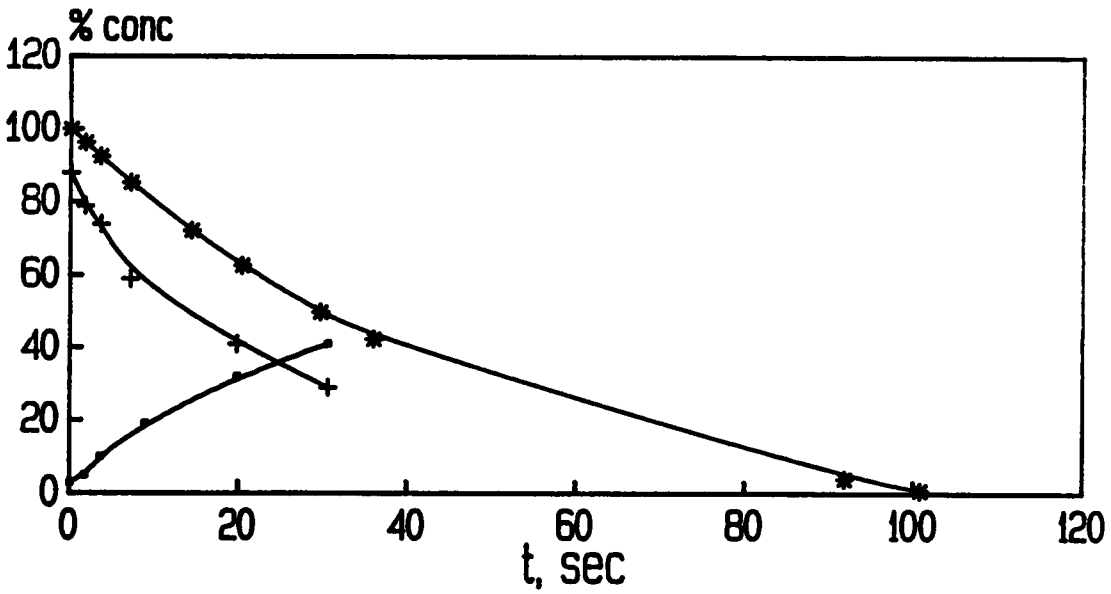

\+ Represents ethyl ether (25b) thermolysis.

■ Represents hydrocarbon (27) formation.

• Represents independent study of hydrocarbon (27) decomposition.

Figure 25. Comparison plot of % concentration versus time for thermolysis of ethyl ether (25b), formation of hydrocarbon (27), and independent study of hydrocarbon (27) decomposition all measured @ 230.0 ± 0.5°C.

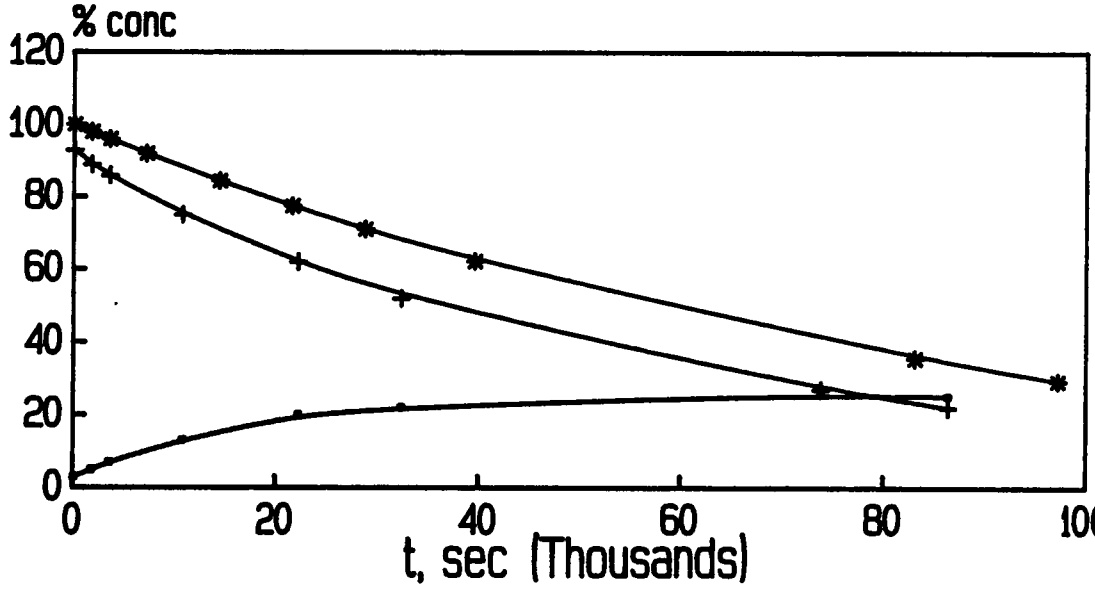

\+ Represents ethyl ether (25b) thermolysis.

■ Represents hydrocarbon (27) formation.

* Represents independent study of hydrocarbon (27) decomposition.

Figure 26. Comparison plot of % concentration versus time for thermolysis of ethyl ether (25b), formation of hydrocarbon (27), and independent study of hydrocarbon (27) decomposition all measured @ 220.0 ± 0.5°C.

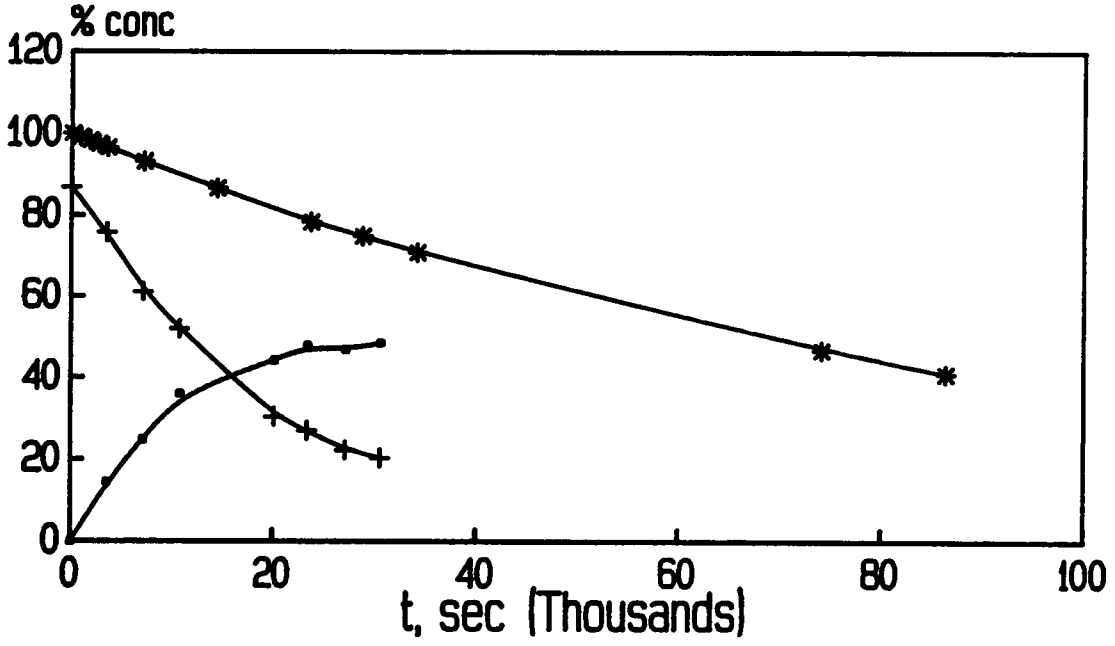

\+ Represents n-propyl ether (25c) thermolysis.

■ Represents hydrocarbon (27) formation.

* Represents independent study of hydrocarbon (27) decomposition.

Figure 27. Comparison plot of % concentration versus time for thermolysis of n-propyl ether (25c), formation of hydrocarbon (27), and independent study of hydrocarbon (27) decomposition all measured @ 240.0 ± 0.5°C.

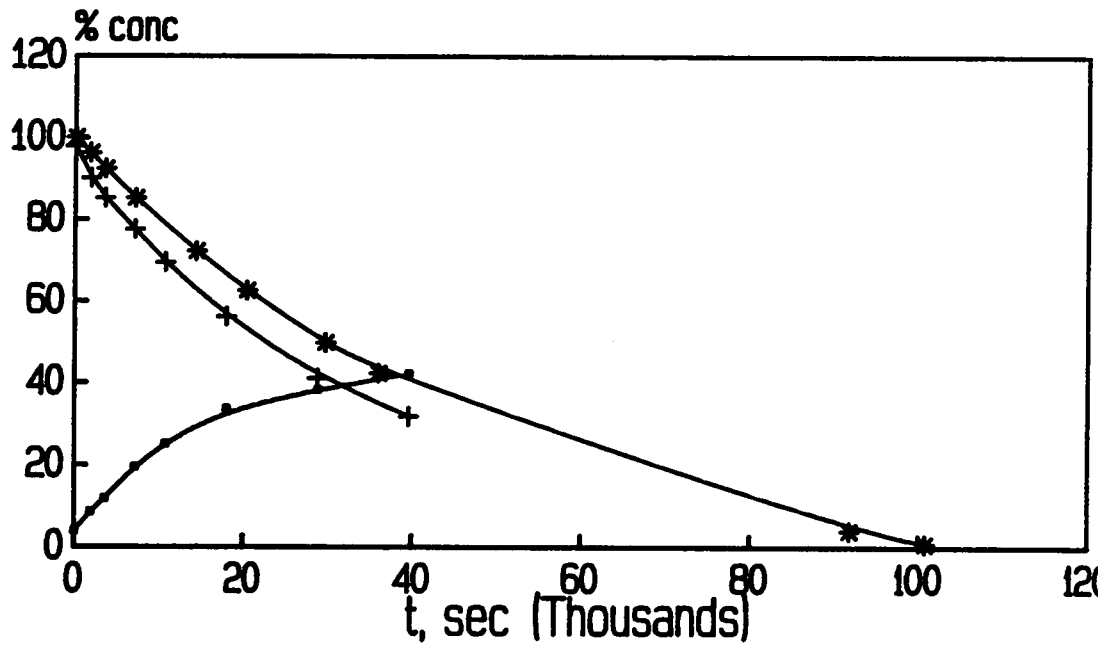

\+ Represents n-propyl ether (25c) thermolysis.

■ Represents hydrocarbon (27) formation.

* Represents independent study of hydrocarbon (27) decomposition.

Figure 28. Comparison plot of % concentration versus time for thermolysis of n-propyl ether (25c), formation of hydrocarbon (27), and independent study of hydrocarbon (27) decomposition all measured @ 230.0 ± 0.5°C.

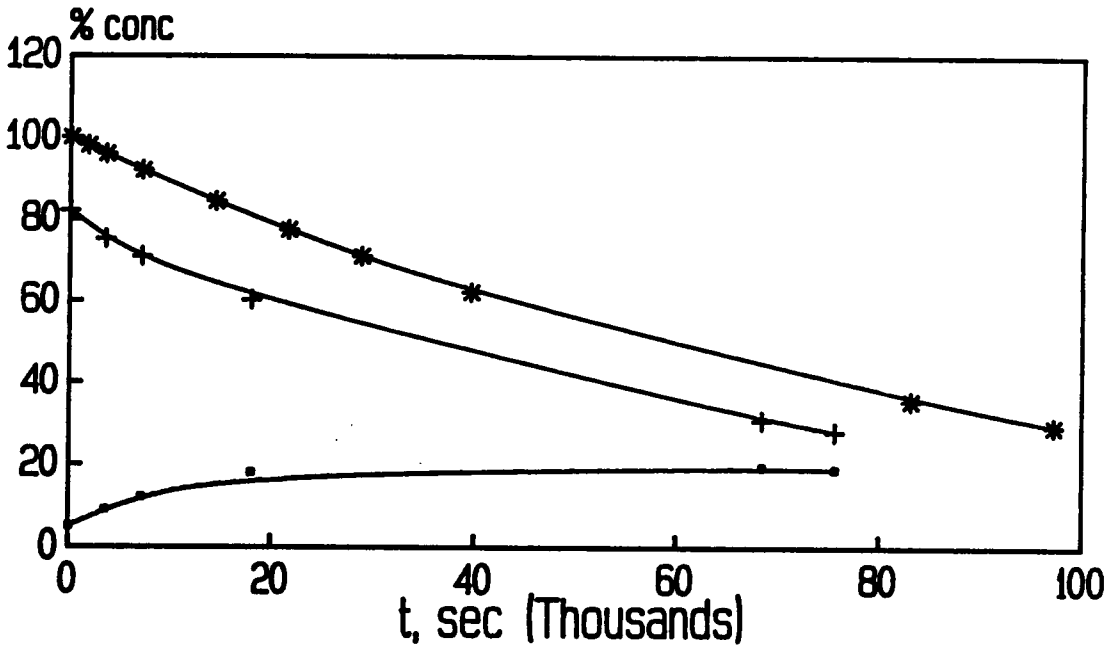

\+ Represents n-propyl ether (25c) thermolysis.

■ Represents hydrocarbon (27) formation.

* Represents independent study of hydrocarbon (27) decomposition.

Figure 29. Comparison plot of % concentration versus time for thermolysis of n-propyl ether (25c), formation of hydrocarbon (27), and independent study of hydrocarbon (27) decomposition all measured @ 220.0 ± 0.5°C.

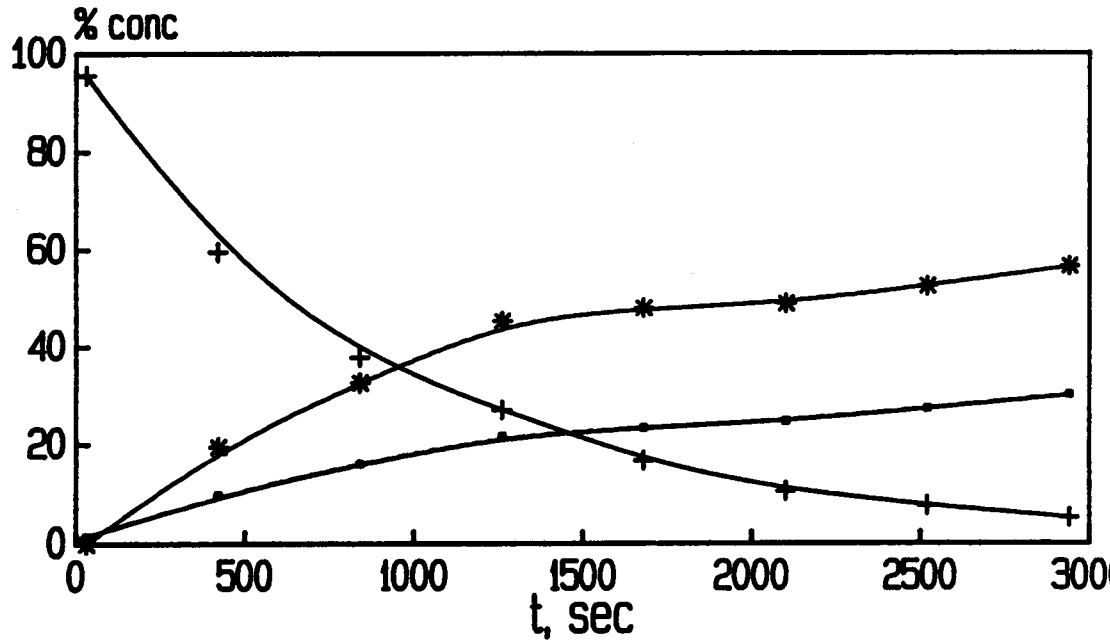

\+ Represents benzyl ether (25e) thermolysis.

■ Represents hydrocarbon (27) formation.

* Represents benzyl ketone (39e) formation.

Figure 30. Comparison plot of % concentration versus time for thermolysis of benzyl ether (25e), formation of hydrocarbon (27), and formation of benzyl ketone (39e) all measured @ 240.0 ± 0.5°C.

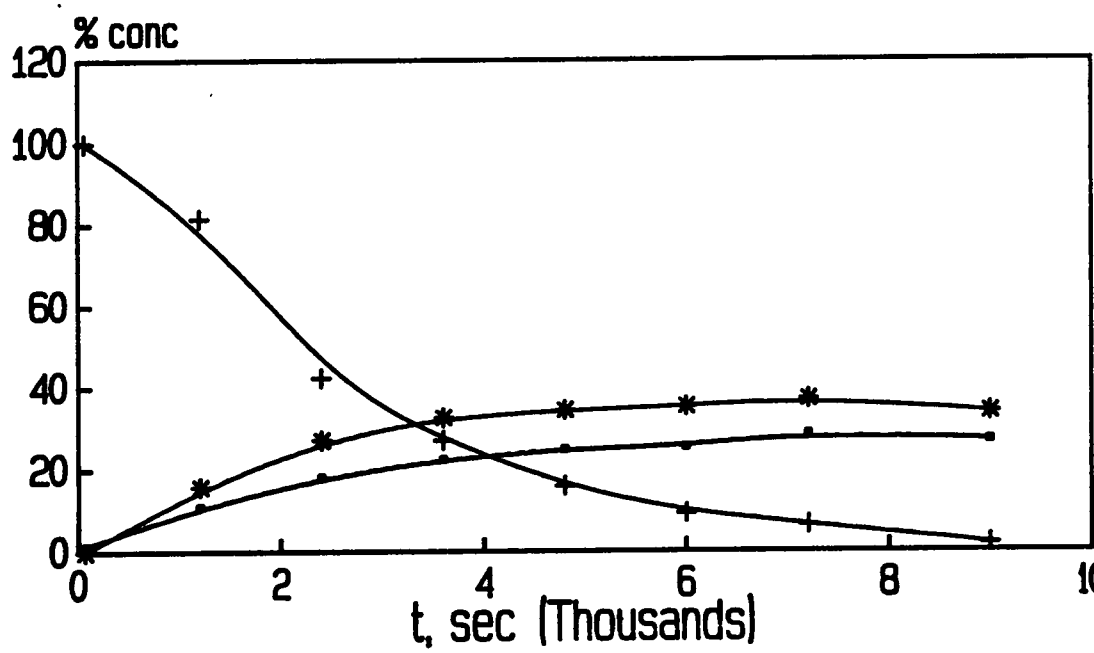

+ Represents benzyl ether (25e) thermolysis.

■ Represents hydrocarbon (27) formation.

• Represents benzyl ketone (39e) formation.

Figure 31. Comparison plot of % concentration versus time for thermolysis of benzyl ether (25e), formation of hydrocarbon (27), and formation of benzyl ketone (39e) all measured @ 225.0 ± 0.5°C.

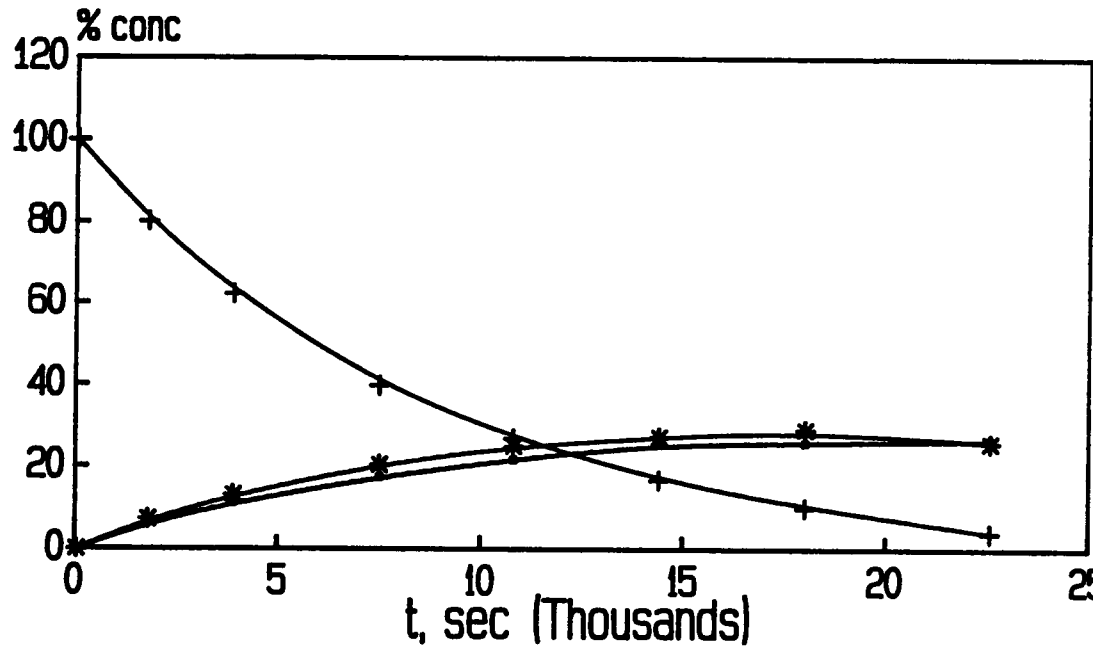

\+ Represents benzyl ether (25e) thermolysis.

■ Represents hydrocarbon (27) formation.

* Represents benzyl ketone (39e) formation.

Figure 32. Comparison plot of % concentration versus time for thermolysis of benzyl ether (25e), formation of hydrocarbon (27), and formation of benzyl ketone (39e) all measured @ 210.0 ± 0.5°C.

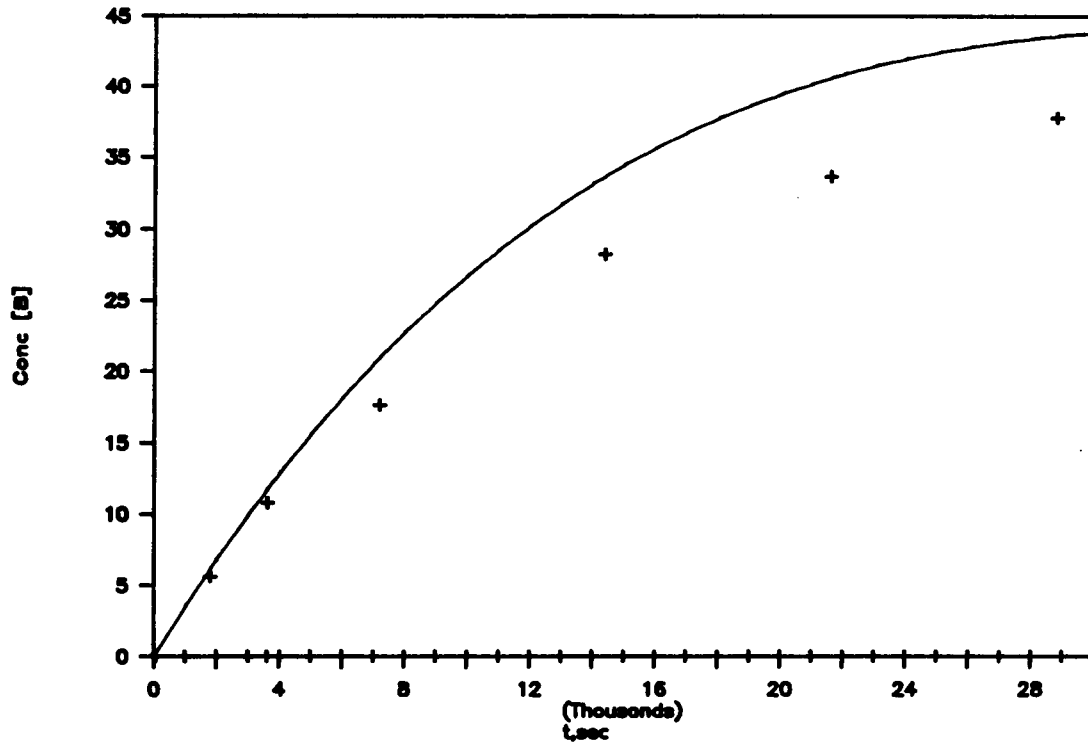

\+ Represents experimental data points for hydrocarbon (27) formation.

— Represents theoretically generated curve for hydrocarbon (27) formation.

Figure 33. Comparison plot of experimentally obtained data points with a theoretically generated plot illustrating % concentration versus time for the formation of hydrocarbon compound (27) from the thermolysis of methyl ether (25a) @ 240.0 ± 0.5°C.

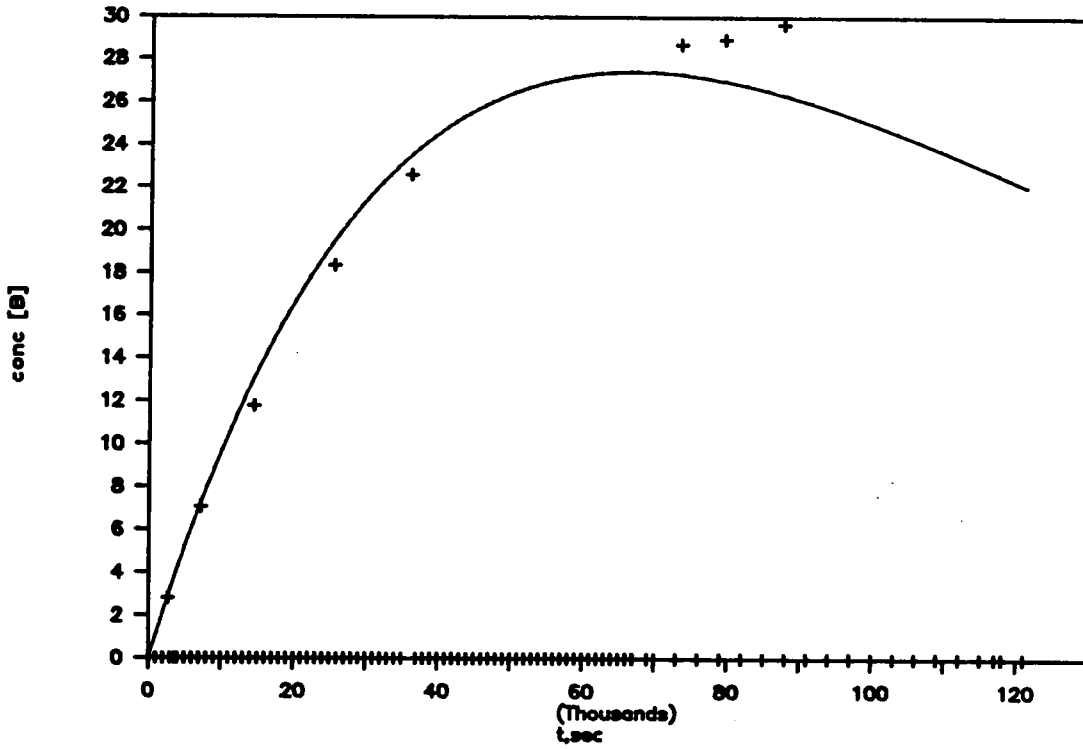

\+ Represents experimental data points for hydrocarbon (27) formation.

— Represents theoretically generated curve for hydrocarbon (27) formation.

Figure 34. Comparison plot of experimentally obtained data points with a theoretically generated plot illustrating % concentration versus time for the formation of hydrocarbon compound (27) from the thermolysis of methyl ether (25a) @ 225.0 ± 0.5°C.

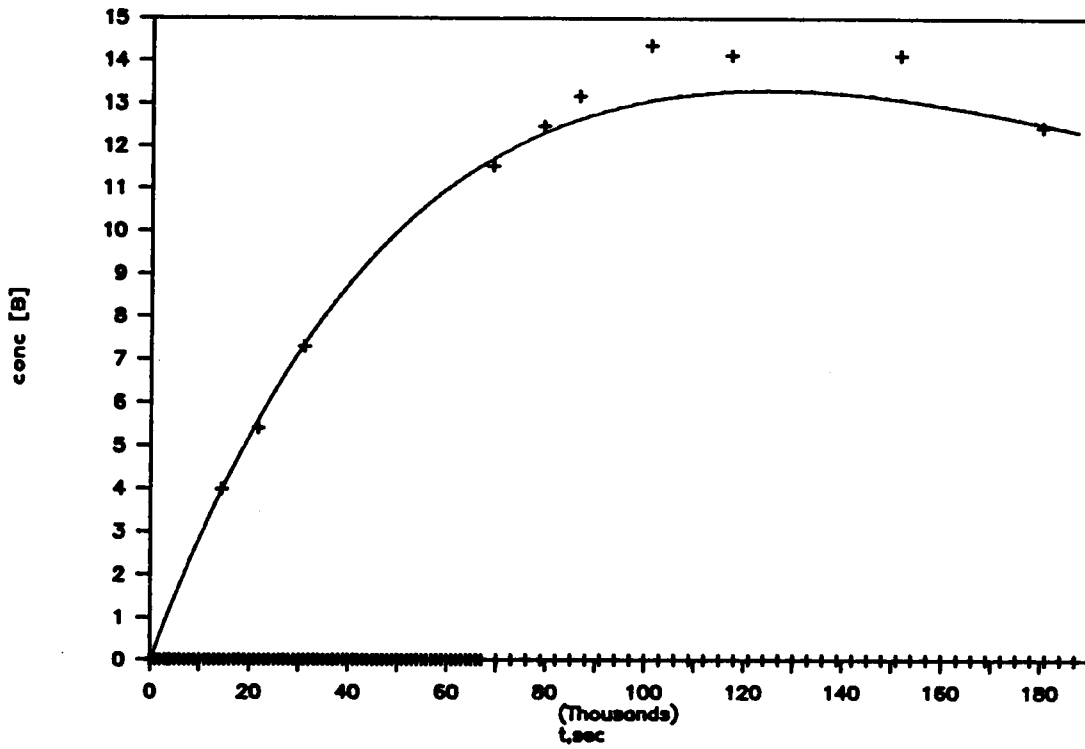

\+ Represents experimental data points for hydrocarbon (27) formation.

— Represents theoretically generated curve for hydrocarbon (27) formation.

Figure 35. Comparison plot of experimentally obtained data points with a theoretically generated plot illustrating % concentration versus time for the formation of hydrocarbon compound (27) from the thermolysis of methyl ether (25a) @ 210.0 ± 0.5°C.

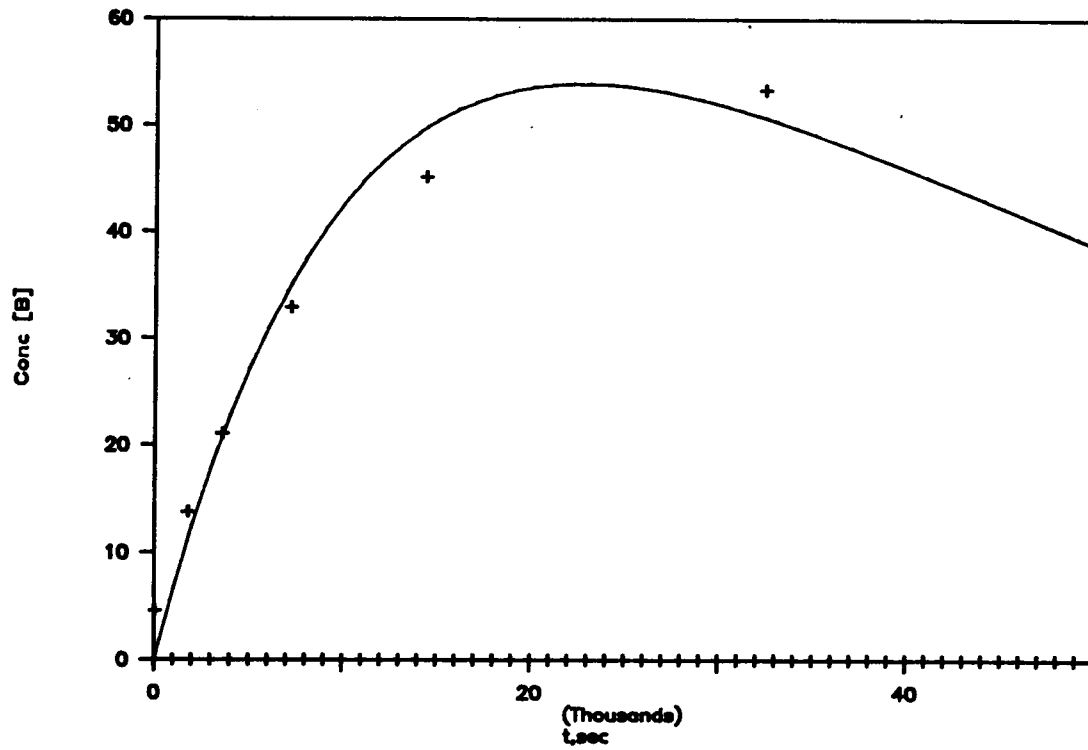

\+ Represents experimental data points for hydrocarbon (27) formation.

— Represents theoretically generated curve for hydrocarbon (27) formation.

Figure 36. Comparison plot of experimentally obtained data points with a theoretically generated plot illustrating % concentration versus time for the formation of hydrocarbon compound (27) from the thermolysis of ethyl ether (25b) @ 240.0 ± 0.5°C.

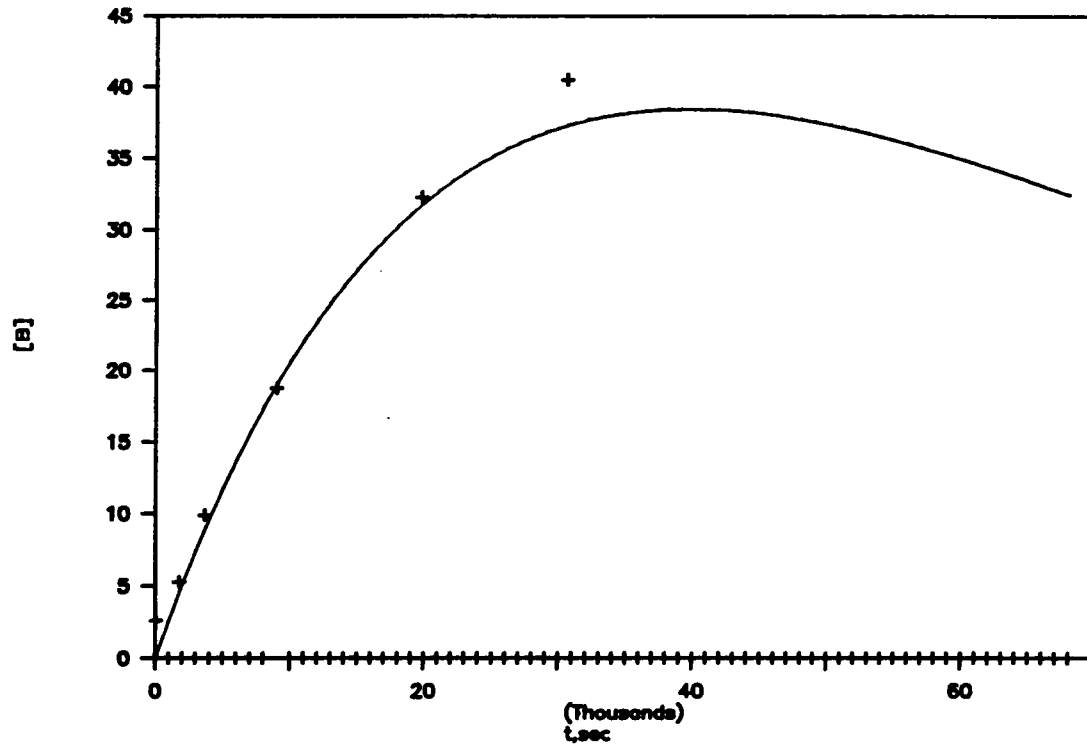

\+ Represents experimental data points for hydrocarbon (27) formation.

— Represents theoretically generated curve for hydrocarbon (27) formation.

Figure 37. Comparison plot of experimentally obtained data points with a theoretically generated plot illustrating % concentration versus time for the formation of hydrocarbon compound (27) from the thermolysis of ethyl ether (25b) @ 230.0 ± 0.5°C.

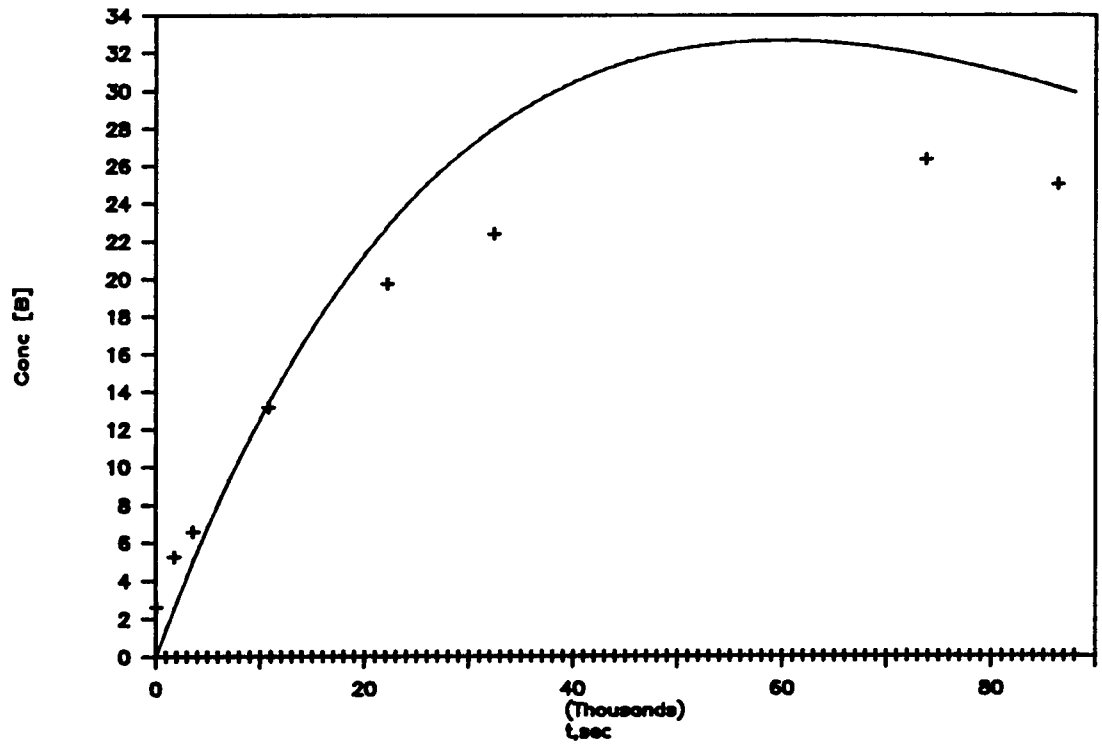

\+ Represents experimental data points for hydrocarbon (27) formation.

— Represents theoretically generated curve for hydrocarbon (27) formation.

Figure 38. Comparison plot of experimentally obtained data points with a theoretically generated plot illustrating % concentration versus time for the formation of hydrocarbon compound (27) from the thermolysis of ethyl ether (25b) @ 220.0 ± 0.5°C.

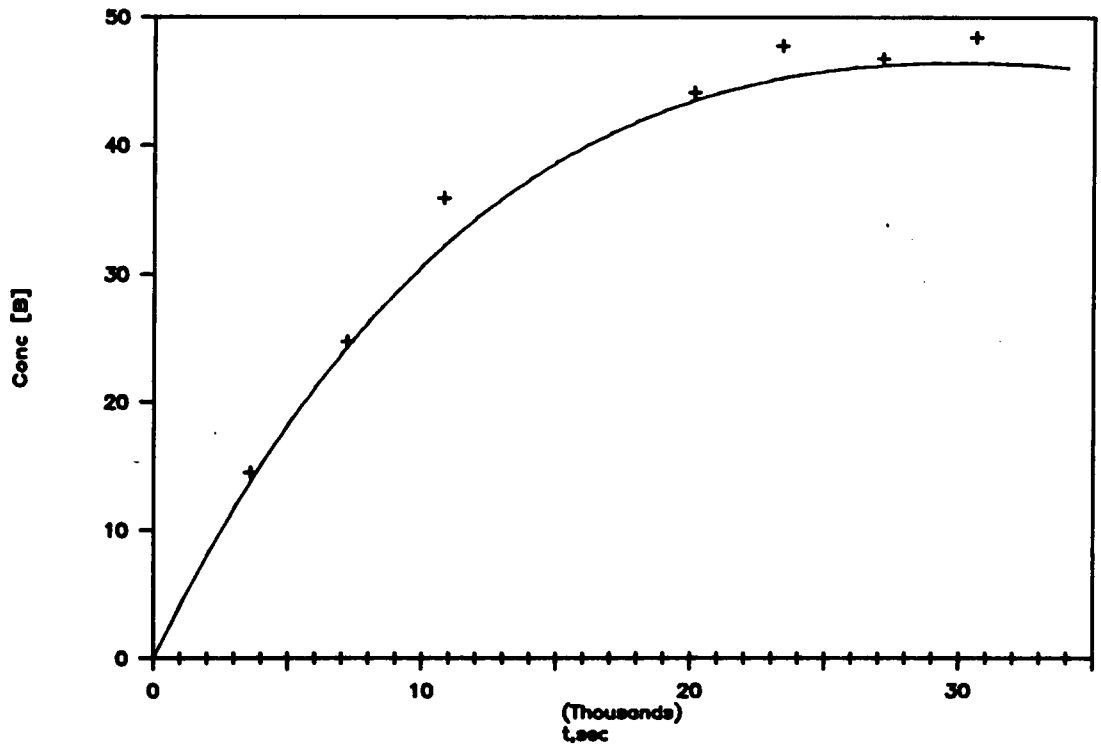

\+ Represents experimental data points for hydrocarbon (27) formation.

— Represents theoretically generated curve for hydrocarbon (27) formation.

Figure 39. Comparison plot of experimentally obtained data points with a theoretically generated plot illustrating % concentration versus time for the formation of hydrocarbon compound (27) from the thermolysis of n-propyl ether (25c) @ 240.0 ± 0.5°C.

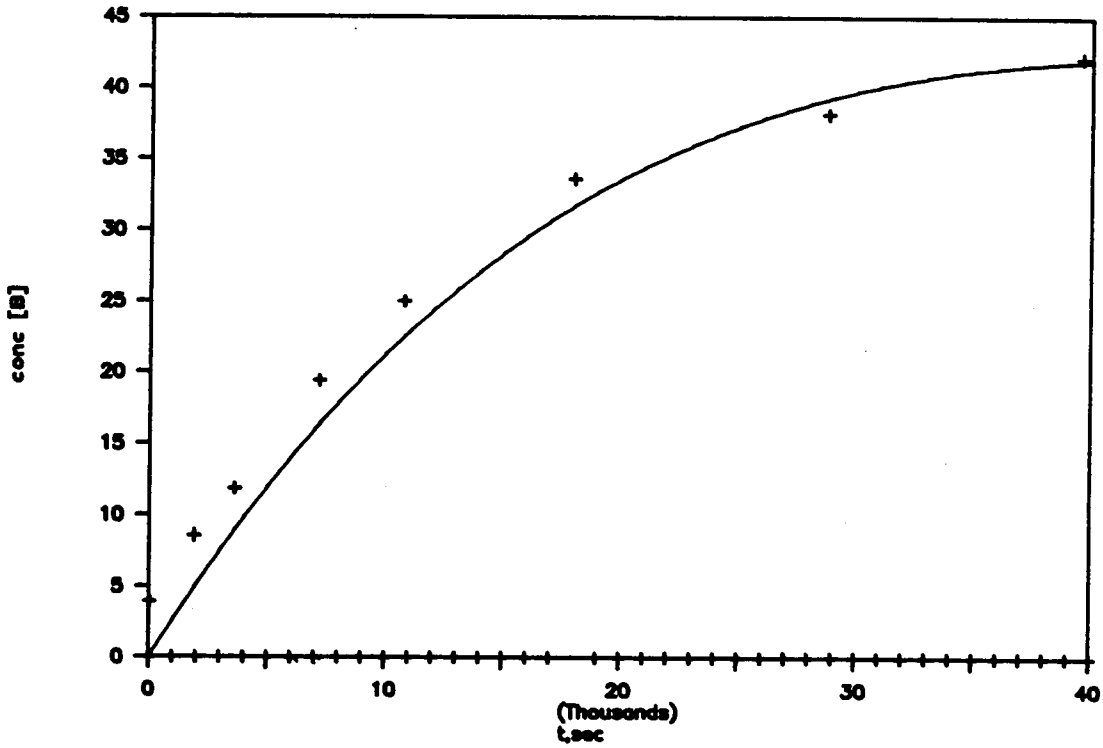

\+ Represents experimental data points for hydrocarbon (27) formation.

— Represents theoretically generated curve for hydrocarbon (27) formation.

Figure 40. Comparison plot of experimentally obtained data points with a theoretically generated plot illustrating % concentration versus time for the formation of hydrocarbon compound (27) from the thermolysis of n-propyl ether (25c) @ 230.0 ± 0.5°C.

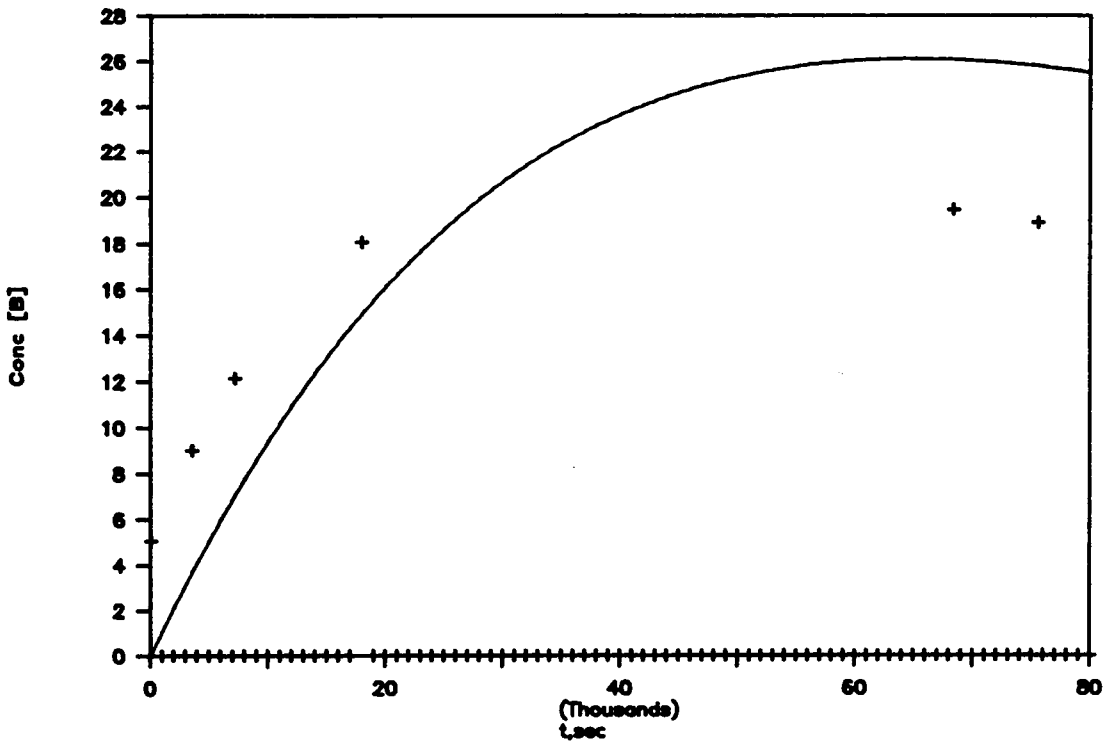

\+ Represents experimental data points for hydrocarbon (27) formation.

— Represents theoretically generated curve for hydrocarbon (27) formation.

Figure 41. Comparison plot of experimentally obtained data points with a theoretically generated plot illustrating % concentration versus time for the formation of hydrocarbon compound (27) from the thermolysis of n-propyl ether (25c) @ 220.0 ± 0.5°C.

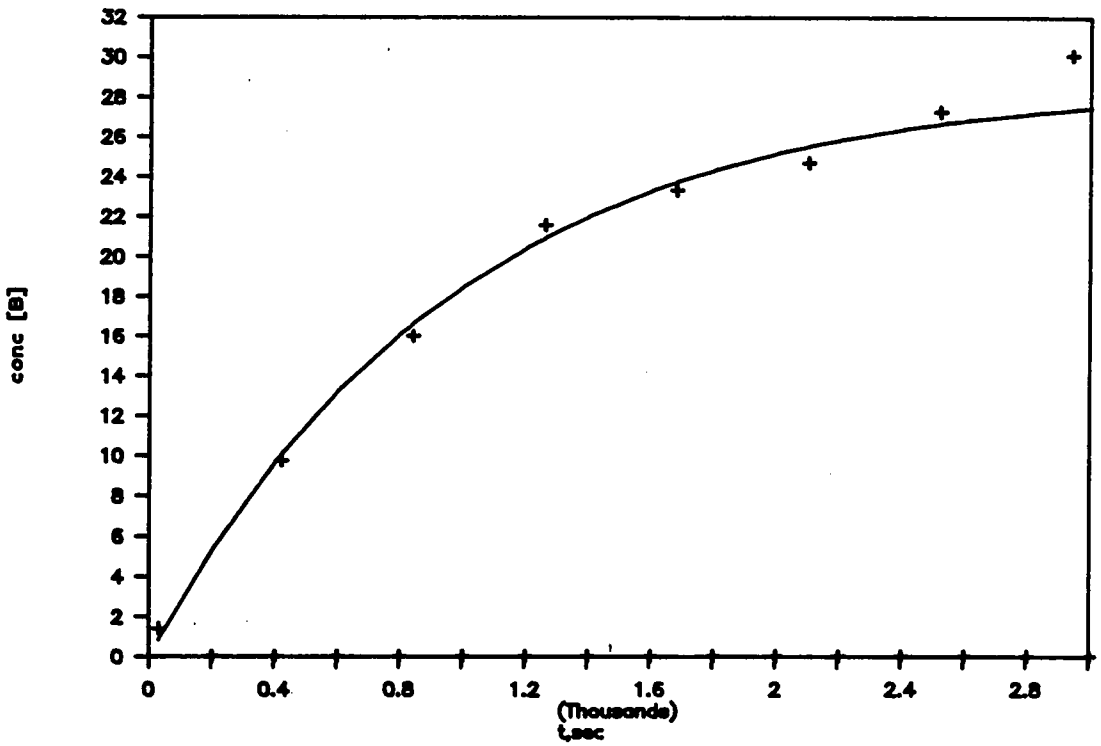

\+ Represents experimental data points for hydrocarbon (27) formation.

— Represents theoretically generated curve for hydrocarbon (27) formation.

Figure 42. Comparison plot of experimentally obtained data points with a theoretically generated plot illustrating % concentration versus time for the formation of hydrocarbon compound (27) from the thermolysis of benzyl ether (25e) @ 240.0 ± 0.5°C.

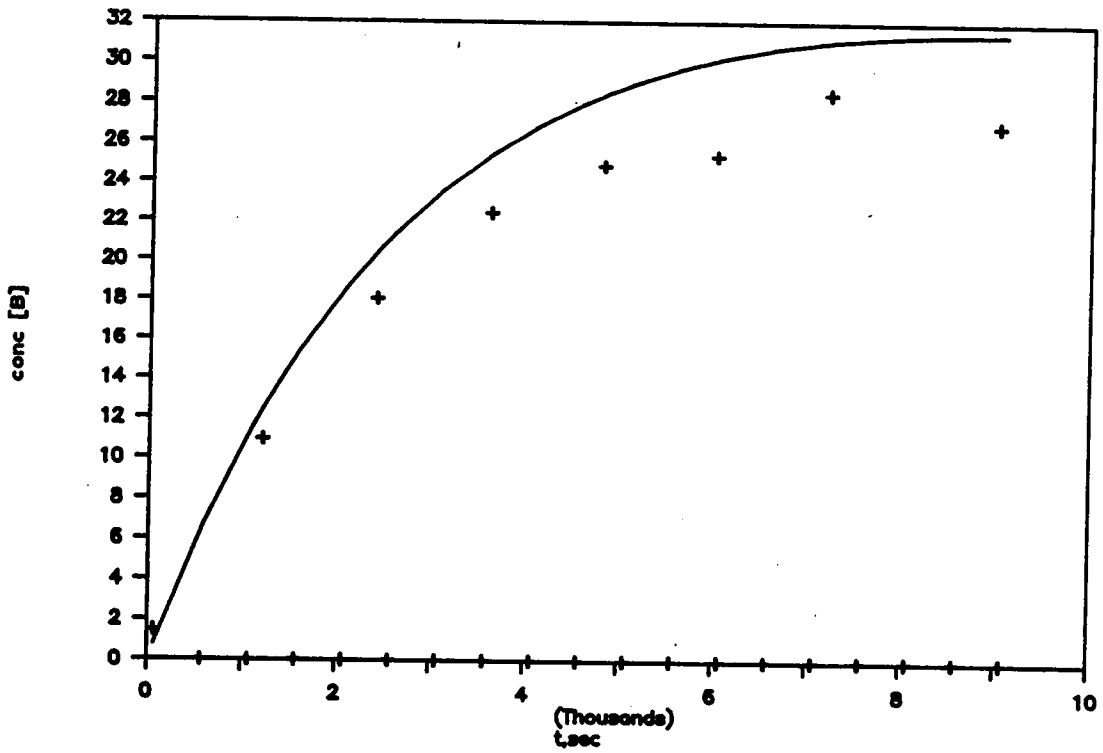

\+ Represents experimental data points for hydrocarbon (27) formation.

— Represents theoretically generated curve for hydrocarbon (27) formation.

Figure 43. Comparison plot of experimentally obtained data points with a theoretically generated plot illustrating % concentration versus time for the formation of hydrocarbon compound (27) from the thermolysis of benzyl ether (25e) @ 225.0 ± 0.5°C.

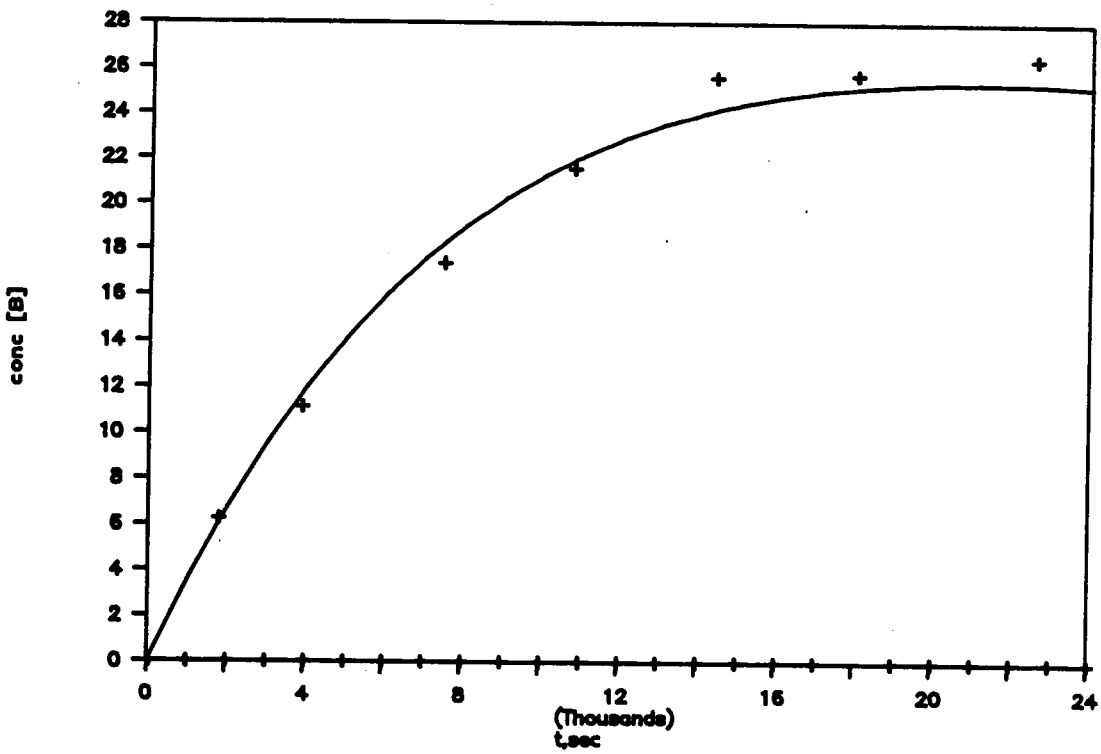

\+ Represents experimental data points for hydrocarbon (27) formation.

— Represents theoretically generated curve for hydrocarbon (27) formation.

Figure 44. Comparison plot of experimentally obtained data points with a theoretically generated plot illustrating % concentration versus time for the formation of hydrocarbon compound (27) from the thermolysis of benzyl ether (25e) @ 210.0 ± 0.5°C.

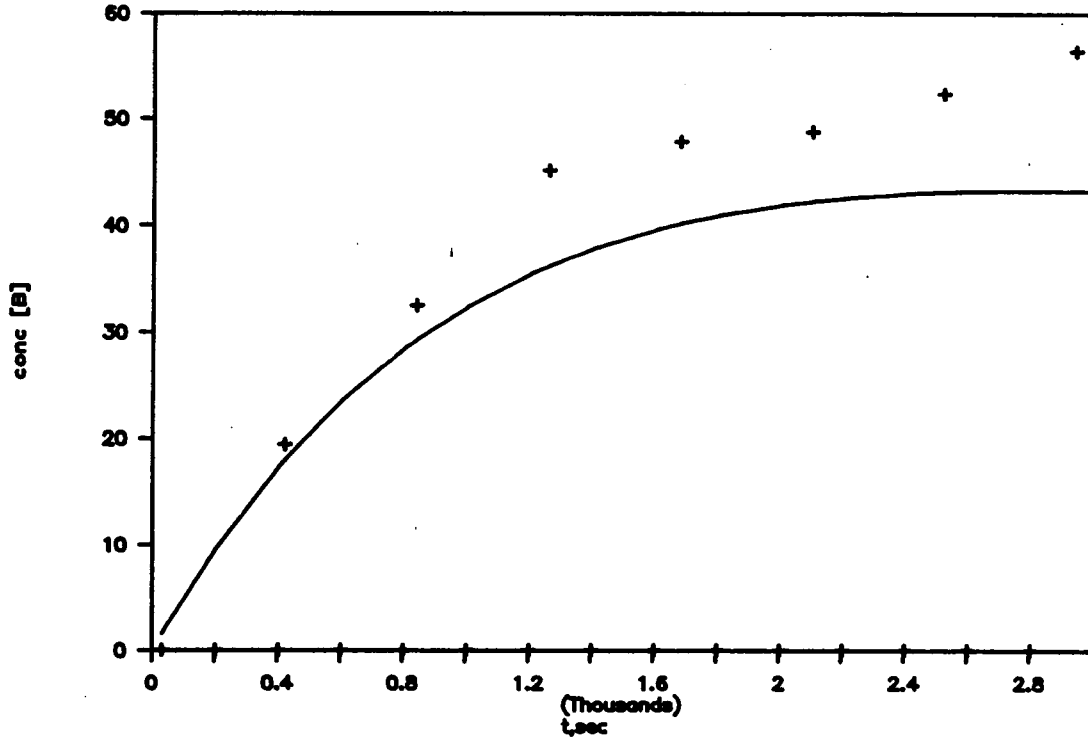

\+ Represents experimental data points for benzyl ketone (39e) formation.

— Represents theoretically generated curve for benzyl ketone (39e) formation.

Figure 45. Comparison plot of experimentally obtained data points with a theoretically generated plot illustrating % concentration versus time for the formation of benzyl ketone (39e) from the thermolysis of benzyl ether (25e) @ 240.0 ± 0.5°C.

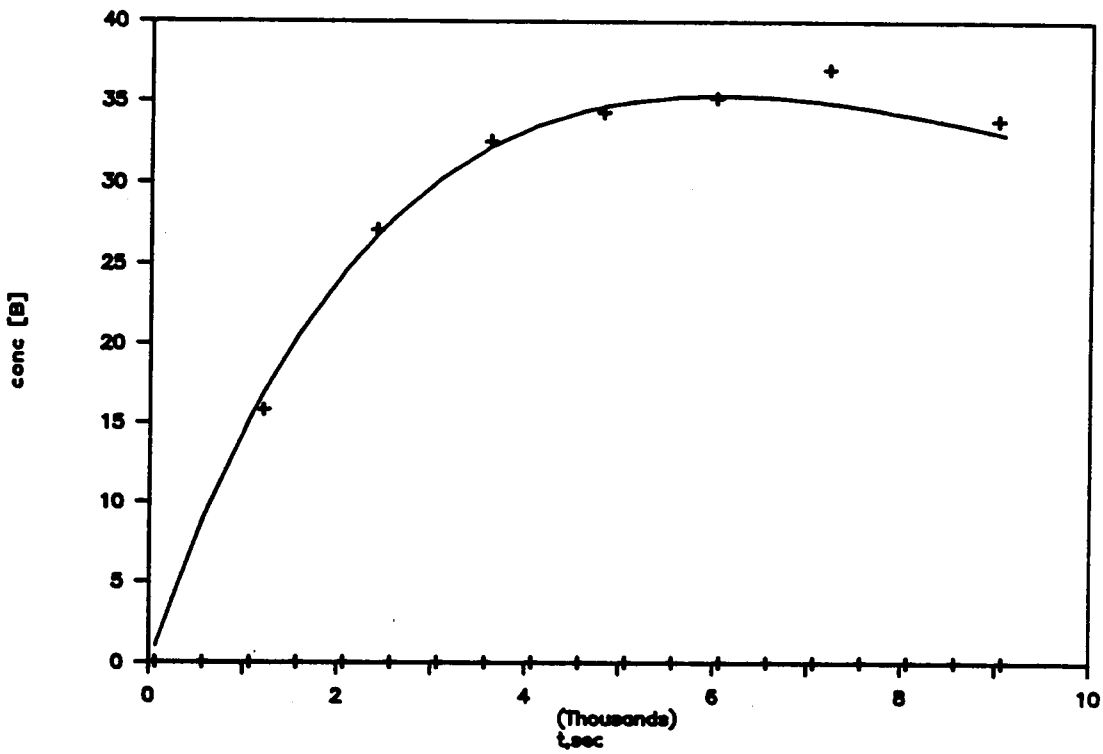

\+ Represents experimental data points for benzyl ketone (39e) formation.

— Represents theoretically generated curve for benzyl ketone (39e) formation.

Figure 46. Comparison plot of experimentally obtained data points with a theoretically generated plot illustrating % concentration versus time for the formation of benzyl ketone (39e) from the thermolysis of benzyl ether (25e) @ 225.0 ± 0.5°C.

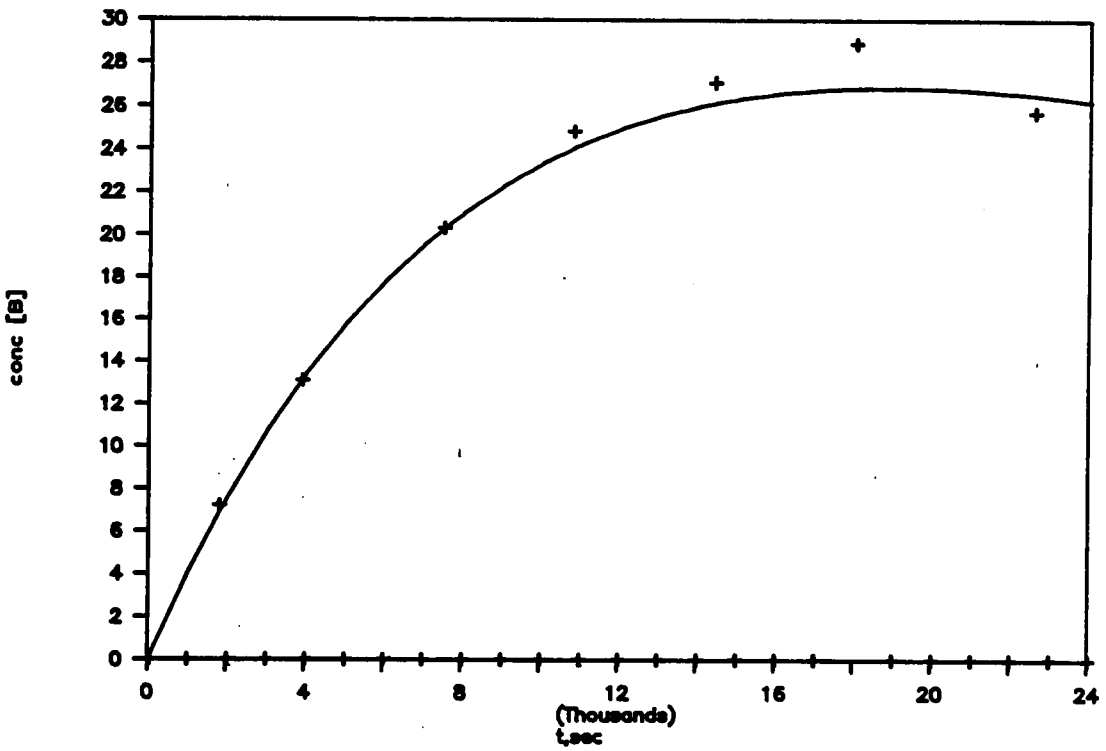

\+ Represents experimental data points for benzyl ketone (39e) formation.

— Represents theoretically generated curve for benzyl ketone (39e) formation.

Figure 47. Comparison plot of experimentally obtained data points with a theoretically generated plot illustrating % concentration versus time for the formation of benzyl ketone (39e) from the thermolysis of benzyl ether (25e) @ 210.0 ± 0.5°C.

Summary

In conclusion, four major points can be made.

First, a comparative study proved the most efficient method of synthesizing the 1,2,3,4,5-pentaphenyl-2,4-cyclopentadiene alkyl ethers (**25a-f**) to be by means of a solvolysis type Williamson ether synthesis. The ethers (**25a-f**) were synthesized in good yield (78-93%) by refluxing the bromo compound (**40**) in the appropriate alcohol to give the corresponding ether.

Second, the enol ethers (**26**) (the product of a [1,5]-sigmatropic phenyl shift in the alkylic ethers (**25a-f**)) can only be synthesized from the enolate (**38**) if a very hard electrophile is used as the alkylating agent. And, these enol ethers can be detected in the ^{1}H NMR as different from the allylic ethers due to an upfield shift of the alkyl protons caused by a shielding effect from the phenyl substituents.

Third, instead of the expected [1,5]-sigmatropic phenyl shift occuring in the 1,2,3,4,5-pentaphenyl-2,4-cyclopentadiene alkyl ethers (**25a-f**) when they are heated to approximately 200°C, a retro ene elimination was observed yielding the hydrocarbon compound (**27**) and the corresponding aldehydes.

And fourth, the thermolysis of the 1,2,3,4,5-pentaphenyl-2,4-cyclopentadiene alkyl ethers meets all the criteria of a retro ene elimination reaction. The reaction, being a concerted cyclic elimination, is unimolecular exhibiting first order kinetics, shows a deuterium isotope effect and displays a negative entropy of activation. The activation energy to reach the transition state of the

retro ene elimination must be lower than the activation energy associated with a [1,5]-sigmatropic phenyl shift in this particular allylic ether system (**25a-f**). This fact is due directly to the geometrical features and constraints of these allylic ethers (**25a-f**).

LITERATURE CITED

1. Youssef A. K.; Ogliaruso, M. A. *J. Org. Chem.* **1972**, 37, 2601.

2. Oldaker, G. B.; Perfetti, T. A.; Ogliaruso, M. A. *J. Org. Chem.* **1980**, 45, 3910.

3. Brubaker, W. F.; Ph.D. Dissertation, Virginia Polytechnic Institute and State University, **1982**.

4. Eagan, R. L.; Ph.D. Dissertation, Virginia Polytechnic Institute and State University, **1986**.

5. Allen, C. F. H.; Van Allan, J. A. *J. Am. Chem. Soc.* **1943**, 65, 1384.

6. Dufraisse, C.; Rio, G.; Ranjon, A. *C. R. Acad. Sci.* **1961**, 253, 244.

7. Woodward, R. B.; Hoffmann, R. *Angew. Chem. Int. Ed.* **1969**, 11, 781.

8. McLean, S.; Haynes, P. *Tetrahedron* **1965**, 21, 2329.

9. Miller, L. L.; Greisinger, R.; Boyer, R. F. *J. Am. Chem. Soc.* **1969**, 91, 1578.

10. Miller, L. L.; Boyer, R. F. *J. Am. Chem. Soc.* **1971**, 93, 650.

11. Breslow, R.; Hoffman, J. H.; Perchonock, C. *Tetrahedron Lett.* **1973**, 3273.

12. Youssef, A. K.; Ogliaruso, M. A. *J. Org. Chem.* **1973**, 38, 487.

13. McCullough, J. J.; McClory, M. R. *J. Am. Chem. Soc.* **1974**, 96.

14. Berg, R. G.; Ogliaruso, M. A.; McNair, H. M. *J. Chromatographic Sci.* **1975**, 13, 69.

15. Davis, D. M.; Ph.D. Dissertation, Virginia Polytechnic Institute and State University, **1985**.

16. DuFraisse, C.; Etienne, A.; Aubry, J. *Compt. Rend* **1954**, 239, 1170.

17. DuFraisse, C. *Experientia, Supplementum II* up 2 **1955**, p. 30.

18. Rio, G.; Ranjon, A.; Dufraisse, C. *Compt. Rend.* **1959**, 1834.

19. Ranjon, A.; Dufraisse, C. *Compt. Rend.* **1962**, 2997.

20. Rio, G.; Ranjon, A.; Dufraisse, C. *Compt. Rend.* **1962**, 2997.

21. Dufraisse, C.; Rio, G.; Liberles, R. *Compt. Rend.* **1963**, 256, 1873.

22. Johnson, J. R.; Grummitt, O. *Organic Synthesis*; Wiley: New York, 1953; Collect. Vol. III, p. 806.

23. Morrison, R. T.; Boyd, R. N. *Organic Chemistry*, 3rd Ed., Allyn and Bacon, Inc.: Boston, 1973.

24. Carey, F. A.; Sundberg, R. J. *Advanced Organic Chemistry*, Part A; Plenum Press: New York, 1977.

25. Ho, T. L. *J. Chem. Ed.* **1978**, 55, 355.

26. Mukhopadhyay, T.; Seebach, D. *Helv. Chem. Acta* **1982**, 65, 385.

27. Smith, G. G.; Kelly, F. W. *Prog. Phys. Org. Chem.* **1961**, 8, 75.

28. Cookson, R. C.; Wallis, S. R. *J. Chem. Soc. (B)* **1966**, 1245.

29. Kwart, H.; Sarner, S. F.; Slutsky, J. *J. Am. Chem. Soc.* **1973**, 95, 5234.

30. Kwart, H.; Sarner, S. F.; Slutsky, J. *J. Am. Chem. Soc.* **1973**, 95, 5242.

31. Lowry, T. H.; Richardson, K. T. *Mechanism and Theory in Organic Chemistry*, 2nd Ed.; Harper & Row, Publishers: New York, 1981.

32. Hoffman, H. M. R. *Angew. Chem. Int. Ed.* **1969**, 8, 556.

33. Gilchrist, T. L.; Stork, R. C. *Organic Reactions and Orbital Symmetry*; Cambridge University Press: London, 1972.

34. Ohloff, G. *Chem. Ber.* **1960**, 93, 2673.

35. Carpenter, *Determination of Organic Reaction Mechanisms*; John Wiley & Sons: New York, 1984, p. 83.

36. Espenson, J. H. *Chemical Kinetics and Reaction Mechanisms*, McGraw-Hill: New York, 1981, p. 55 and p. 65.

37. Daniels, F.; Alberty, R. A. *Physical Chemistry*, 4th Ed., John Wiley & Sons, Inc.: New York, 1975, p. 300-322.

Appendix

A: Derivation of the rate constant (k) for a first-order reaction[36,37]

$$-\frac{d[A]}{dt} = k[A]$$

$$-\frac{d[A]}{[A]} = k\,dt$$

$$-\int_{[A]_1}^{[A]_2} \frac{d[A]}{[A]} = k\int_{t_1}^{t_2} dt$$

$$-(\ln[A]_2 - \ln[A]_1) = k(t_2 - t_1)$$

$$\ln[A]_2 - \ln[A]_1 = -k(t_2 - t_1)$$

$$\ln([A]_2 / [A]_1) = -k(t_2 - t_1)$$

If $t_1 = 0$

$$\ln([A]_2 / [A]_1) = -k t_2$$

$$2.303 \log([A]_2 / [A]_1) = -k t_2$$

$$\log([A]_2 / [A]_1) = -\frac{k}{2.303} t_2$$

$$\log[A]_2 - \log[A]_1 = -\frac{k}{2.303} t_2$$

$$\log[A]_2 = -\frac{k}{2.303} t_2 + \log[A]_1$$

If $[A]_1 = 100\%$

$$\log[A]_2 = -\frac{k}{2.303} t_2 + \log[100]$$

$$\log[A]_2 = -\frac{k}{2.303} t_2 + 2.00$$

Plotting $\log[A]_2$ versus t_2

$$slope = -\frac{k}{2.303}$$

$$k = -2.303\,(slope)$$

$$y_{intercept} = 2.00$$

B: Derivation of the activation energy (E_a) from the Arrhenius equation[36,37]

$$k = Ae^{-E_a/RT}$$

$$\log k = \log A + \log (e^{-E_a/RT})$$

$$\log k = \log A - \frac{E_a}{2.303\ R\ T}$$

Plotting $\log k$ versus $\frac{1}{T}$

$$\text{slope} = -\frac{E_a}{2.303\ R}$$

$$E_a = -2.303\,(R)\,(slope)$$

$$E_a = -2.303\,(1.987\ \text{cal mol}^{-1}\ \text{K}^{-1})\,(slope)$$

$$E_a = -4.576\ \text{cal mol}^{-1}\ \text{K}^{-1}\,(slope)$$

C: Derivation of the enthalpy ($\Delta H^{\neq}$) and entropy ($\Delta S^{\neq}$) of activation from the Eyring equation [36,37]

$$k = \frac{R\,T}{N_A\,h}\; e^{\Delta S^{\neq}/R}\; e^{-\Delta H^{\neq}/RT}$$

where

$$R = 1.987\ \text{cal mol}^{-1}\ \text{K}^{-1}$$

$$N_A = 6.022 \times 10^{23}\ \text{mol}^{-1}$$

$$h = 1.584 \times 10^{-34}\ \text{cal sec}$$

thus

$$k = 2.083 \times 10^{10}\ T\ e^{\Delta S^{\neq}/R}\ e^{-\Delta H^{\neq}/RT}$$

$$\frac{k}{T} = 2.083 \times 10^{10}\ e^{\Delta S^{\neq}/R}\ e^{-\Delta H^{\neq}/RT}$$

$$\log\left(\frac{k}{T}\right) = \log(2.083 \times 10^{10}) + \log\left(e^{\Delta S^{\neq}/R}\right) + \log\left(e^{-\Delta H^{\neq}/RT}\right)$$

$$\log\left(\frac{k}{T}\right) = 10.32 + \frac{\Delta S^{\neq}}{2.303\,R} - \frac{\Delta H^{\neq}}{2.303\,R\,T}$$

Plotting $\log\left(\frac{k}{T}\right)$ versus $\frac{1}{T}$

$$slope = -\frac{\Delta H^{\neq}}{2.303\,R}$$

$$\Delta H^{\neq} = -2.303\,R\,(slope)$$

$$\Delta H^{\neq} = -2.303\,(1.987\ \text{cal mol}^{-1}\ \text{K}^{-1})\,(slope)$$

$$\Delta H^{\neq} = -4.576\ \text{cal mol}^{-1}\ \text{K}^{-1}\,(slope)$$

$$y_{intercept} = \frac{\Delta S^{\neq}}{2.303\,R} + 10.32$$

$$\Delta S^{\neq} = 2.303\,R\,(y_{intercept} - 10.32)$$

$$\Delta S^{\neq} = 2.303\,(1.987\ \text{cal mol}^{-1}\ \text{K}^{-1})\,(y_{intercept} - 10.32)$$

$$\Delta S^{\neq} = 4.576\ \text{cal mol}^{-1}\ \text{K}^{-1}\,(y_{intercept} - 10.32)$$

D: For consecutive first-order reactions[36]:

$$A \xrightarrow{k_1} B \xrightarrow{k_2} C$$

The differential equations and their solutions are:

$$\frac{-d[A]}{dt} = k_1[A]$$

$$[A] = [A]_o \exp(-k_1 t)$$

$$\frac{d[B]}{dt} = k_1[A] - k_2[B]$$

$$\frac{d[B]}{dt} = k_1[A]_o \exp(-k_1 t) - k_2[B]$$

multiplying by exp (k_2t):

$$\exp(k_2 t)\frac{d[B]}{dt} + \exp(k_2 t)[B]k_2 = k_1[A]_o \exp(k_2 - k_1)t$$

integrating where [B] = 0 at t = 0 and rearranging:

$$[B] = \frac{k_1[A]_o}{k_2 - k_1}[\exp(-k_1 t) - \exp(-k_2 t)]$$

differentiation and setting $\frac{d[B]}{dt} = 0$ yields:

$$[B]_{max} = [A]_o\left(\frac{k_2}{k_1}\right)^{k_2/(k_1 - k_2)}$$

$$t_{max} = \frac{\ln(k_2/k_1)}{k_2 - k_1}$$

D: For the proposed case[36]:

A = benzyl ether 25e

B = benzyl ketone 35e

C = decomposition products

D = decomposition products

$$-\frac{d[A]}{dt} = (k_1 + k_2)[A]$$

$$[A] = [A]_o e^{-(k_1 + k_2)T}$$

$$\frac{d[B]}{dt} = k_1[A] - k_3[B] = k_1[A]_o e^{-(k_1 + k_2)t} - k_3[B]$$

$$\frac{d[B]}{dt} e^{k_3 t} + k_3[B]e^{k_3 t} = k_1[A]_o e^{[k_3 - (k_1 + k_2)]t}$$

$$e^{k_3 t} d[B] + [B]k_3 e^{k_3 t} dt = k_1[A]_o e^{[k_3 - (k_1 + k_2)]t} dw$$

Integration yields:

$$[B]e^{k_3 t} = \frac{k_1[A]_o e^{[k_3 - (k_1 + k_2)]t}}{[k_3 - (k_1 + k_2)]}$$

Evaluating at t = 0.

[B] = 0

$$[B]e^{k_3 t} = \left[\frac{k_1[A]_o}{k_3 - (k_1 + k_2)}\right]\left[e^{k_3 - (k_1 + k_2)t} - 1\right]$$

$$[B] = \frac{k_1[A]_o}{k_3 - (k_1 + k_2)}\left[e^{-(k_1 + k_2)t} - e^{-k_3 t}\right]$$

Similarly

$$[D] = \frac{k_2[A]_o}{k_4 - (k_1 + k_2)} \left[e^{-(k_1 + k_2)t} - e^{-k_4 t} \right]$$

E: Data from thermolysis of the pentaphenylcyclopentadiene-alkyl ethers 25a-f

Table IV.

The Thermolysis of 1,2,3,4,5-Pentaphenyl-2,4-cyclopentadiene-1-methyl ether (25a) @ 240.0 ± 0.5°C

Aliquot #	Time (sec)	% Concentration	log (% conc.)
1	60	91	1.96
2	1810	86	1.93
3	3620	79	1.90
4	7200	67	1.83
5	14400	50	1.69
6	21600	37	1.56
7	28800	27	1.44

k

Plotting log (% conc) versus time

k = -2.303 (slope)

$k = 4.04 \times 10^{-5} sec^{-1}$

slope = -1.75×10^{-5}

y intercept = 1.96

corr = 0.999

Table V.

The Formation of 1,2,3,4,5-Pentaphenyl-2,4-Cyclopentadiene (27) from the Thermolysis of 1,2,3,4,5-Pentaphenyl-2,4-Cyclopentadiene-1-methyl ether (25a) @ 240.0 ± 0.5°C.

Aliquot #	Time (sec)	% Concentration	log (% conc.)
1	60	0	-
2	1810	6	0.75
3	3620	11	1.03
4	7200	18	1.25
5	14400	28	1.45
6	21600	34	1.52
7	28800	38	1.58

Table VI.

The Thermolysis of
1,2,3,4,5-Pentaphenyl-2,4-cyclopentadiene-1-methyl ether (25a)
@ 225.0 ± 0.5°C

Aliquot #	Time (sec)	% Concentration	log (% conc.)
1	60	94	1.97
2	2705	90	1.96
3	7200	85	1.93
4	14400	76	1.88
5	25410	67	1.82
6	36000	58	1.77
7	73220	38	1.58
8	79205	35	1.55

k

Plotting log (% conc) versus time

k = -2.303 (slope)

k = $1.23 \times 10^{-5} sec^{-1}$

slope = -5.33×10^{-6}

y intercept = 1.96

corr = 0.999

Table VII.

The Formation of 1,2,3,4,5-Pentaphenyl-2,4-Cyclopentadiene (27) from the Thermolysis of 1,2,3,4,5-Pentaphenyl-2,4-Cyclopentadiene-1-methyl ether (25a) @ 225.0 ± 0.5°C.

Aliquot #	Time (sec)	% Concentration	log (% conc.)
1	60	3	0.45
2	2705	7	0.85
3	7200	12	1.07
4	14400	18	1.26
5	25410	23	1.35
6	36000	29	1.46
7	73220	29	1.46
8	79205	30	1.47

Table VIII.

The Thermolysis of
1,2,3,4,5-Pentaphenyl-2,4-cyclopentadiene-1-methyl ether (25a)
@ 210.0 ± 0.5°C

Aliquot #	Time (sec)	% Concentration	log (% conc.)
1	90	88	1.95
2	12600	85	1.93
3	18000	81	1.91
4	32400	82	1.92
5	39600	78	1.89
6	75840	70	1.84
7	93600	66	1.82

k

Plotting log (% conc) versus time

k = -2.303 (slope)

$k = 3.04 \times 10^{-6} sec^{-1}$

slope = -1.32×10^{-6}

y intercept = 1.94

corr = 0.974

Table IX.

The Formation of 1,2,3,4,5-Pentaphenyl-2,4-Cyclopentadiene (27) from the Thermolysis of 1,2,3,4,5-Pentaphenyl-2,4-Cyclopentadiene-1-methyl ether (25a) @ 210.0 ± 0.5°C.

Aliquot #	Time (sec)	% Concentration	log (% conc.)
1	90	4	0.56
2	12600	7	0.84
3	18000	9	0.95
4	32400	12	1.07
5	39600	13	1.10
6	75840	16	1.20
7	93600	17	1.22

Table X.

The Thermolysis of 1,2,3,4,5-Pentaphenyl-2,4-cyclopentadiene-1-methyl (d_3) ether (25f) @ 240.0 ± 0.5°C

Aliquot #	Time (sec)	% Concentration	log (% conc.)
1	60	94	1.97
2	1800	91	1.96
3	3600	84	1.92
4	7200	84	1.93
5	10800	80	1.90
6	14400	76	1.88
7	21600	67	1.83
8	28800	59	1.77
9	64800	34	1.53
10	79200	27	1.44

k

Plotting log (% conc) versus time

k = -2.303 (slope)

k = $1.55 \times 10^{-5} sec^{-1}$

slope = -6.75×10^{-6}

y intercept = 1.97

corr = 0.998

Table XI.

The Thermolysis of
1,2,3,4,5-Pentaphenyl-2,4-cyclopentadiene-1-methyl (d_3) ether
(25f) @ 225.0 ± 0.5°C

Aliquot #	Time (sec)	% Concentration	log (% conc.)
1	60	94	1.97
2	16200	86	1.93
3	28800	80	1.90
4	42300	74	1.87
5	86400	62	1.80
6	130260	45	1.65
7	172925	36	1.56
8	194405	35	1.54

k

Plotting log (% conc) versus time

k = -2.303 (slope)

k = 5.34 x 10^{-6} sec^{-1}

slope = -2.32 x 10^{-6}

y intercept = 1.97

corr = 0.993

Table XII.

The Thermolysis of 1,2,3,4,5-Pentaphenyl-2,4-cyclopentadiene-1-methyl (d_3) ether (25f) @ 210.0 ± 0.5°C

Aliquot #	Time (sec)	% Concentration	log (% conc.)
1	60	99	1.99
2	46800	93	1.97
3	93600	91	1.96
4	149400	85	1.93
5	179100	82	1.91
6	227100	78	1.89
7	266700	78	1.89
8	318660	71	1.85

k

Plotting log (% conc) versus time

k = -2.303 (slope)

k = 9.81 x 10^{-7}sec^{-1}

slope = -4.26 x 10^{-7}

y intercept = 1.99

corr = 0.986

Table XIII.

The Thermolysis of
1,2,3,4,5-Pentaphenyl-2,4-cyclopentadiene-1-ethyl ether (25b)
@ 240.0 ± 0.5°C

Aliquot #	Time (sec)	% Concentration	log (% conc.)
1	90	93	1.97
2	1800	77	1.89
3	3600	66	1.82
4	7210	47	1.67
5	14400	25	1.40
6	32400	7	0.84

k

Plotting log (% conc) versus time

k = -2.303 (slope)

$k = 7.961 \times 10^{-5} sec^{-1}$

slope = -3.46×10^{-5}

y intercept = 1.94

corr = 0.996

Table XIV.

The Formation of 1,2,3,4,5-Pentaphenyl-2,4-Cyclopentadiene (27) from the Thermolysis of 1,2,3,4,5-Pentaphenyl-2,4-Cyclopentadiene-1-ethyl ether (25b) @ 240.0 ± 0.5°C.

Aliquot #	Time (sec)	% Concentration	log (% conc.)
1	60	5	0.66
2	1800	14	1.14
3	3600	21	1.32
4	7210	33	1.52
5	14400	45	1.65
6	32400	53	1.73

Table XV.

The Thermolysis of
1,2,3,4,5-Pentaphenyl-2,4-cyclopentadiene-1-ethyl ether (25b)
@ 230.0 ± 0.5°C

Aliquot #	Time (sec)	% Concentration	log (% conc.)
1	60	88	1.94
2	1800	79	1.90
3	3690	74	1.87
4	9000	59	1.77
5	19800	41	1.62
6	30600	29	1.47

k

Plotting log (% conc) versus time

k = -2.303 (slope)

$k = 3.25 \times 10^{-5} sec^{-1}$

slope = -1.41×10^{-5}

y intercept = 1.92

corr = 0.996

Table XVI.

The Formation of 1,2,3,4,5-Pentaphenyl-2,4-Cyclopentadiene (27) from the Thermolysis of 1,2,3,4,5-Pentaphenyl-2,4-Cyclopentadiene-1-ethyl ether (25b) @ 230.0 ± 0.5°C.

Aliquot #	Time (sec)	% Concentration	log (% conc.)
1	60	3	0.42
2	1800	5	0.72
3	3690	10	0.99
4	9000	19	1.27
5	19800	32	1.51
6	30600	41	1.61

Table XVII.

The Thermolysis of
1,2,3,4,5-Pentaphenyl-2,4-cyclopentadiene-1-ethyl ether (25b)
@ 220.0 ± 0.5°C

Aliquot #	Time (sec)	% Concentration	log (% conc.)
1	70	93	1.97
2	1800	89	1.95
3	3600	86	1.93
4	10800	75	1.87
5	22200	62	1.79
6	32400	52	1.72
7	73805	27	1.43
8	86400	22	1.35

k

Plotting log (% conc) versus time

k = -2.303 (slope)

k = $1.65 \times 10^{-5} sec^{-1}$

slope = -7.14×10^{-6}

y intercept = 1.96

corr = 0.999

Table XVIII.

The Formation of 1,2,3,4,5-Pentaphenyl-2,4-Cyclopentadiene (27) from the Thermolysis of 1,2,3,4,5-Pentaphenyl-2,4-Cyclopentadiene-1-ethyl ether (25b) @ 220.0 ± 0.5°C.

Aliquot #	Time (sec)	% Concentration	log (% conc.)
1	70	3	0.42
2	1800	5	0.72
3	3600	7	0.82
4	10800	13	1.12
5	22200	20	1.29
6	32400	22	1.35
7	73805	26	1.42
8	86400	25	1.40

Table XIX.

The Thermolysis of
1,2,3,4,5-Pentaphenyl-2,4-cyclopentadiene-1-n-propyl ether (25c)
@ 240.0 ± 0.5°C

Aliquot #	Time (sec)	% Concentration	log (% conc.)
1	60	87	1.94
2	3602	76	1.88
3	7200	61	1.78
4	10805	52	1.71
5	20120	31	1.48
6	23400	27	1.43
7	27150	22	1.35
8	30600	20	1.31

k

Plotting log (% conc) versus time

k = -2.303 (slope)

$k = 4.97 \times 10^{-5} sec^{-1}$

slope = -2.16×10^{-5}

y intercept = 1.94

corr = 0.996

Table XX.

The Formation of 1,2,3,4,5-Pentaphenyl-2,4-Cyclopentadiene (27) from the Thermolysis of 1,2,3,4,5-Pentaphenyl-2,4-Cyclopentadiene-1-n-propyl ether (25c) @ 240.0 ± 0.5°C.

Aliquot #	Time (sec)	% Concentration	log (% conc.)
1	60	0	
2	3602	15	1.16
3	7200	25	1.39
4	10805	36	1.56
5	20120	44	1.64
6	23400	48	1.68
7	27150	47	1.67
8	30600	48	1.69

Table XXI.

The Thermolysis of
1,2,3,4,5-Pentaphenyl-2,4-cyclopentadiene-1-n-propyl ether (25c)
@ 230.0 ± 0.5°C

Aliquot #	Time (sec)	% Concentration	log (% conc.)
1	35	98	1.99
2	1920	90	1.96
3	3620	85	1.93
4	7200	78	1.89
5	10800	70	1.84
6	18000	56	1.75
7	28800	41	1.61
8	39605	32	1.50

k

Plotting log (% conc) versus time

k = -2.303 (slope)

k = $2.84 \times 10^{-5} sec^{-1}$

slope = -1.23×10^{-5}

y intercept = 1.98

corr = 0.997

Table XXII.

The Formation of 1,2,3,4,5-Pentaphenyl-2,4-Cyclopentadiene (27) from the Thermolysis of 1,2,3,4,5-Pentaphenyl-2,4-Cyclopentadiene-1-n-propyl ether (25c) @ 230.0 ± 0.5°C.

Aliquot #	Time (sec)	% Concentration	log (% conc.)
1	35	4	0.59
2	1920	9	0.93
3	3620	12	1.07
4	7200	19	1.29
5	10800	25	1.40
6	18000	34	1.52
7	28800	38	1.58
8	39605	42	1.62

Table XXIII.

The Thermolysis of
1,2,3,4,5-Pentaphenyl-2,4-cyclopentadiene-1-n-propyl ether (25c)
@ 220.0 ± 0.5°C

Aliquot #	Time (sec)	% Concentration	log (% conc.)
1	60	82	1.92
2	3600	75	1.88
3	7200	71	1.85
4	18000	60	1.78
5	68400	31	1.49
6	75600	28	1.45

k

Plotting log (% conc) versus time

k = -2.303 (slope)

k = $1.39 \times 10^{-5} sec^{-1}$

slope = -6.01×10^{-6}

y intercept = 1.90

corr = 0.998

Table XXIV.

The Formation of 1,2,3,4,5-Pentaphenyl-2,4-Cyclopentadiene (27) from the Thermolysis of 1,2,3,4,5-Pentaphenyl-2,4-Cyclopentadiene-1-n-propyl ether (25c) @ 220.0 ± 0.5°C.

Aliquot #	Time (sec)	% Concentration	log (% conc.)
1	60	5	0.71
2	3600	9	0.96
3	7200	12	1.08
4	18000	18	1.26
5	68400	20	1.29
6	75600	19	1.28

Table XXV.

The Thermolysis of
1,2,3,4,5-Pentaphenyl-2,4-cyclopentadiene-1-benzyl ether (25e)
@ 240.0 ± 0.5°C

Aliquot #	Time (sec)	% Concentration	log (% conc.)
1	30	96	1.98
2	420	60	1.77
3	840	38	1.58
4	1260	27	1.43
5	1680	17	1.22
6	2100	11	1.02
7	2520	8	0.88
8	2940	5	0.72

k

Plotting log (% conc) versus time

k = -2.303 (slope)

k = $9.95 \times 10^{-4} sec^{-1}$

slope = -4.32×10^{-4}

y intercept = 1.96

corr = 0.997

Table XXVI.

The Formation of 2-Benzyl-2,3,4,5,5-pentaphenyl-2,4-cyclopentadienone (39e) from the Thermolysis of 1,2,3,4,5-Pentaphenyl-2,4-Cyclopentadiene-1-benzyl ether (25e) @ 240.0 ± 0.5°C.

Aliquot #	Time (sec)	% Concentration	log (% conc.)
1	30	0	-
2	420	19	1.29
3	840	33	1.51
4	1260	45	1.65
5	1680	48	1.68
6	2100	49	1.69
7	2520	52	1.72
8	2940	56	1.75

Table XXVII.

The Formation of 1,2,3,4,5-Pentaphenyl-2,4-Cyclopentadiene (27) from the Thermolysis of 1,2,3,4,5-Pentaphenyl-2,4-Cyclopentadiene-1-benzyl ether (25e) @ 240.0 ± 0.5°C.

Aliquot #	Time (sec)	% Concentration	log (% conc.)
1	30	1	0.14
2	420	10	0.99
3	840	16	1.20
4	1260	22	1.33
5	1680	23	1.37
6	2100	25	1.39
7	2520	27	1.44
8	2940	30	1.48

Table XXVIII.

The Thermolysis of
1,2,3,4,5-Pentaphenyl-2,4-cyclopentadiene-1-benzyl ether (25e)
@ 225.0 ± 0.5°C

Aliquot #	Time (sec)	% Concentration	log (% conc.)
1	60	103	2.01
2	1200	85	1.93
3	2400	45	1.66
4	3600	30	1.48
5	4800	19	1.28
6	6000	12	1.09
7	7200	10	0.98
8	9000	5	0.70

k

Plotting log (% conc) versus time

k = -2.303 (slope)

k = $3.48 \times 10^{-4} sec^{-1}$

slope = -1.51×10^{-4}

y intercept = 2.03

corr = 0.993

Table XXIX.

The Formation of 2-Benzyl-2,3,4,5,5-pentaphenyl-2,4-cyclopentadienone (39e) from the Thermolysis of 1,2,3,4,5-Pentaphenyl-2,4-Cyclopentadiene-1-benzyl ether (25e) @ 225.0 ± 0.5°C.

Aliquot #	Time (sec)	% Concentration	log (% conc.)
1	60	0	-
2	1200	16	1.19
3	2400	27	1.43
4	3600	33	1.51
5	4800	34	1.54
6	6000	35	1.55
7	7200	37	1.56
8	9000	34	1.53

Table XXX.

The Formation of 1,2,3,4,5-Pentaphenyl-2,4-Cyclopentadiene (27) from the Thermolysis of 1,2,3,4,5-Pentaphenyl-2,4-Cyclopentadiene-1-benzyl ether (25c) @ 225.0 ± 0.5°C.

Aliquot #	Time (sec)	% Concentration	log (% conc.)
1	60	2	0.16
2	1200	11	1.04
3	2400	18	1.26
4	3600	22	1.35
5	4800	25	1.40
6	6000	25	1.40
7	7200	29	1.45
8	9000	27	1.43

Table XXXI.

The Thermolysis of
1,2,3,4,5-Pentaphenyl-2,4-cyclopentadiene-1-benzyl ether (25e)
@ 210.0 ± 0.5°C

Aliquot #	Time (sec)	% Concentration	log (% conc.)
1	30	105	2.02
2	1800	85	1.93
3	3900	67	1.83
4	7500	45	1.65
5	10800	32	1.50
6	14400	22	1.33
7	18000	15	1.17
8	22580	9	0.95

k

Plotting log (% conc) versus time

k = -2.303 (slope)

k = $1.09 \times 10^{-4} sec^{-1}$

slope = -4.72×10^{-5}

y intercept = 2.01

corr = 0.999

Table XXXII.

The Formation of 2-Benzyl-2,3,4,5,5-pentaphenyl-2,4-cyclopentadienone (39e) from the Thermolysis of 1,2,3,4,5-Pentaphenyl-2,4-Cyclopentadiene-1-benzyl ether (25e) @ 210.0 ± 0.5°C.

Aliquot #	Time (sec)	% Concentration	log (% conc.)
1	30	0	-
2	1800	7	0.86
3	3900	13	1.12
4	7500	20	1.31
5	10800	25	1.39
6	14400	27	1.43
7	18000	29	1.46
8	22580	26	1.41

Table XXXIII.

The Formation of 1,2,3,4,5-Pentaphenyl-2,4-Cyclopentadiene (27) from the Thermolysis of 1,2,3,4,5-Pentaphenyl-2,4-Cyclopentadiene-1-benzyl ether (25e) @ 210.0 ± 0.5°C.

Aliquot #	Time (sec)	% Concentration	log (% conc.)
1	30	0	-
2	1800	6	0.80
3	3900	11	1.04
4	7500	17	1.24
5	10800	22	1.33
6	14400	26	1.41
7	18000	26	1.41
8	22580	26	1.42

F: Decomposition of 1,2,3,4,5-Pentaphenyl-2,4-Cyclopentadiene 27 @ 240.0-210.0°C.

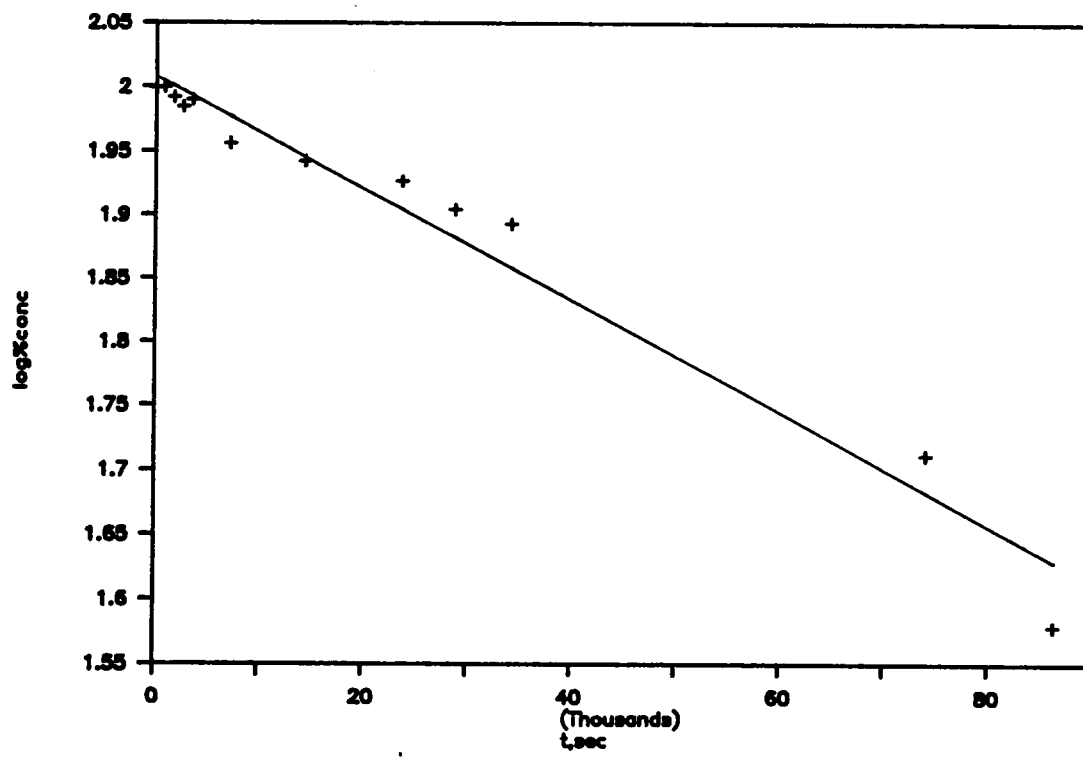

k

plotting log (% conc) versus time

k = -2.303 (slope)

k = 9.47 x 10^{-6} sec^{-1}

slope = -4.11 x 10^{-6}

y intercept = 2.02

corr = 0.968

Figure 48. The thermal decomposition of hydrocarbon (27) @ 240.0 ± 0.5°C.

Table XXXIV.

The Thermal Decomposition of Hydrocarbon (27) @ 240.0 ± 0.5°C.

Aliquot #	Time (sec)	% Concentration	log (% conc.)
1	60	100	2.00
2	900	100	2.00
3	1800	99	1.99
4	2700	97	1.99
5	3600	98	1.99
6	7200	91	1.96
7	14400	88	1.94
8	23700	85	1.93
9	28800	81	1.91
10	34200	79	1.89
11	74100	52	1.72
12	86400	38	1.58

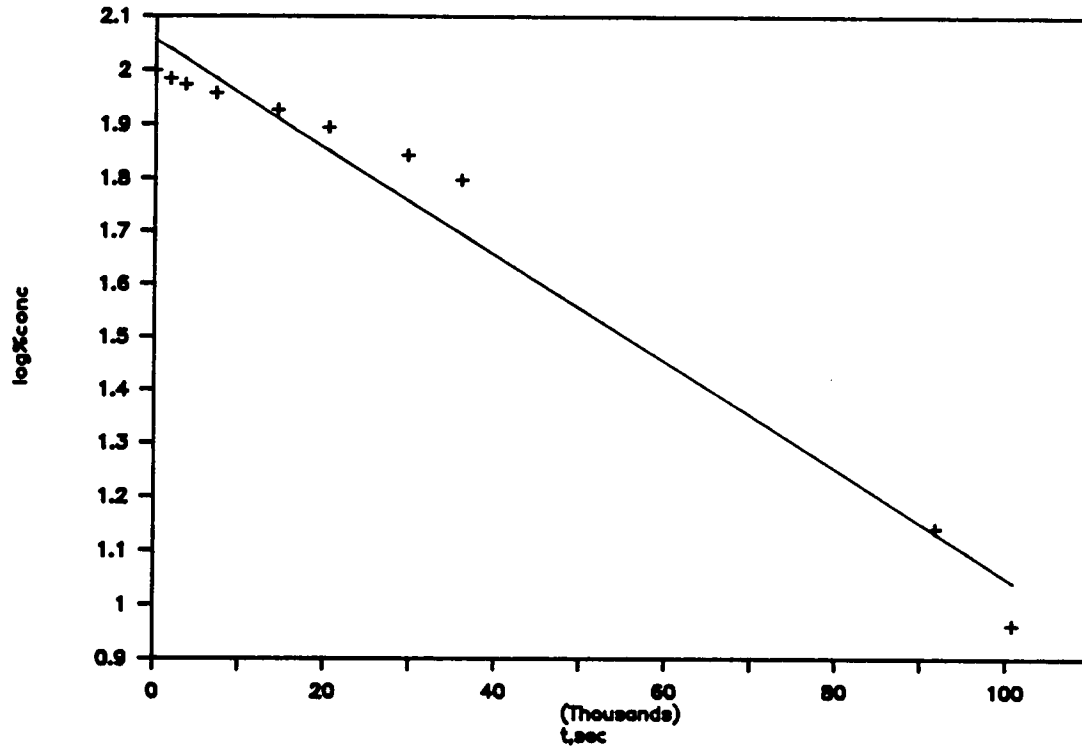

k

plotting log (% conc) versus time	slope = -8.34×10^{-6}
k = -2.303 (slope)	y intercept = 2.06
k = $1.92 \times 10^{-5} sec^{-1}$	corr = 0.980

Figure 49. The thermal decomposition of hydrocarbon (27) @ 230.0 ± 0.5°C.

Table XXXV.

The Thermal Decomposition of Hydrocarbon (27) @ 230.0 ± 0.5°C.

Aliquot #	Time (sec)	% Concentration	log (% conc.)
1	60	100	2.00
2	1800	97	1.99
3	3600	94	1.97
4	7200	91	1.96
5	14400	85	1.93
6	20400	79	1.90
7	29700	70	1.85
8	36000	63	1.80
9	91800	14	1.15
10	100800	9	0.95

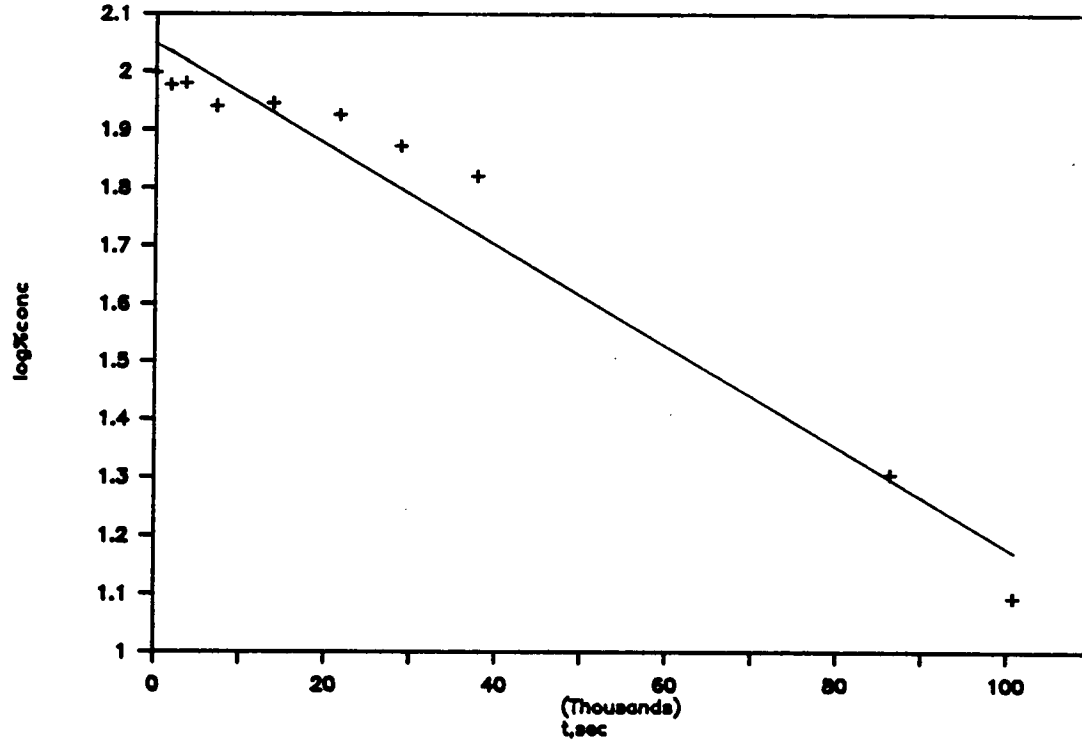

k

plotting log (% conc) versus time

k = -2.303 (slope)

k = $1.83 \times 10^{-5} sec^{-1}$

slope = -7.93×10^{-6}

y intercept = 2.05

corr = 0.965

Figure 50. The thermal decomposition of hydrocarbon (27) @ 225.0 ± 0.5°C.

Table XXXVI.

The Thermal Decomposition of Hydrocarbon (27) @ 225.0 ± 0.5°C.

Aliquot #	Time (sec)	% Concentration	log (% conc.)
1	60	100	2.00
2	1800	95	1.98
3	3600	96	1.98
4	7200	88	1.94
5	13800	89	1.95
6	21600	85	1.93
7	28800	75	1.88
8	37800	67	1.83
9	86400	21	1.32
10	100800	13	1.11

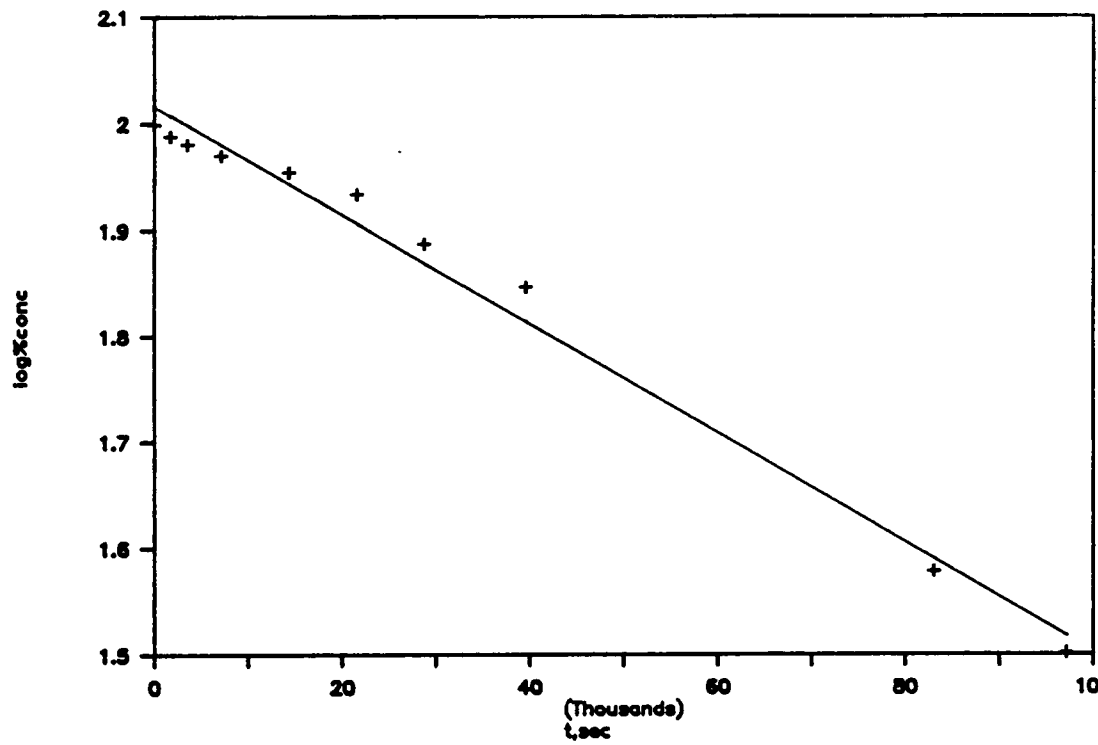

k

plotting log (% conc) versus time	slope = -4.72×10^{-6}
k = -2.303 (slope)	y intercept = 2.03
k = $1.09 \times 10^{-5} sec^{-1}$	corr = 0.988

Figure 51. The thermal decomposition of hydrocarbon (27) @ 220.0 ± 0.5°C.

Table XXXVII.

The Thermal Decomposition of Hydrocarbon (27) @ 220.0 ± 0.5°C.

Aliquot #	Time (sec)	% Concentration	log (% conc.)
1	68	100	2.00
2	1800	97	1.99
3	3600	96	1.98
4	7200	93	1.97
5	14400	90	1.95
6	21600	86	1.93
7	28804	77	1.88
8	39600	70	1.85
9	83100	38	1.58
10	97200	32	1.51

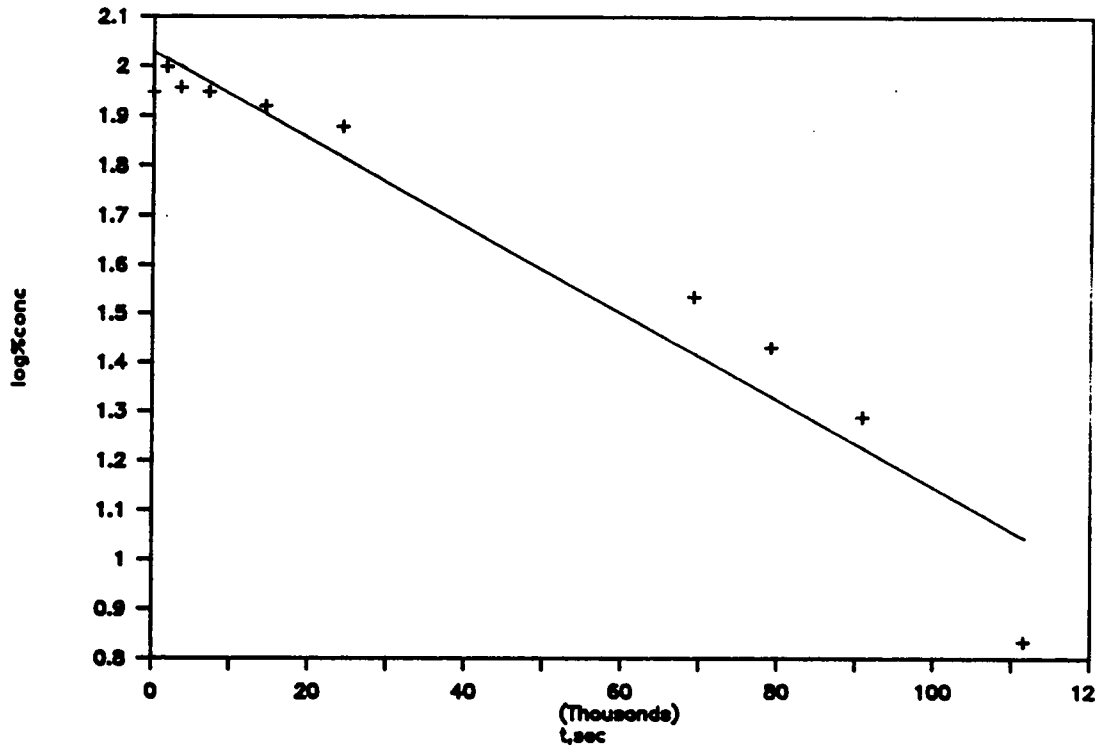

k

plotting log (% conc) versus time	slope = 6.66×10^{-6}
k = -2.303 (slope)	y intercept = 2.05
k = $1.53 \times 10^{-5} sec^{-1}$	corr = 0.974

Figure 52. The thermal decomposition of hydrocarbon (27) @ 210.0 ± 0.5°C.

Table XXXVIII.

The Thermal Decomposition of Hydrocarbon (27) @ 210.0 ± 0.5°C.

Aliquot #	Time (sec)	% Concentration	log (% conc.)
1	60	89	1.95
2	1800	100	2.00
3	3600	91	1.96
4	7200	88	1.94
5	14400	83	1.92
6	24300	75	1.88
7	69300	34	1.53
8	79200	27	1.43
9	90900	19	1.28
10	111600	7	0.84

G: Decomposition of 2-Benzyl-2,3,4,5,5-Pentaphenyl-2,4-Cyclopentadienone 39e @ 240.0-210.0°C.

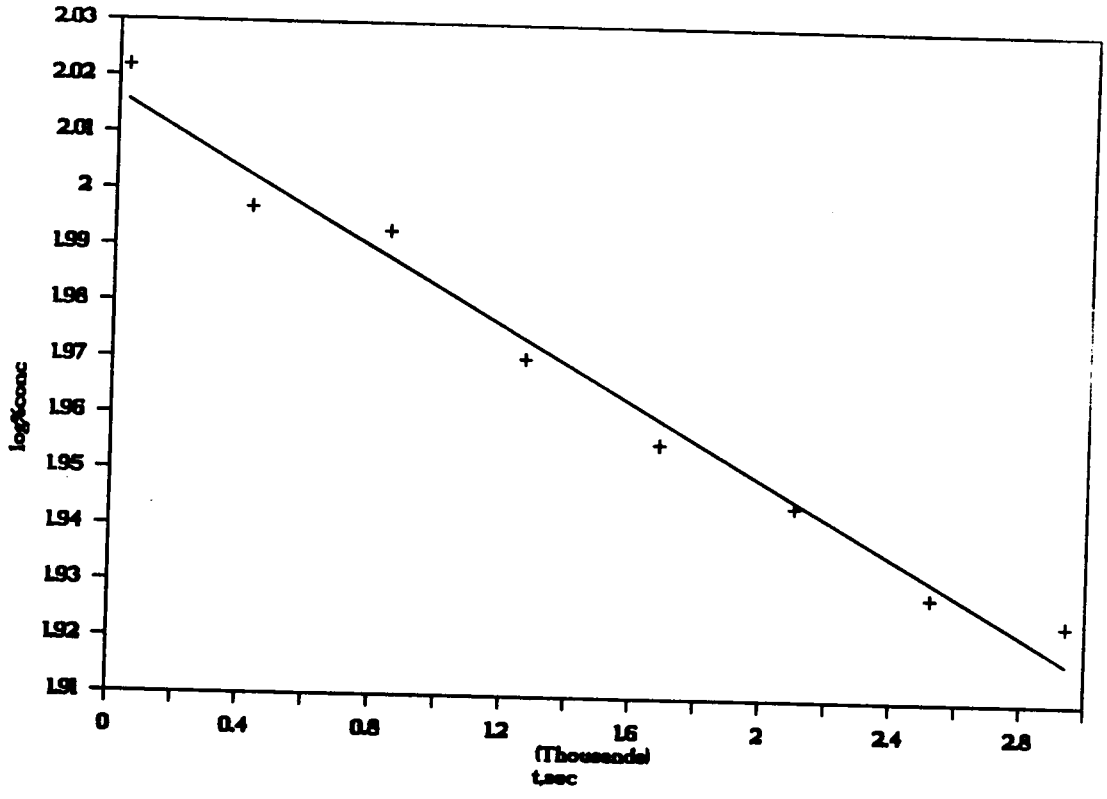

k

plotting log (% conc) versus time

k = -2.303 (slope)

k = 7.78 x 10^{-5}sec^{-1}

slope = -3.38 x 10^{-5}

y intercept = 2.01

corr = 0.979

Figure 53. The thermal decomposition of benzyl ketone (39e) @ 240.0 ± 0.5°C.

Table XXXIX.

The Thermal Decomposition of Benzyl Ketone (39c) @ 240.0 ± 0.5°C.

Aliquot #	Time (sec)	% Concentration	log (% conc.)
1	30	105	2.02
2	420	99	2.00
3	840	98	1.99
4	1260	93	1.97
5	1680	90	1.96
6	2100	88	1.94
7	2520	85	1.93
8	2940	84	1.92

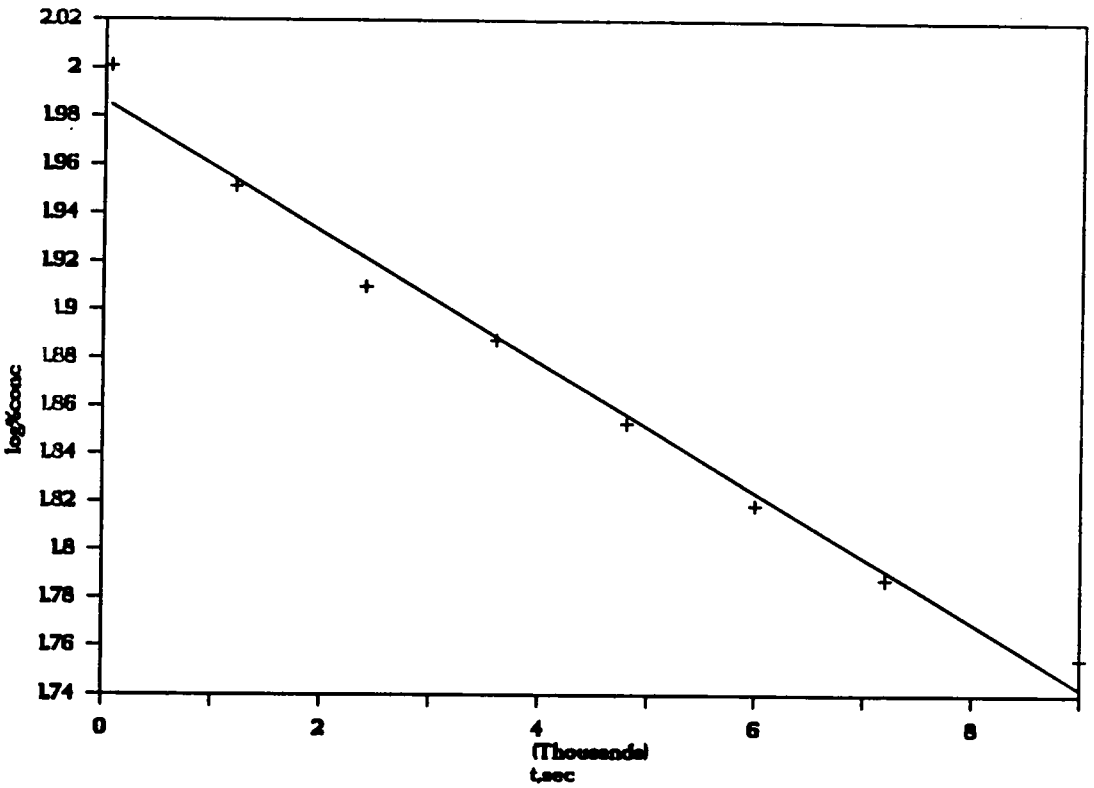

k

plotting log (% conc) versus time	slope = -2.71×10^{-5}
k = -2.303 (slope)	y intercept = 1.98
k = $6.24 \times 10^{-5} sec^{-1}$	corr = 0.987

Figure 54. The thermal decomposition of benzyl ketone (39e) @ 225.0 ± 0.5°C.

Table XXXX.

The Thermal Decomposition of Benzyl Ketone (39e) @ 225.0 ± 0.5°C.

Aliquot #	Time (sec)	% Concentration	log (% conc.)
1	60	100	2.00
2	1200	89	1.95
3	2400	81	1.91
4	3600	77	1.89
5	4800	71	1.85
6	6000	66	1.82
7	7200	61	1.79
8	9000	57	1.75

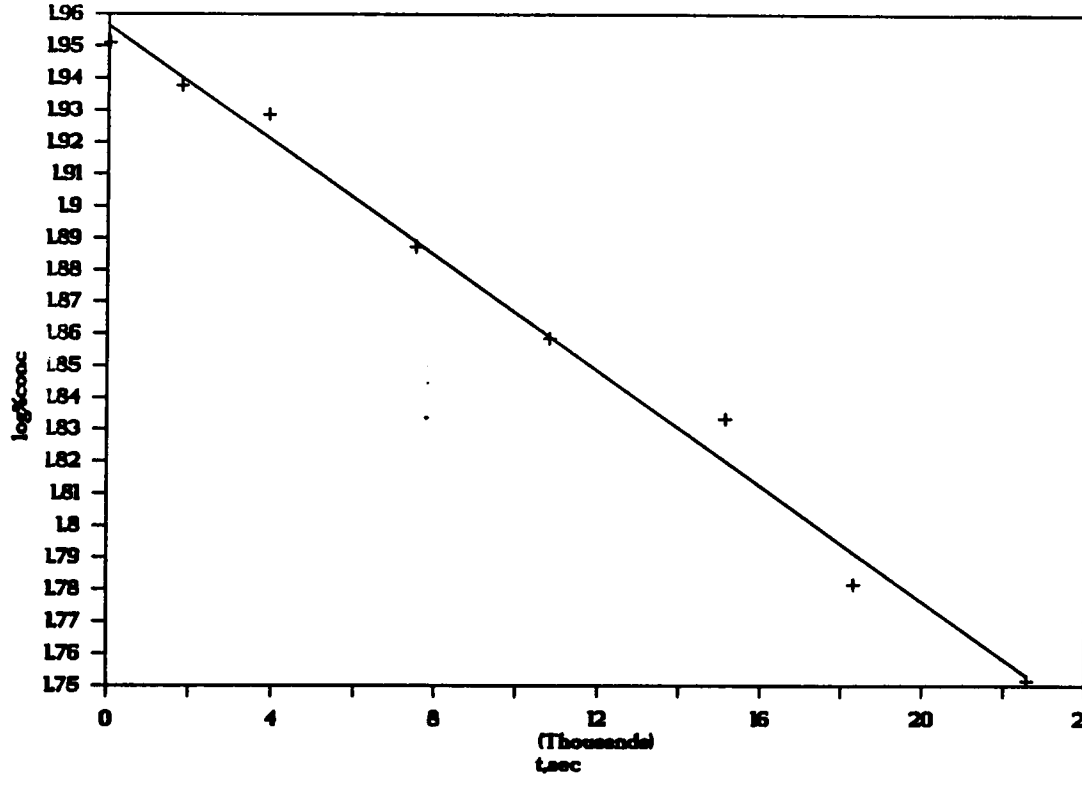

k

plotting log (% conc) versus time

k = -2.303 (slope)

k = 2.08 x 10^{-5}sec^{-1}

slope = -9.02 x 10^{-6}

y intercept = 1.95

corr = 0.990

Figure 55. The thermal decomposition of benzyl ketone (39e) @ 210.0 ± 0.5°C.

Table XXXXI.

The Thermal Decomposition of Benzyl Ketone (39e) @ 210.0 ± 0.5°C.

Aliquot #	Time (sec)	% Concentration	log (% conc.)
1	30	89	1.95
2	1800	87	1.94
3	3900	85	1.93
4	7500	77	1.89
5	10800	72	1.86
6	15120	68	1.83
7	18300	61	1.78
8	22580	56	1.75

H: Calculation of $[B]_{max}$ and t_{max} for the formation of hydrocarbon (27) from the thermolysis of the pentaphenylcyclopentadiene-alkyl ethers (25a-f)

Ether	Temperature (°C)	$[B]_{max}$	t_{max}
25a	240	38.47	46928.59
[B] = **27**	225	27.45	66374.94
	210	11.70	131610.05
25b	240	64.62	30376.38
[B] = **27**	230	38.47	39596.24
	220	40.51	74237.96
25c	240	59.51	41235.52
[B] = **27**	230	42.08	42563.16
	220	32.63	81847.79
25e	240	26.54	3946.6
[B] = **27**	225	31.48	8946.0
	210	25.40	20973.95
25e	240	43.6	2780.0
[B] = **39e**	225	35.38	6024.0
	210	26.90	18819.39

I: Kinetic data on pentaphenyl cyclopentadiene ethers (25a-f)

Calculation of the E_a, $\Delta H^{\neq}$ and $\Delta S^{\neq}$ for the thermolysis of 1,2,3,4,5-pentaphenyl-2,4-cyclopentadiene-1-methyl ether (25a)

For the case $A \overset{k_1}{\rightarrow} B \overset{k_2}{\rightarrow} C$

$\quad\; k_3$

$\quad\; D$

assume $k_3 <<< k_1 \quad k_3 \simeq 0$

therefore $k_{obs} = k_1$ *(at maximum)*

Temperature 0°C	°K	k sec^{-1}	1/T $°K^{-1}$	log k	log (k/T)
240	513.15	4.04×10^{-5}	1.949×10^{-3}	-4.394	-7.104
225	498.15	1.23×10^{-5}	2.007×10^{-3}	-4.910	-7.607
210	483.15	3.53×10^{-6}	2.070×10^{-3}	-5.452	-8.136

E_a

Plotting log k versus 1/T

E_a = -4.576 cal $mol^{-1}K^{-1}$(slope)

E_a = 40.0 kcal mol^{-1}

slope = -8.742×10^3

y intercept = 12.64

corr = 0.999

<u>$\Delta H^{\neq}$&$\Delta S^{\neq}$</u>

Plotting log (k/T) versus 1/T

$\Delta H^{\neq}$ = -4.576 cal $mol^{-1}K^{-1}$ (slope)

$\Delta H^{\neq}$ = 39.0 kcal $mol^{-1}K^{-1}$

slope = -8.527×10^3

y intercept = 9.51

corr = 0.999

$\Delta S^{\neq}$ = 4.576 cal $mol^{-1}K^{-1}$ (y intercept -10 .32)

$\Delta S^{\neq}$ = -3.7 cal $mol^{-1}K^{-1}$

Calculation of the E_a, $\Delta H^{\neq}$ and $\Delta S^{\neq}$ for the thermolysis of 1,2,3,4,5-pentaphenyl-2,4-cyclopentadiene-1-methyl (d_3) ether (25f)

For the case $A \xrightarrow{k_1} B \xrightarrow{k_2} C$

k_3

D

assume $k_3 <<< k_1 \quad k_3 \simeq 0$

therefore $k_{obs} = k_1$ *(at maximum)*

0°C	Temperature °K	k sec^{-1}	1/T $°K^{-1}$	log k	log (k/T)
240	513.15	1.55×10^{-5}	1.949×10^{-3}	-4.810	-7.520
225	498.15	5.34×10^{-6}	2.007×10^{-3}	-5.272	-7.970
210	483.15	9.81×10^{-7}	2.070×10^{-3}	-6.008	-8.692

E_a

Plotting log k versus 1/T

slope = -9.926×10^3

E_a = -4.576 cal $mol^{-1}K^{-1}$(slope)

y intercept = 14.58

E_a = 45.4 kcal mol^{-1}

corr = 0.988

$\Delta H^{\neq}$&$\Delta S^{\neq}$

Plotting log (k/T) versus 1/T

$\Delta H^{\neq}$ = -4.576 cal $mol^{-1}K^{-1}$ (slope)

slope = -9.711×10^3

$\Delta H^{\neq}$ = 44.4 kcal $mol^{-1}K^{-1}$

y intercept = 11.45

corr = 0.988

$\Delta S^{\neq}$ = 4.576 cal $mol^{-1}K^{-1}$ (y intercept -10 .32)

$\Delta S^{\neq}$ = 5.17 cal $mol^{-1}K^{-1}$

Calculation of the E_a, $\Delta H^{\neq}$ and $\Delta S^{\neq}$ for the thermolysis of 1,2,3,4,5-pentaphenyl-2,4-cyclopentadiene-1-ethyl ether (25b)

For the case $A \xrightarrow{k_1} B \xrightarrow{k_2} C$

k_3

D

assume $k_3 <<< k_1 \quad k_3 \simeq 0$

therefore $k_{obs} = k_1$ *(at maximum)*

Temperature 0°C	°K	k sec^{-1}	1/T °K^{-1}	log k	log (k/T)
240	513.15	7.96 x 10^{-5}	1.949 x 10^{-3}	-4.099	-6.809
230	503.15	3.25 x 10^{-5}	1.987 x 10^{-3}	-4.488	-7.190
220	493.15	1.65 x 10^{-5}	2.028 x 10^{-3}	-4.783	-7.475

E_a

Plotting log k versus 1/T

E_a = -4.576 cal mol^{-1}K^{-1}(slope)

E_a = 39.5 kcal mol^{-1}

slope = -8.639 x 10^3

y intercept = 12.72

corr = 0.989

<u>$\Delta H^{\neq}$&$\Delta S^{\neq}$</u>

Plotting log (k/T) versus 1/T

$\Delta H^{\neq}$ = -4.576 cal mol^{-1}K^{-1} (slope)

$\Delta H^{\neq}$ = 38.5 kcal mol^{-1}K^{-1}

slope = -8.410 x 10^3

y intercept = 9.56

corr = 0.989

$\Delta S^{\neq}$ = 4.576 cal mol^{-1}K^{-1} (y intercept -10 .32)

$\Delta S^{\neq}$ = -3.48 cal mol^{-1}K^{-1}

Calculation of the E_a, $\Delta H^{\neq}$ and $\Delta S^{\neq}$ for the thermolysis of 1,2,3,4,5-pentaphenyl-2,4-cyclopentadiene-1-n-propyl ether (25c)

For the case $A \xrightarrow{k_1} B \xrightarrow{k_2} C$, $A \xrightarrow{k_3} D$

assume $k_3 < < < k_1 \quad k_3 \simeq 0$
therefore $k_{obs} = k_1$ *(at maximum)*

0°C	Temperature °K	k sec^{-1}	1/T $°K^{-1}$	log k	log (k/T)
240	513.15	4.97×10^{-5}	1.949×10^{-3}	-4.304	-7.014
230	503.15	2.84×10^{-5}	1.987×10^{-3}	-4.547	-7.248
220	493.15	1.37×10^{-5}	2.028×10^{-3}	-4.864	-7.557

E_a

Plotting log k versus 1/T

slope = -7.097×10^3

E_a = -4.576 cal $mol^{-1}K^{-1}$(slope)

y intercept = 9.537

E_a = 32.43 kcal mol^{-1}

corr = 0.997

<u>$\Delta H^{\neq}$&$\Delta S^{\neq}$</u>

Plotting log (k/T) versus 1/T

$\Delta H^{\neq}$ = -4.576 cal $mol^{-1}K^{-1}$ (slope)

slope = -6.882×10^3

$\Delta H^{\neq}$ = 31.49 kcal $mol^{-1}K^{-1}$

y intercept = 6.409

corr = 0.996

$\Delta S^{\neq}$ = 4.576 cal $mol^{-1}K^{-1}$ (y intercept -10 .32)

$\Delta S^{\neq}$ = -17.8 cal $mol^{-1}K^{-1}$

Calculation of the E_a, $\Delta H^{\neq}$ and $\Delta S^{\neq}$ for the formation of benzyl ketone (39e) from the thermolysis of 1,2,3,4,5-pentaphenyl-2,4-cyclopentadiene-1-benzyl ether (25e)

For the case $A \xrightarrow{k_1} B \xrightarrow{k_3} C$ $\quad$ B = *benzyl ketone* 39e

k_2, k_4: $D \rightarrow E$

$$[B] = \frac{k_1[A]_o}{k_3 - (k_1 + k_2)}\left[e^{-(k_1 + k_2)t} - e^{-k_3 t}\right]$$

solve for k_1

0°C	Temperature °K	k sec^{-1}	1/T $°K^{-1}$	log k	log (k/T)
240	513.15	5.86×10^{-4}	1.949×10^{-3}	-3.232	-5.9423
225	498.15	1.64×10^{-4}	2.007×10^{-3}	-3.785	-6.4826
210	483.15	4.2×10^{-5}	2.070×10^{-3}	-4.377	-7.0607

E_a

Plotting log k versus 1/T

slope = -9.461×10^3

E_a = -4.576 cal $mol^{-1}K^{-1}$(slope)

y intercept = 15.2

E_a = 43.3 kcal mol^{-1}

corr = 0.999

<u>$\Delta H^{\neq}$&$\Delta S^{\neq}$</u>

Plotting log (k/T) versus 1/T

$\Delta H^{\neq}$ = -4.576 cal $mol^{-1}K^{-1}$ (slope)

slope = -9.242×10^3

$\Delta H^{\neq}$ = 42.29 kcal $mol^{-1}K^{-1}$

y intercept = 12.068

corr = 0.999

$\Delta S^{\neq}$ = 4.576 cal $mol^{-1}K^{-1}$ (y intercept -10 .32)

$\Delta S^{\neq}$ = 8.0 cal $mol^{-1}K^{-1}$

Calculation of the E_a, $\Delta H^{\neq}$ and $\Delta S^{\neq}$ for the formation of hydrocarbon (27) from the thermolysis of 1,2,3,4,5-pentaphenyl-2,4-cyclopentadiene-1-benzyl ether (25e)

For the case $A \xrightarrow{k_1} B \xrightarrow{k_3} C$, $D \xrightarrow{k_4} E$ (with k_2) D = *hydrocarbon 27*

$$[D] = \frac{k_2[A]_o}{k_4 - (k_1 + k_2)} \left[e^{-(k_1 + k_2)t} - e^{-k_4 t}\right]$$

solve for k_2

0°C	Temperature °K	k sec^{-1}	1/T $°K^{-1}$	log k	log (k/T)
240	513.15	3.125×10^{-4}	1.949×10^{-3}	-3.505	-6.198
225	498.15	1.18×10^{-4}	2.007×10^{-3}	-4.432	-6.626
210	483.15	3.7×10^{-5}	2.070×10^{-3}	-3.928	-7.1158

E_a

Plotting log k versus 1/T

slope = -7.205×10^3

E_a = -4.576 cal $mol^{-1}K^{-1}$(slope)

y intercept = 10.535

E_a = 33.0 kcal mol^{-1}

corr = 0.999

<u>$\Delta H^{\neq}$&$\Delta S^{\neq}$</u>

Plotting log (k/T) versus 1/T

$\Delta H^{\neq}$ = -4.576 cal $mol^{-1}K^{-1}$ (slope)

slope = -7.589×10^3

$\Delta H^{\neq}$ = 34.73 kcal $mol^{-1}K^{-1}$

y intercept = 8.596

corr = 0.999

$\Delta S^{\neq}$ = 4.576 cal $mol^{-1}K^{-1}$ (y intercept -10 .32)

$\Delta S^{\neq}$ = -7.8852 cal $mol^{-1}K^{-1}$

J: Arrhenius and Eyring Plots for the Pentaphenylcyclopentadiene ethers (25a-f)

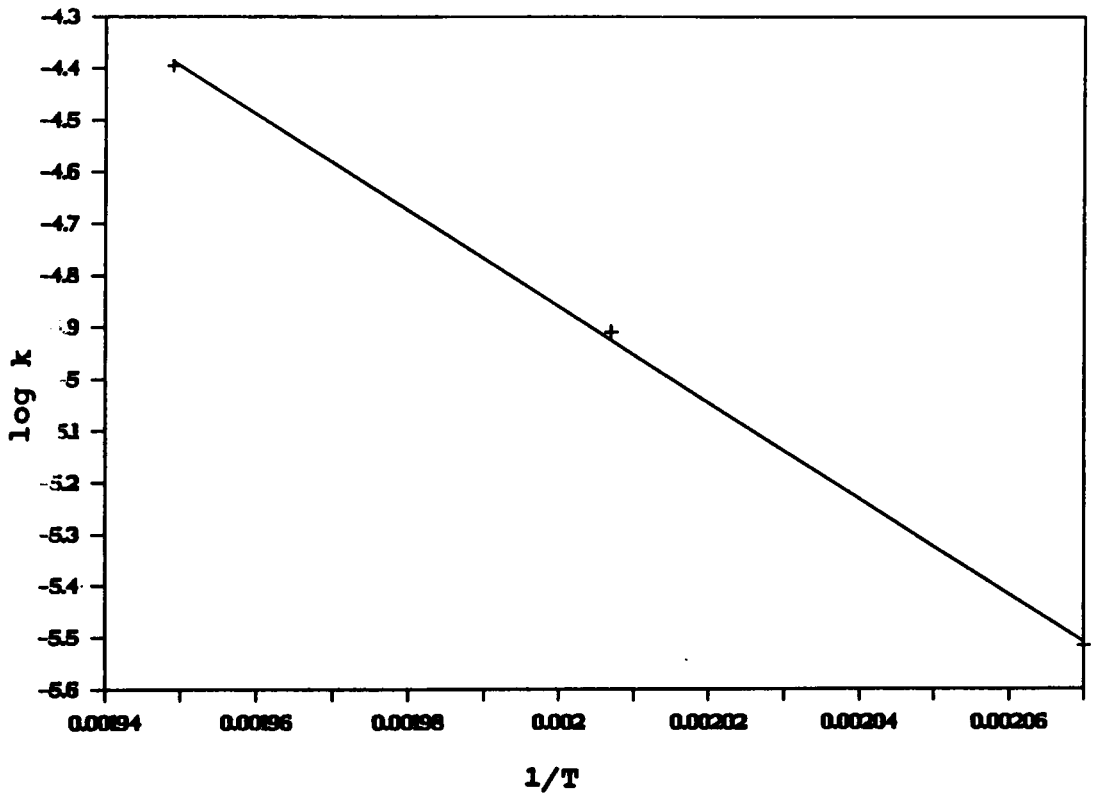

Figure 56. Arrhenius plot of the thermolysis of 1,2,3,4,5-pentaphenyl-2,4-cyclopentadiene-1-methyl ether (25a).

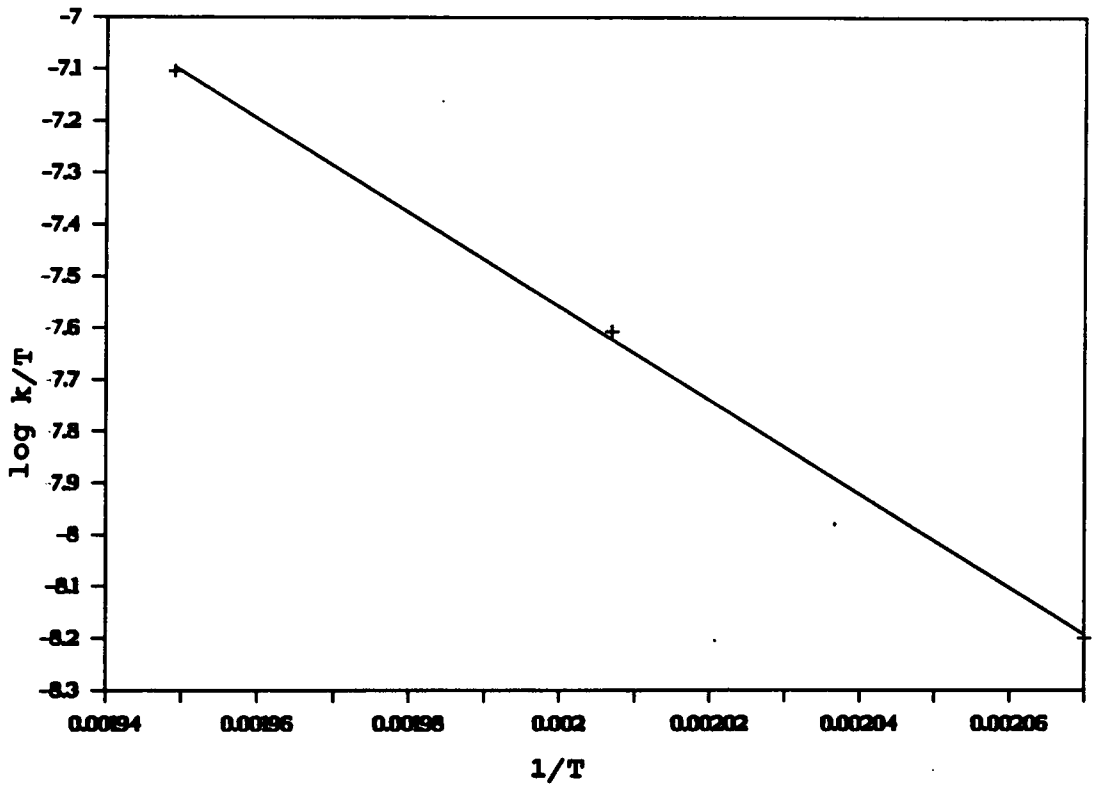

Figure 57. Eyring plot of the thermolysis of 1,2,3,4,5-pentaphenyl-2,4-cyclopentadiene-1-methyl ether (25a).

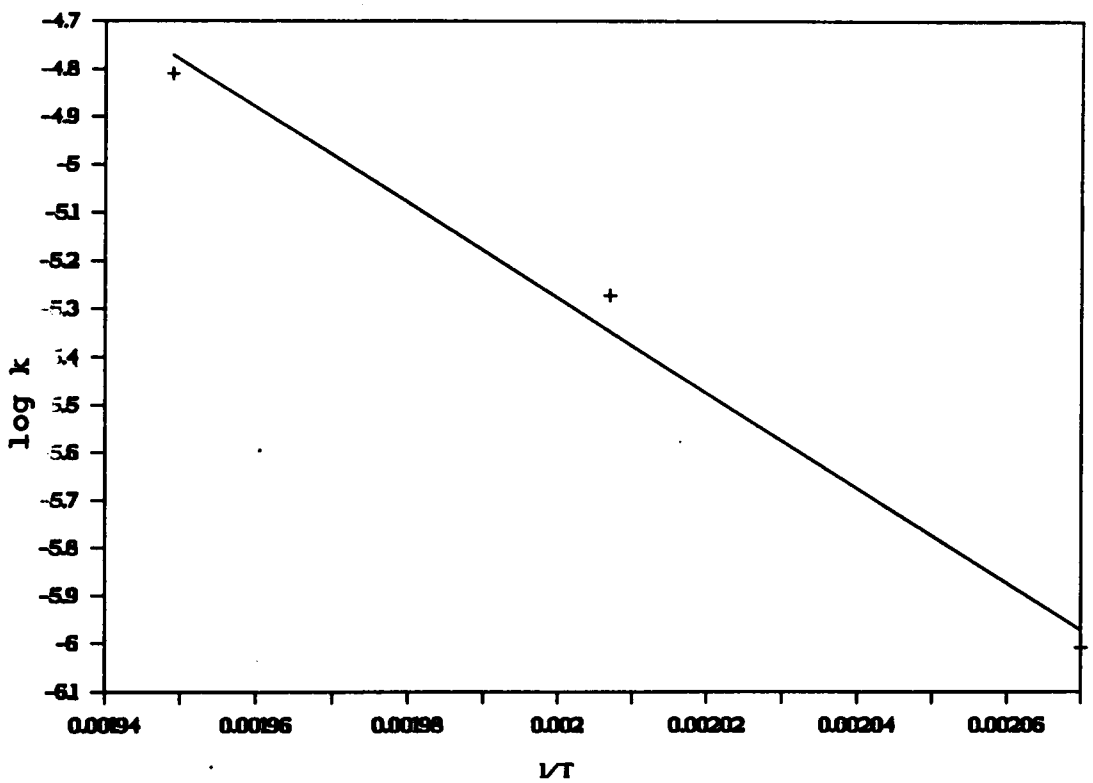

Figure 58. Arrhenius plot of the thermolysis of 1,2,3,4,5-pentaphenyl-2,4-cyclopentadiene-1-methyl (d_3) ether (25f).

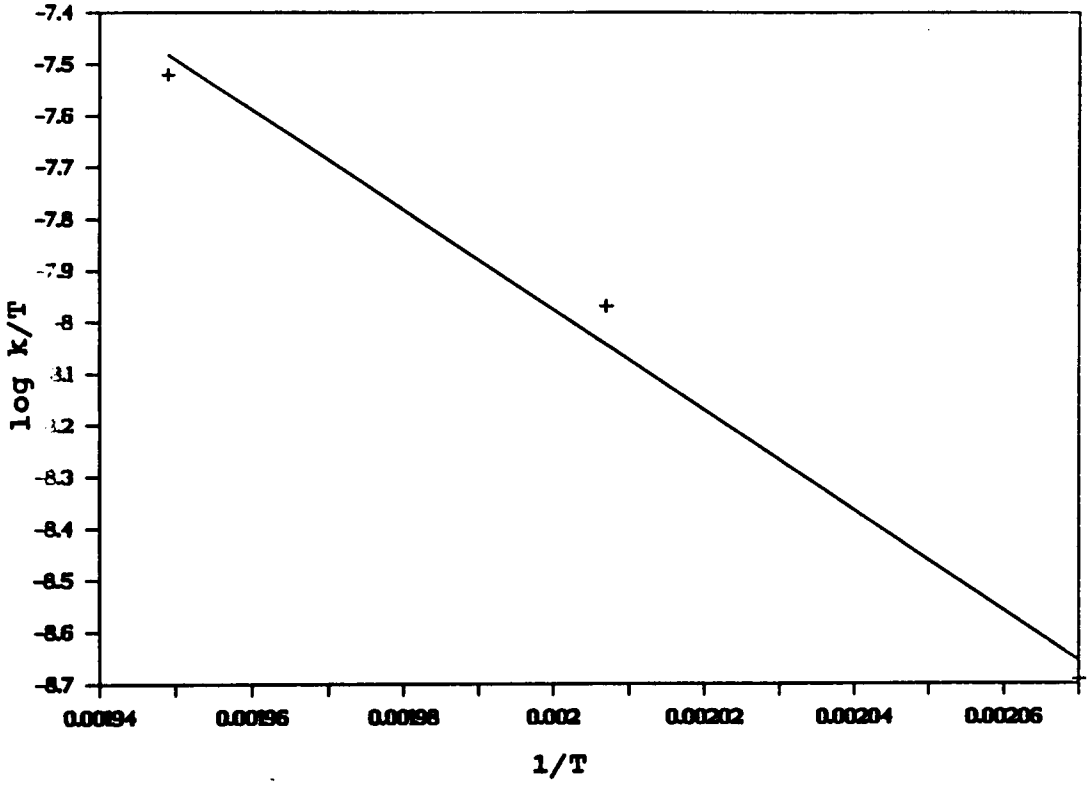

Figure 59. Eyring plot of the thermolysis of 1,2,3,4,5-pentaphenyl-2,4-cyclopentadiene-1-methyl (d_3) ether (25f).

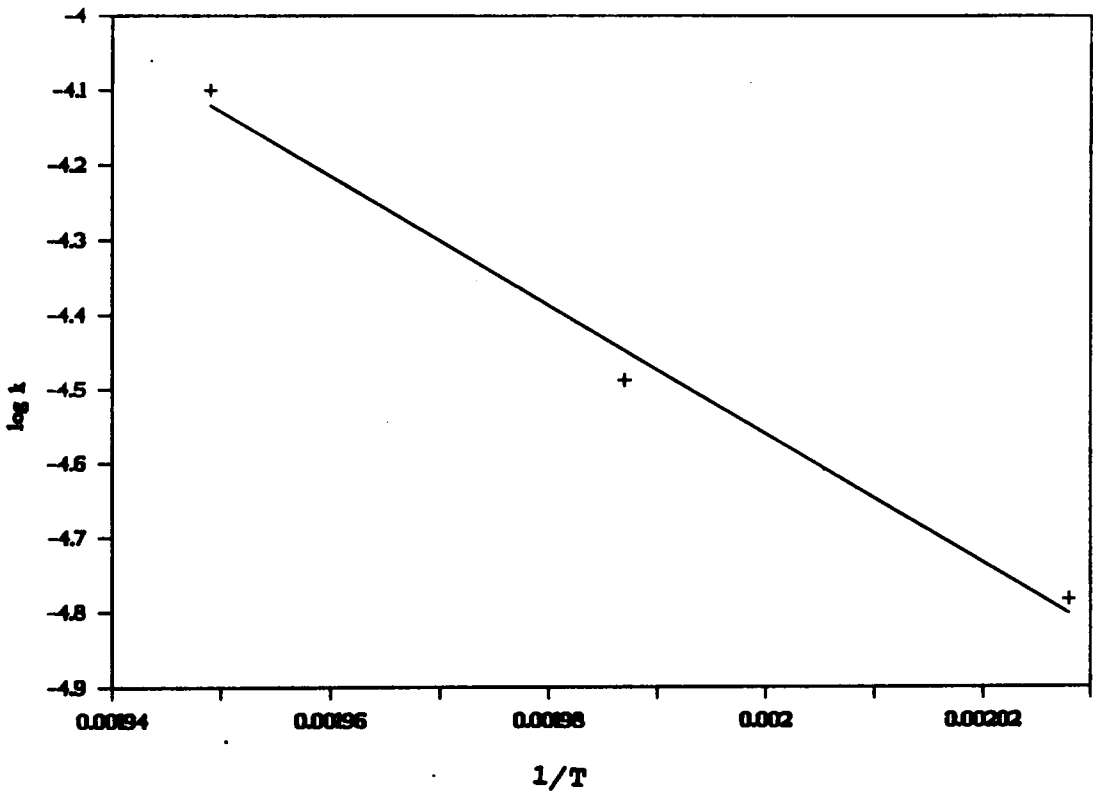

Figure 60. Arrhenius plot of the thermolysis of 1,2,3,4,5-pentaphenyl-2,4-cyclopentadiene-1-ethyl ether (25b).

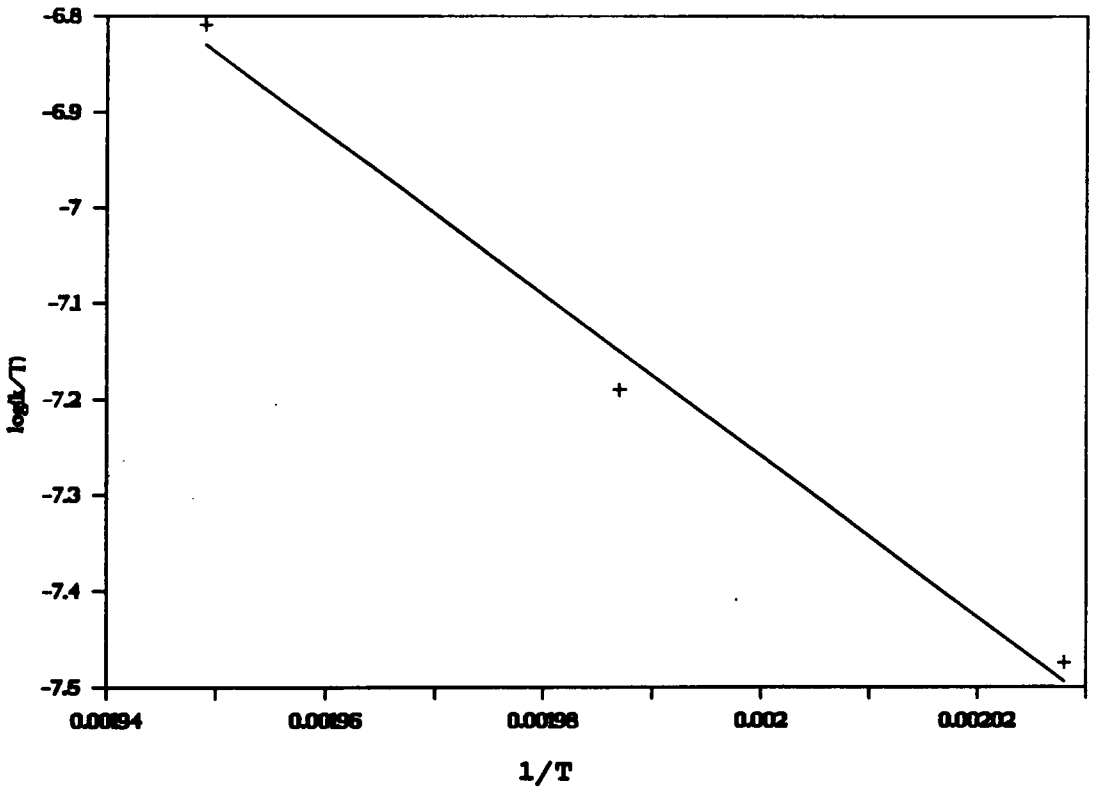

Figure 61. Eyring plot of the thermolysis of 1,2,3,4,5-pentaphenyl-2,4-cyclopentadiene-1-ethyl ether (25b).

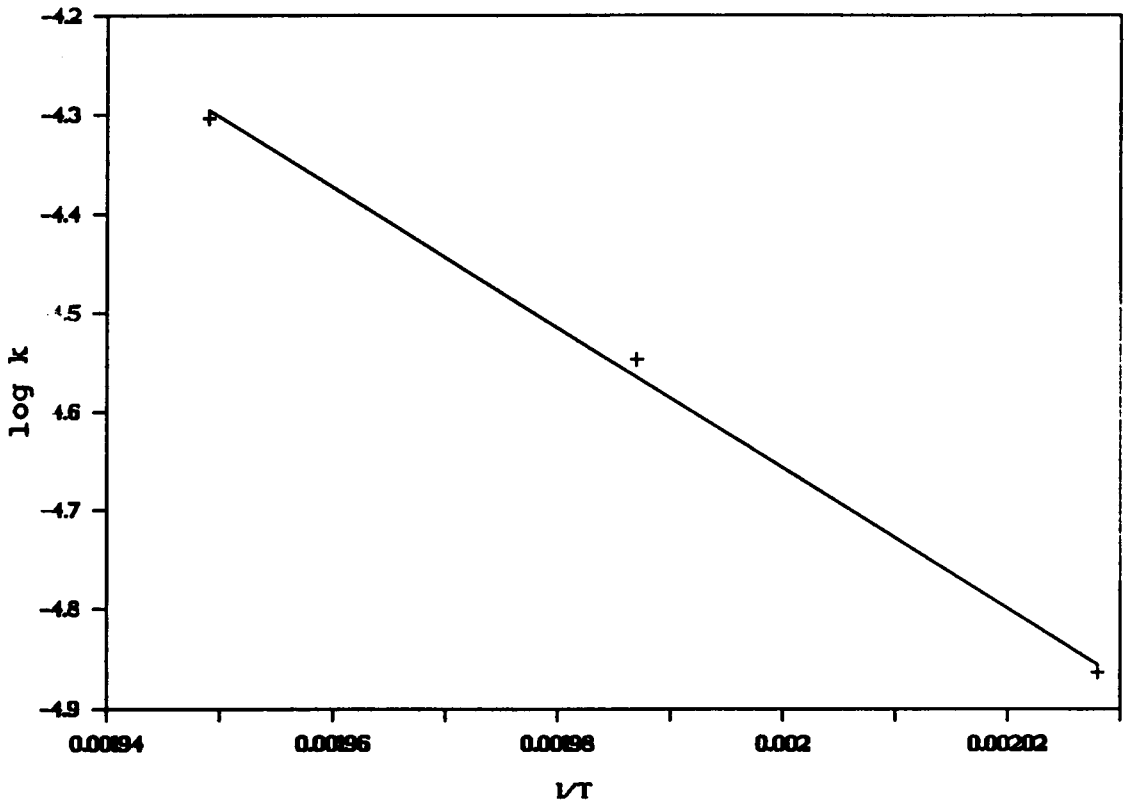

Figure 62. Arrhenius plot of the thermolysis of 1,2,3,4,5-pentaphenyl-2,4-cyclopentadiene-1-n-propyl ether (25c).

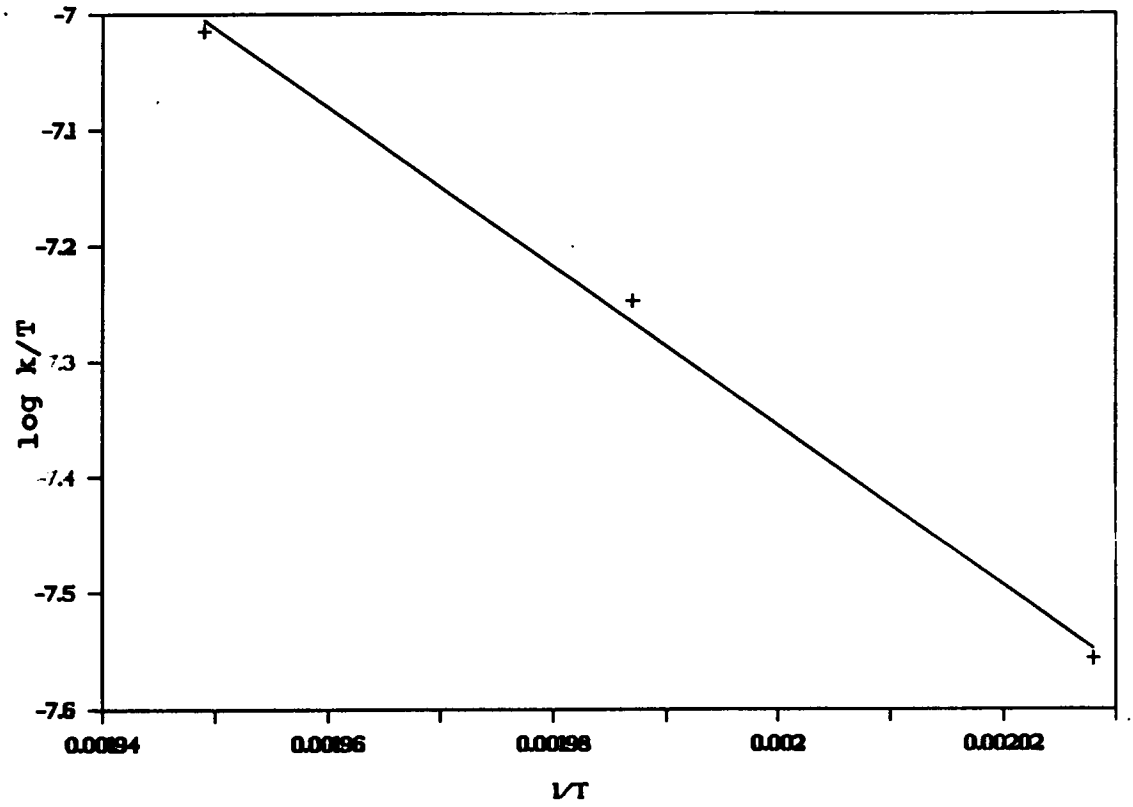

Figure 63. Eyring plot of the thermolysis of 1,2,3,4,5-pentaphenyl-2,4-cyclopentadiene-1-n-propyl ether (25c).

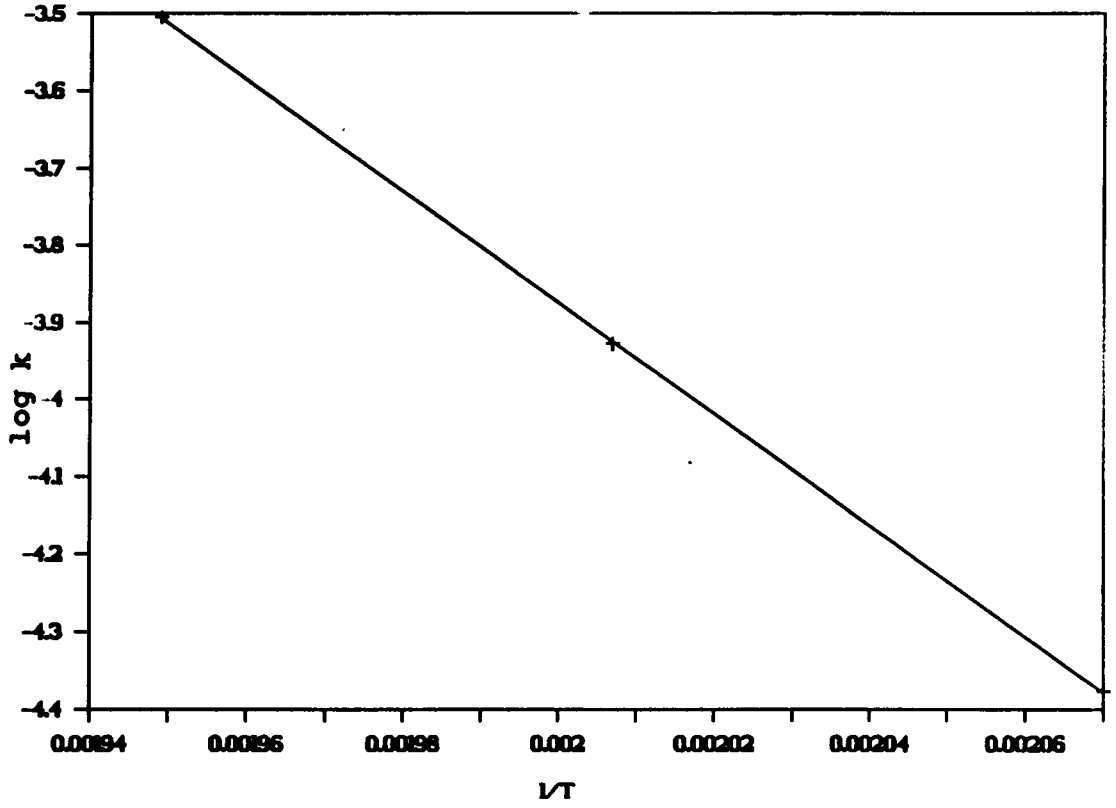

Figure 64. Arrhenius plot of the thermolysis of 1,2,3,4,5-pentaphenyl-2,4-cyclopentadiene-1-benzyl ether (25e).

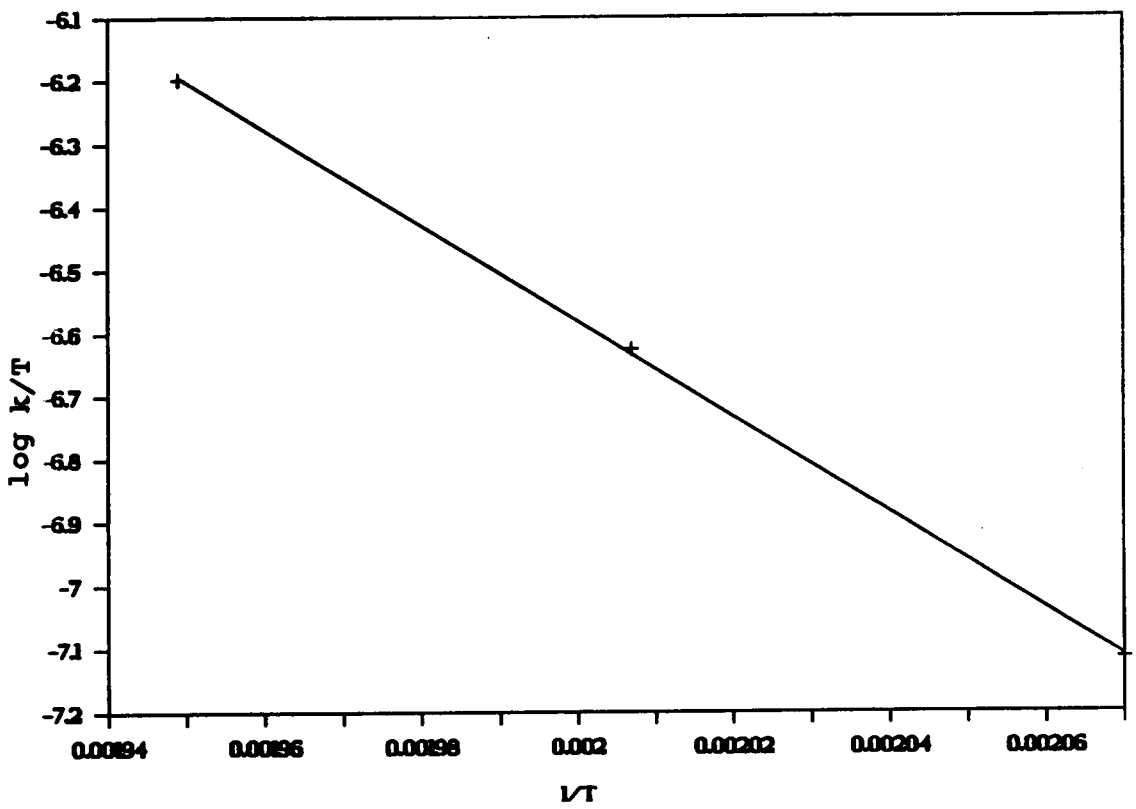

Figure 65. Eyring plot of the thermolysis of 1,2,3,4,5-pentaphenyl-2,4-cyclopentadiene-1-benzyl ether (25e).

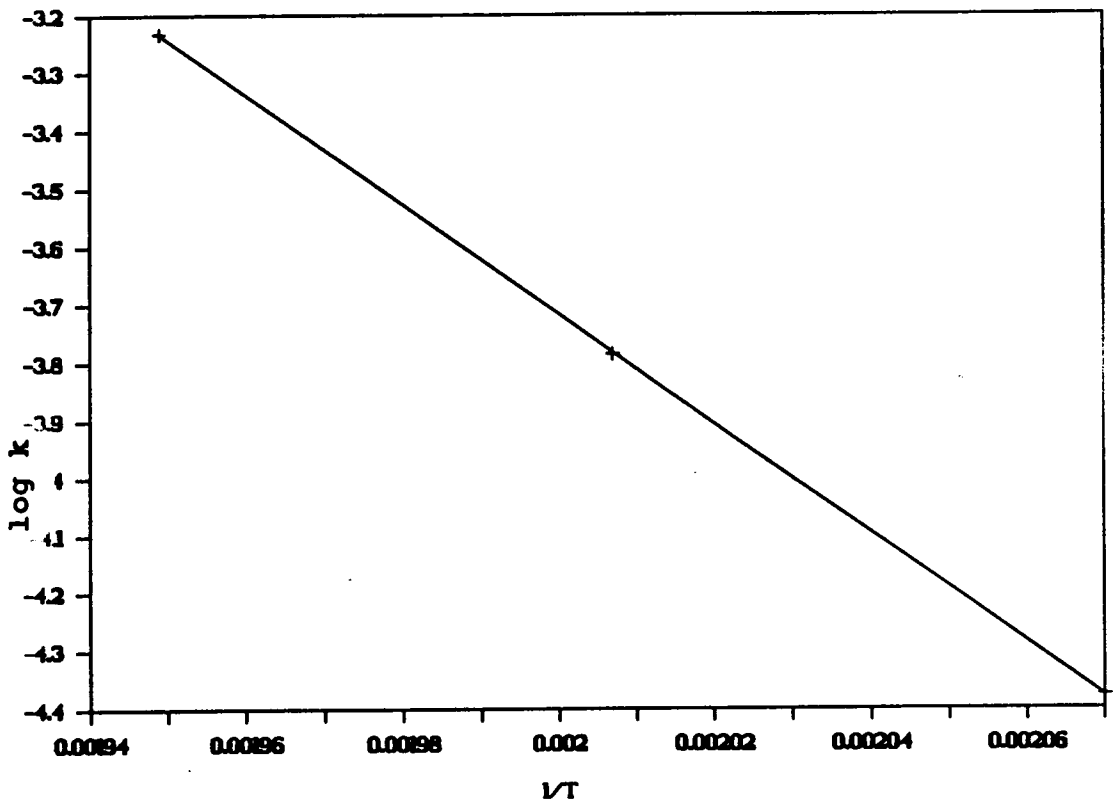

Figure 66. Arrhenius plot of the thermolysis of 1,2,3,4,5-pentaphenyl-2,4-cyclopentadiene-1-benzyl ether (25e).

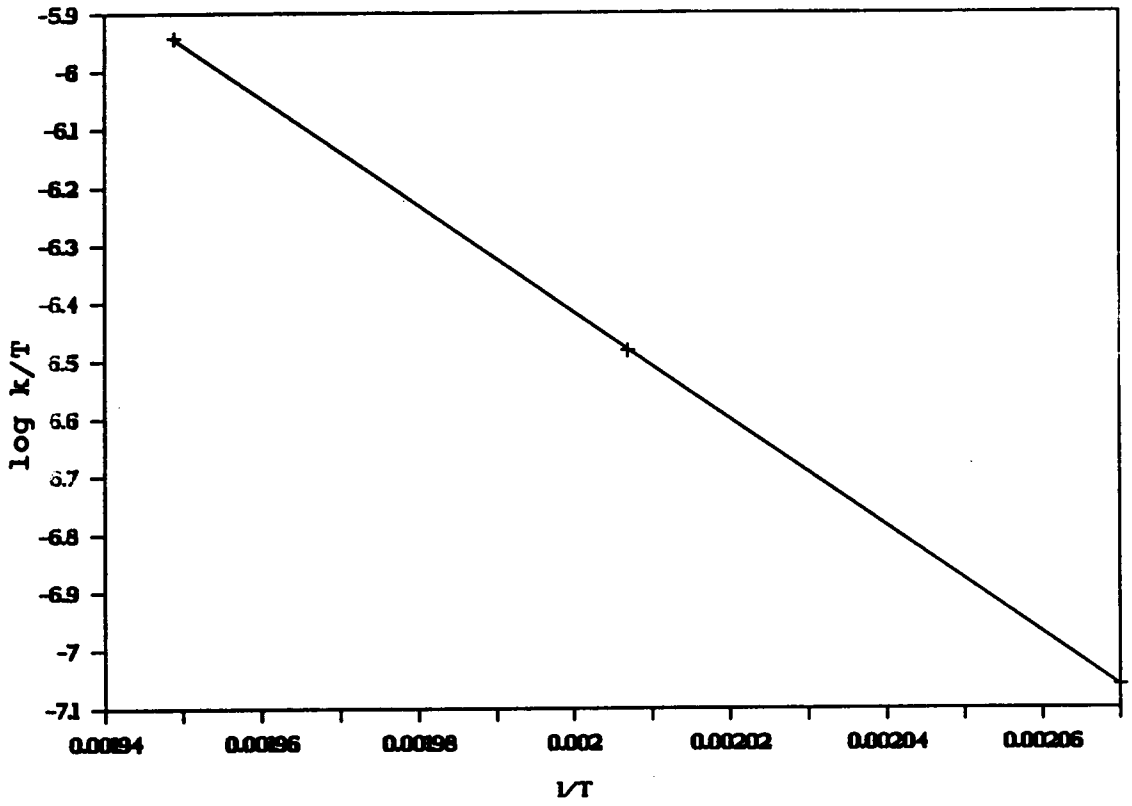

Figure 67. Eyring plot of the thermolysis of 1,2,3,4,5-pentaphenyl-2,4-cyclopentadiene-1-benzyl ether (25e).

K: Data on 1,2,3,4,5-Pentaphenyl-2,4-Cyclopentadien-1-ol (3)

Table XXXXII.

The Isomerization of 1,2,3,4,5-Pentaphenyl-2,4-cyclopentadien-1-ol (3) @ 175.0 ± 0.5°C

Aliquot #	Time (sec)	% Concentration	log (% conc.)
1	30	100	1.99
2	2700	84	1.93
3	5400	71	1.85
4	8100	58	1.76
5	10810	51	1.70
6	13500	39	1.59
7	16200	29	1.46
8	18900	21	1.32
9	21617	17	1.22

k

Plotting log (% conc) versus time

k = -2.303 (slope)

$k = 8.34 \times 10^{-5} sec^{-1}$

slope = -3.62×10^{-5}

y intercept = 2.04

corr = 0.984

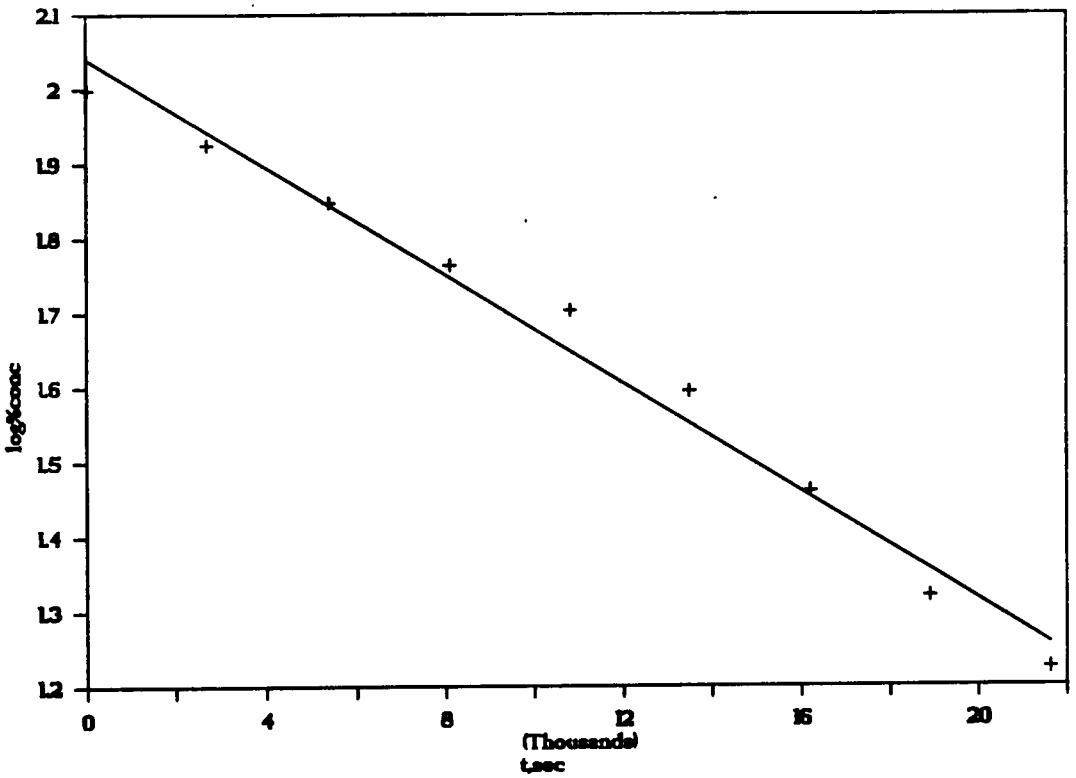

k

Plotting log (% conc) versus time

k = -2.303 (slope)

k = $8.34 \times 10^{-5} sec^{-1}$

slope = -3.62×10^{-5}

y intercept = 2.04

corr = 0.984

Figure 68. First-order plot of the isomerization of 1,2,3,4,5-pentaphenyl-2,4-cyclopentadien-1-ol (3) @ 175.0 ± 0.5°C.

Table XXXXIII.

The Isomerization of
1,2,3,4,5-Pentaphenyl-2,4-cyclopentadien-1-ol (3)
@ 190.0 ± 0.5°C

Aliquot #	Time (sec)	% Concentration	log (% conc.)
1	30	101	2.00
2	870	83	1.92
3	1800	67	1.83
4	2711	52	1.72
5	3600	42	1.62
6	4260	36	1.56
7	5400	31	1.49
8	5300	28	1.44
9	7200	22	1.35

k

Plotting log (% conc) versus time

k = -2.303 (slope)

k = $2.09 \times 10^{-4} sec^{-1}$

slope = -9.08×10^{-5}

y intercept = 1.98

corr = 0.988

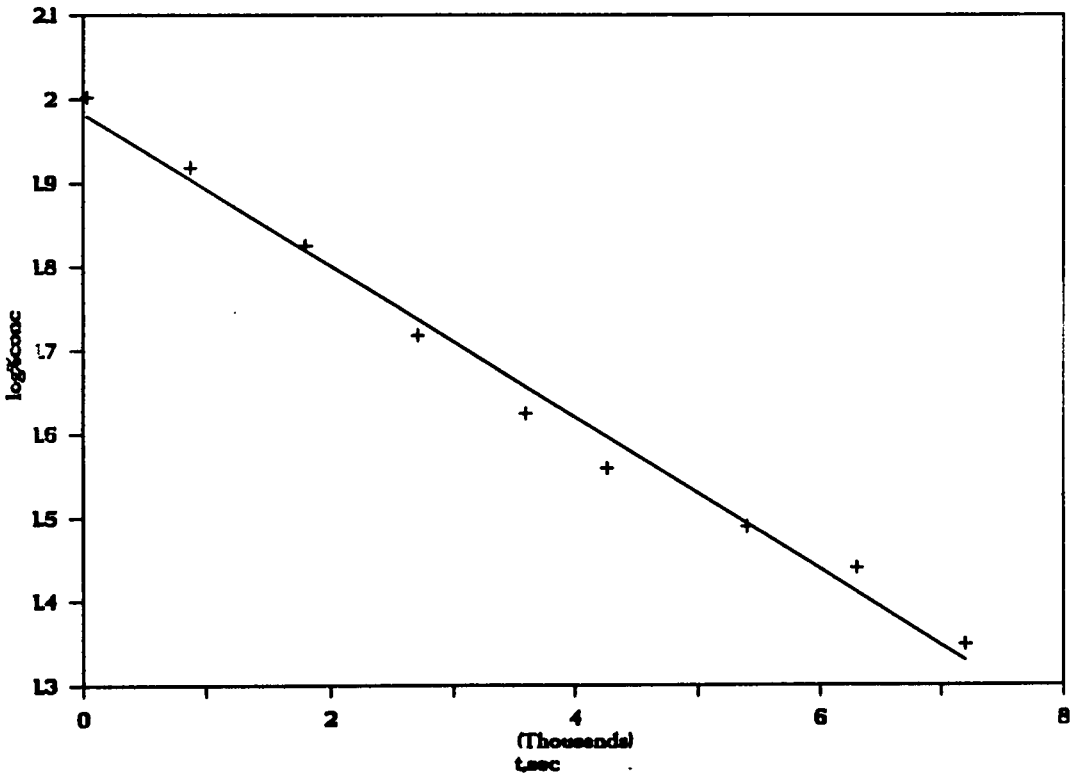

k

Plotting log (% conc) versus time

k = -2.303 (slope)

k = 2.09 x 10^{-4}sec^{-1}

slope = -9.08 x 10^{-5}

y intercept = 1.98

corr = 0.988

Figure 69. First-order plot of the isomerization of 1,2,3,4,5-pentaphenyl-2,4-cyclopentadien-1-ol (3) @ 190.0 ± 0.5°C.

Table XXXXIV.

The Isomerization of 1,2,3,4,5-Pentaphenyl-2,4-cyclopentadien-1-ol (3) @ 205.0 ± 0.5°C

Aliquot #	Time (sec)	% Concentration	log (% conc.)
1	30	106	2.02
2	300	88	1.94
3	600	73	1.86
4	900	59	1.77
5	1200	51	1.71
6	1560	37	1.56
7	1800	33	1.52
8	2100	23	1.35
9	2400	20	1.30
10	2700	15	1.18

k

Plotting log (% conc) versus time

k = -2.303 (slope)

k = 7.28 x 10^{-4} sec^{-1}

slope = -3.16 x 10^{-4}

y intercept = 2.05

corr = 0.993

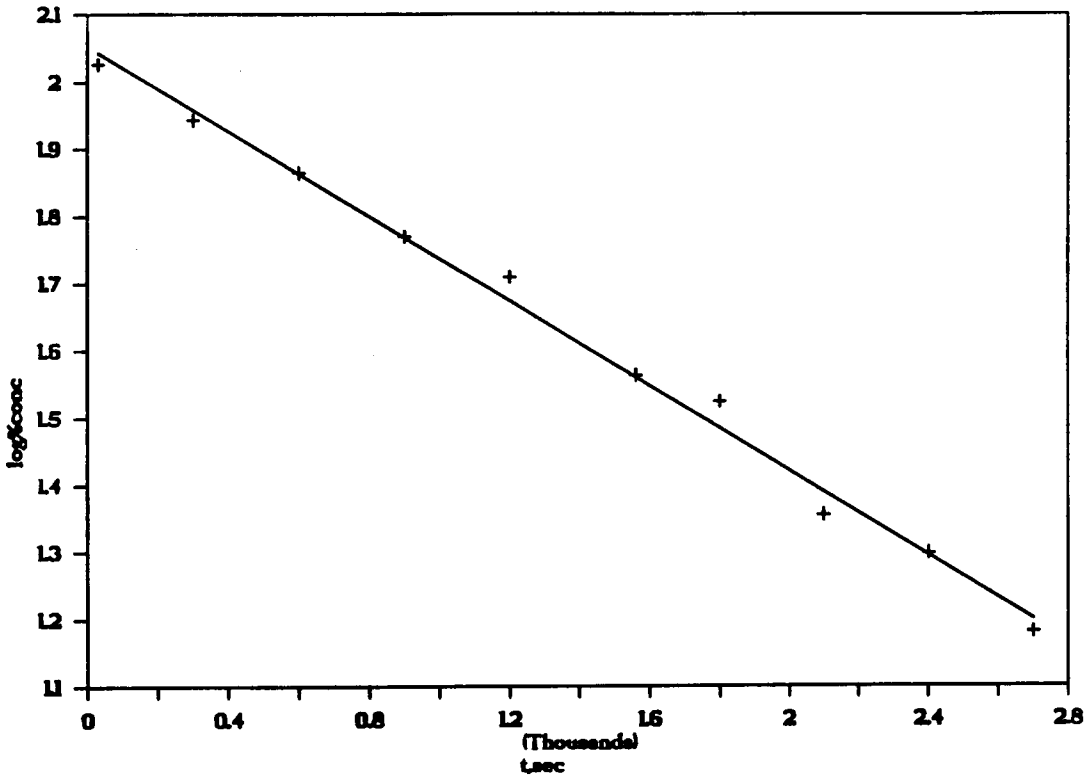

k

Plotting log (% conc) versus time

k = -2.303 (slope)

k = 7.28 x 10^{-4}sec^{-1}

slope = -3.16 x 10^{-4}

y intercept = 2.05

corr = 0.993

Figure 70. First-order plot of the isomerization of 1,2,3,4,5-pentaphenyl-2,4-cyclopentadien-1-ol (3) @ 205.0 ± 0.5°C.

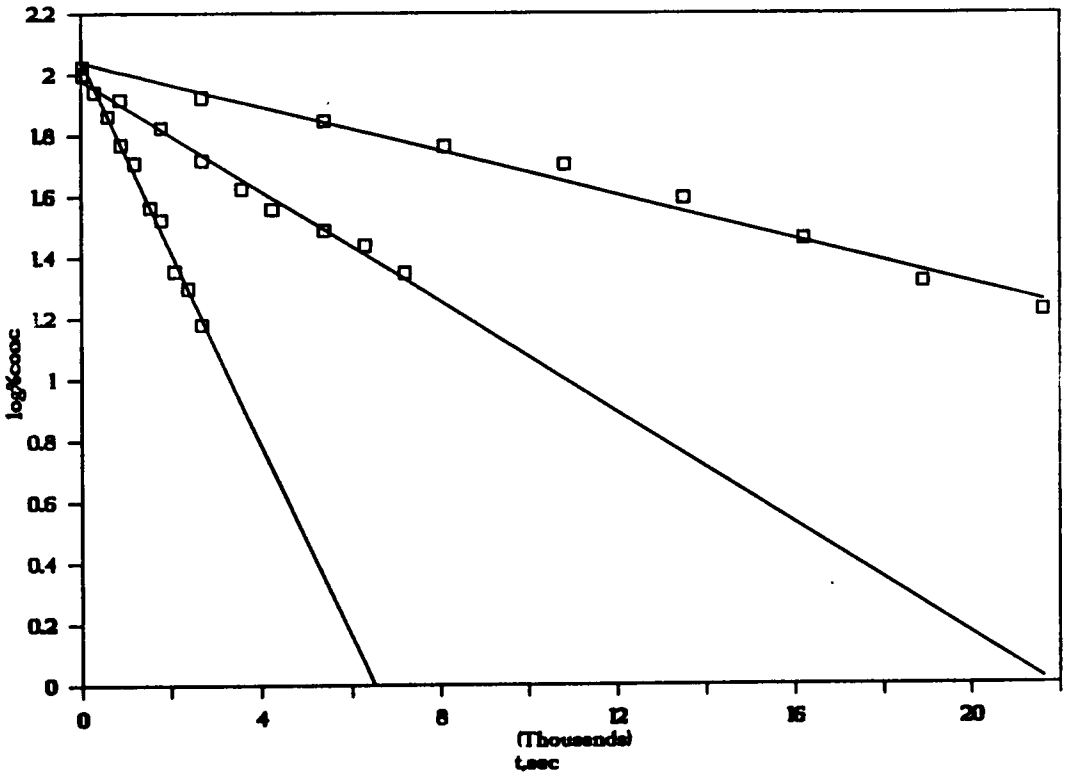

Figure 71. First-order plot of the isomerization of 1,2,3,4,5-pentaphenyl-2,4-cyclopentadien-1-ol (3) @ 175.0-205.0°C.

Calculation of the E_a, $\Delta H^{\neq}$ and $\Delta S^{\neq}$ for the thermolysis of 1,2,3,4,5-pentaphenyl-2,4-cyclopentadien-1-ol (3)

For the case $A \xrightarrow{k_1} B \xrightarrow{k_2} C$
k_3
D

assume $k_3 < < < k_1 \quad k_3 \simeq 0$
therefore $k_{obs} = k_1$ *(at maximum)*

Temperature 0°C	°K	k sec^{-1}	1/T $°K^{-1}$	log k	log (k/T)
205	478.15	7.27×10^{-4}	2.09×10^{-3}	-3.138	-5.818
190	463.15	2.09×10^{-4}	2.16×10^{-3}	-3.679	-6.345
175	448.15	8.34×10^{-5}	2.23×10^{-3}	-4.079	-6.731

E_a

Plotting log k versus 1/T

E_a = -4.576 cal $mol^{-1}K^{-1}$(slope)

E_a = 30.8 kcal mol^{-1}

slope = -6.721×10^3

y intercept = 10.88

corr = 0.992

$\Delta H^{\neq}$&$\Delta S^{\neq}$

Plotting log (k/T) versus 1/T

$\Delta H^{\neq}$ = -4.576 cal $mol^{-1}K^{-1}$ (slope)

$\Delta H^{\neq}$ = 29.8 kcal $mol^{-1}K^{-1}$

slope = -6.521×10^3

y intercept = 7.78

corr = 0.992

$\Delta S^{\neq}$ = 4.576 cal $mol^{-1}K^{-1}$ (y intercept -10 .32)

$\Delta S^{\neq}$ = -11.62 cal $mol^{-1}K^{-1}$

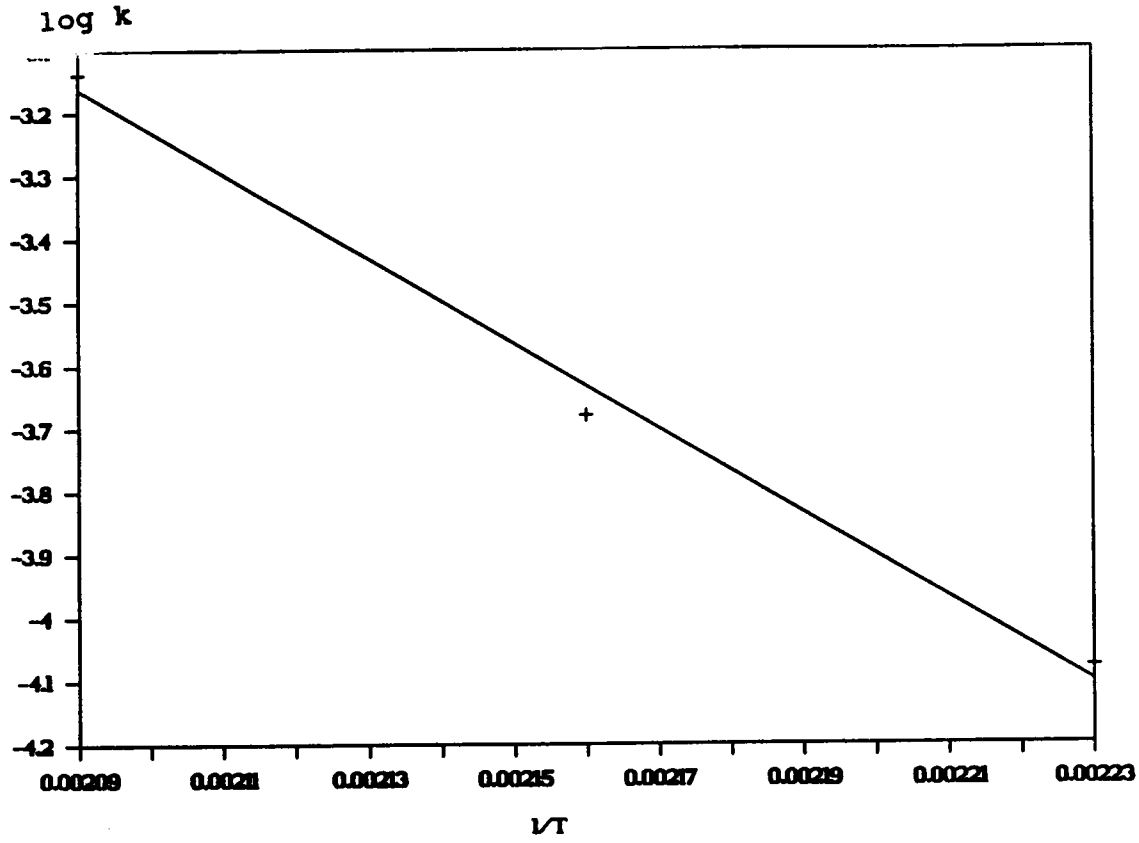

Figure 72. Arrhenius plot of the isomerization of 1,2,3,4,5-pentaphenyl-2,4-cyclopentadien-1-ol (3).

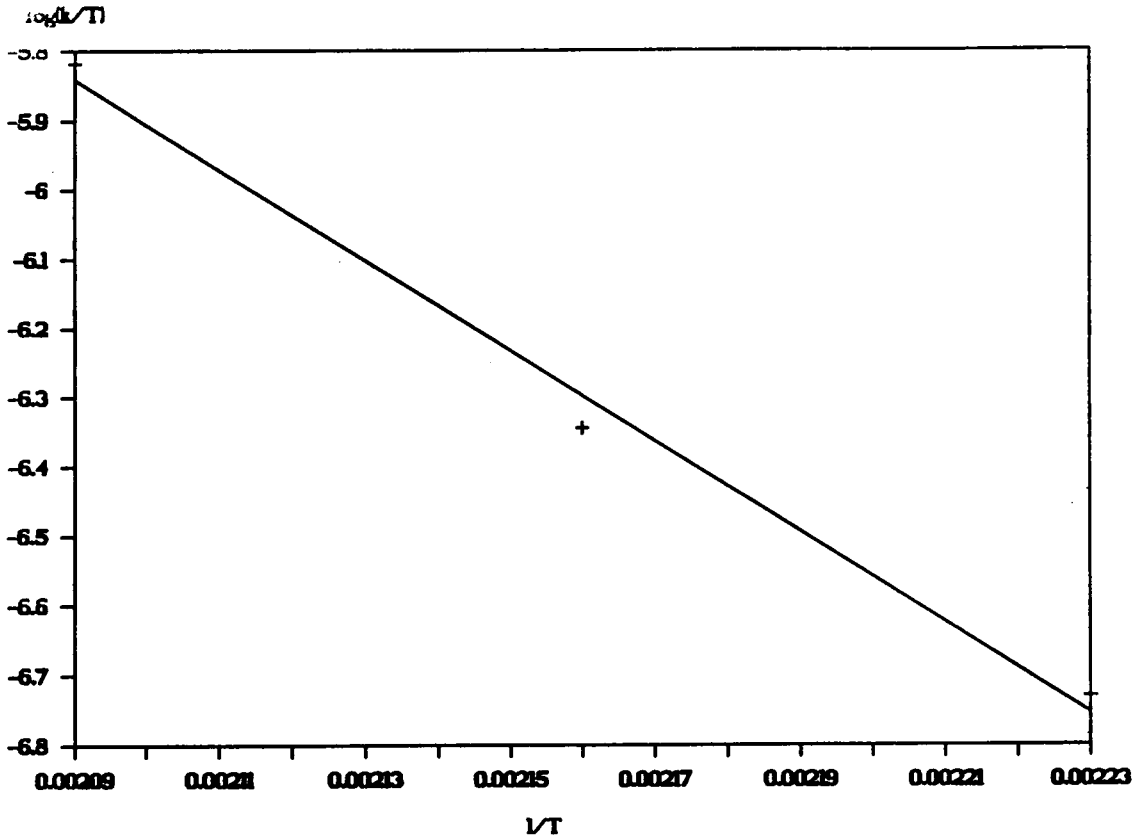

Figure 73. Eyring plot of the isomerization of 1,2,3,4,5-pentaphenyl-2,4-cyclopentadien-1-ol (3).

L: HPLC Conditions and Retention Times for the Pentaphenylcyclopentadiene-Alkyl Ethers.

Normal Phase - Micro Pak NH_2-10 Column

Ether (Hydrocarbon (32))	Retention Time	Mobil Phase
Methyl (**25a**) Hydrocarbon (**32**)	8.6 min 12.4 min	92% Hexane/8% THF
Ethyl (**25b**) Hydrocarbon (**32**)	8.2 min 13.2 min	94% Hexane/6% THF
N-Propyl (**25c**) Hydrocarbon (**32**)	7.6 min 12.5 min	94% Hexane/6% THF
Methyl (d_3)(**25f**)	8 min	92% Hexane/8% THF
Parent Alcohol (**3**)	11.4 min	99% Hexane/1% MeOH

Reverse Phase - Radial Pak C-18 Column

Ether (Products)	Retention Time	Mobil Phase
Benzyl (**25e**) Hydrocarbon (**32**) Benzyl Ketone (**35e**)	9.6 min 5.7 min 7.3 min	66% Methanol/12% THF/22% H_2O

The vita has been removed from the scanned document